DIRECTED SYNTHESIS OF POLYMER MESOSTRUCTURES

by

Charles Frederick James Faul

Dissertation presented for the degree

Doctor of Philosophy (Polymer Science)

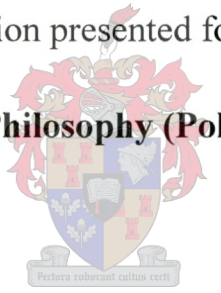

at the

University of Stellenbosch

Promoter

Prof. R.D. Sanderson

Stellenbosch

December 2000

Stellenbosch University http://scholar.sun.ac.za

DECLARATION

I, the undersigned, hereby declare that the work contained in this dissertation is my own original work and that I have not previously in its entirety or in part submitted it at any university for a degree.

Stellenbosch University http://scholar.sun.ac.za

ABSTRACT

The objective of this research was to produce discrete, nano-shaped polymeric structures on the same length scale as, or one to one copies of, templates, deformable templates or structure-directing hosts.

Polymerisation of hydrophobic organic monomers in high concentration surfactant solutions, leads to the formation of shaped particles (rod-like, plank-like and ribbon-like particles) in the micrometer size range. The origin of these regularly shaped particles was investigated. It is proposed that they were not polymeric in nature, but formed by the crystallisation of the surfactant in the presence of electrolytes and ethanol as solvent. The polymeric particles that were formed were found to be of spherical shape, and no directing of the shape was detected.

Mesostructured hosts were then investigated for their possible use as structure-directing agents. A series of polyelectrolyte-surfactant complexes of polydiallylammonium chloride with sodium sulphate surfactants (ranging from C_{10} to C_{16}) were synthesised and characterised in terms of their thermal, mechanical and structural properties. The complex of polydiallylammonium chloride and sodium dodecyl sulphate was selected as an appropriate self-assembled model system for investigations into the structure-directing properties of these new materials.

The polymerisation of hydrophobic organic monomers, such as styrene and the di-functional monomer m-diisopropenylbenzene (m-DIB), within the above mesoscopically structured polyelectrolyte-surfactant complex as host, lead to the formation of unconventionally shaped polymeric particles. The influence of the presence of monomers and guest polymers on the phase morphology of the host was investigated by small angle X-ray analyses (SAXS) and dynamic mechanical analyses (DMA). SAXS analyses showed that these new, stable hosts can hold up to 17 % guest polymer before phase disruption is encountered. These findings were supported by changes in the mechanical properties, as determined by DMA. The transmission electron microscopy (TEM) images of particles obtained after polymerisation showed very clearly that the poly-(m-DIB) did not form a continuous copy of the 3D hexagonal structure of the host, but rather colloidal copies of a part of the host structure that swelled the most. The shapes of the polymer mesostructures were dictated by the morphology of the phase of the structure-directing host, to

Stellenbosch University http://scholar.sun.ac.za

produce nanosized wires (dimensions 4 by 100 nm), cigar-shaped particles (dimensions 8 by 50 nm) and fibrillar bent shapes (larger than 200 nm), as revealed by TEM.

According to literature these are the first shaped, polymer nano-particles produced in a soft, self-assembled, organic templating host.

Stellenbosch University http://scholar.sun.ac.za

OPSOMMING

Die doel van hierdie navorsing was om diskrete, nano-gevormde polimeriese partikels van dieselfde lengteskaal as, of direkte een tot een kopië van, 'n templaat, 'n vervormbare of struktuur-rigtende gasheersisteem te produseer.

Die polimerisasie van hidrofobiese organiese monomere in seep oplossings van hoë konsentrasie, het gelei tot die produksie van gevormde partikels. Die oorsprong van hierdie partikels is ondersoek. Dit word voorgestel dat die partikels nie polimeries van aard is nie, maar gevorm is deur die kristallisasie van die seep in die teenwoordigheid van elekotroliete en etanol as oplosmiddel. Die polimeriese partikels wat wel geproduseer is, was sferies in vorm, en geen rigtende invloed op die vorm van die partikels is waargeneem nie.

Meso-gestruktureerde gasheersisteme is ook ondersoek vir moontlike gebruik as struktuur-rigtende agente. 'n Reeks poliëlektroliet-seep komplekse van polidiallielammoniumchloried en natriumsulfaat sepe (van C_{10} tot C_{16}) is gesintetiseer en gekarakteriseer in terme van hul termiese, meganiese en strukturele eienskappe. Die kompleks van polidiallielammoniumchloried en natrium dodekielsulfaat is gekies as 'n toepaslike self-organiserende modelsisteem vir die ondersoeke na die struktuur-rigtende eienskappe van hierdie nuwe materiale.

Polimerisasie van hidrofobiese organiese monomere, soos byvoorbeeld stireen en die di-funksionele monomeer m-di-isopropenielbenseen (m-DIB), in hierdie mesoskopies-gestruktureerde poliëlektroliet-seep kompleks, het gelei tot die vorming van nie-konvensionele gevormde polimeriese partikels. Die invloed van die teenwoordigheid van monomere en gaspolimere op die fasemorfologie van die gasheersisteem is ondersoek d.m.v. kleinhoek X-straal diffraksie (Eng. SAXS) en dinamiese meganiese analise (DMA). SAXS analises het aangetoon dat hierdie nuwe, stabiele gasheersisteem tot 17 % gaspolimeer kan inkorporeer voordat fasevernietiging plaasvind. Hierdie resultate is verder ondersteun deur veranderinge in die meganiese eienskappe soos waargeneem deur DMA. Transmissie elektronmikroskopie (TEM) afbeeldinge van partikels geïsoleer na polimerisasie het baie duidelik gewys dat, in die geval van poli-(m-DIB), die gaspolimeer nie 'n kontinue kopie van die drie dimensionele heksagonale struktuur van die gasheersisteem produseer nie. Daar word eerder 'kolloïdale kopieë' van dele van die gasheersisteem wat die meeste swel gevorm. Die vorms van die polimeer mesostrukture word dus bepaal deur die morfologie van die fase van die struktuur-rigtende gasheer, om nanogrootte

Stellenbosch University http://scholar.sun.ac.za

draadjies (dimensies 4 x 100 nm), sigaarvormige partikels (8 x 50 nm) en fibrillêre gebuigde vorms (groter as 200 nm) te vorm, soos waargeneem met TEM.

Volgens die literatuur is hierdie die eerste geval van gevormde polimeer nanopartikels geproduseer in ‘n self-organiserende templaat gasheersisteem.

Stellenbosch University http://scholar.sun.ac.za

"We have educated ourselves into imbecility"

Malcolm Muggeridge

Stellenbosch University http://scholar.sun.ac.za

Acknowledgements

I would like to thank all people and institutions that contributed in some way to the completion of my studies, without whom this work would not have been possible. I would like to highlight the following names:

Prof Ron Sanderson, my supervisor, for advice, encouragement, never-ending stream of new ideas, for always trying to go that one step further, and allowing me to enjoy science in all of its international splendour

Prof Dr Markus Antonietti, from the Max Planck Institute for Colloids and Interfaces, Golm, Germany, for accepting me into his laboratories, and, with clear-cut advice and endless email discussions, helping me in the right direction

Prof Engelbrecht, for helpful discussions and his willingness to accommodate me in one of Physical Chemistry's laboratories

Dr Margie Hurndall for help with the proof-reading of my thesis and helpful discussions

Erinda Cooper, Aneli Fourie, Johan Bonthuys at the IPS

Physical Chemistry Department (including Thalma Nieuwoudt, Valeska Cloete, Dr Gawie Wessels, Prof Dillen, Johannes Stuurman and Moebarick Bickerstaff) for many happy hours spent there

Fr Ingrid Zenke, fuer viele SAXS Messungen gemacht (und viele Tasse Tee und freundlichkeit im kalten Teltow Winter)

Prof Dr Christine Göltner, for responding so quickly and helpfully from my first contact, providing the necessary help for my first visit, and for hospitality and friendliness

Dr Hans-Peter Henzte, for guiding me through new learning experiences in the field of directed synthesis, providing the initial idea for many interesting investigations, and helping me settle into life at the MPIKGF

Dr Andreas Thünemann, for friendly advice and many helpful discussion concerning polyelectrolyte-surfactant complexes

Stellenbosch University http://scholar.sun.ac.za

Sascha General, for friendship, and numerous long discussions concerning polyelectrolyte-surfactant complexes

Dr Jurgen Hartman, Dr Helmut Cölfen, Antje Völkel and Dr Heimo Schnablegger for analytical services provided.

The Science Liaison via Video Conferencing Discussion Group

C. Briel, C. Erich and all co-workers at the Max Planck Institute for Colloids and Interfaces

Mr Shaheed Hartley and Mrs Helena Opperman, for friendly and efficient help in order to track down that last bit of funding

National Research Foundation of South Africa -Prestige Scholarship Programme and the Equipment Programme - for making funding available to realise my scientific dreams

Max Planck Gesellschaft, for providing financial support during my visits to the Max Planck Institute for Colloids and Interfaces

John and Nicky Bowmer for a safe haven far from science

My parents, Gert and Cecile Faul, for constant support over the last decade of studies

Jacqueline, for guidance, help, support, freedom to pursue my academic goals and sacrificial love

Stellenbosch University http://scholar.sun.ac.za

Table of Contents

Stellenbosch University http://scholar.sun.ac.za

Stellenbosch University http://scholar.sun.ac.za

List of Figures

Stellenbosch University http://scholar.sun.ac.za

Stellenbosch University http://scholar.sun.ac.za

List of Tables

Stellenbosch University http://scholar.sun.ac.za

List of Important Abbreviations

SDS	Sodium dodecyl sulphate
CTAB	cetyltrimethylammonium bromide
HLB	hydrophilic-lipophilic balance
CMC	critical micelle concentration
ESR	Electron Spin Resonance Spectroscopy
NMR	Nuclear Magnetic Resonance Spectroscopy
P	Packing parameter
v_{hc}	volume of hydrocarbon chain (nm^3)
a_0	effective area per headgroup (nm^2)
l_c	critical length (nm) of an extended saturated hydrocarbon chain
l_{max}	maximum length possible for an extended saturated hydrocarbon chain
M	mean aggregation number
R	radius of the micelle
H	mean curvature at a point on the surface of a micellar aggregate
R_1, R_2	radii of curvature in two perpendicular directions
E	linear charge density of a polyelectrolyte
CAC	concentration where the aggregation of surfactant and polyelectrolyte can first be detected
ß	degree of binding, corresponds to the fraction of available charges on a poly-electrolyte neutralised by the binding of surfactant ions

Stellenbosch University http://scholar.sun.ac.za

IR	infra-red
UV	ultraviolet
SANS	Small Angle Neutron Scattering
SAXS	Small Angle X-ray Scattering
WAXS	Wide Angle X-ray Scattering
ξ	lengthscale of phase separation within a mesoscopically ordered system
SCT	surfactant-containing templates
DNA	Deoxyribonucleic Acid
RNA	Ribonucleic Acid
SEM	Scanning Electron Microscopy
TEM	Transmission Electron Microscopy
MMA	methyl methacrylate
AA	acrylic acid
EGDMA	ethyleneglycoldimethacrylate
HEMA	2-hydroxyethylmethacrylate
ADAB	allyldodecyldimethylammonium bromide
λ	wavelength of electromagnetic radiation
DMA	Dynamic Mechanical Analysis
DSC	Differential Scanning Calorimetry
d	spacing between layers of scattering centers in a sample exposed to X-rays
θ	angle at which the incident beam strikes the strikes the scattering centers in a sample exposed to X-rays

Stellenbosch University http://scholar.sun.ac.za

$I(\vec{s})$	detected scattering intensity
$\rho(\vec{r})$	electron distribution function
$A(\vec{s})$	complex scattering amplitude for N point scatter centres
$P(\vec{r})$	Patterson function (the autocorrelation function of $\rho(\vec{r})$)
ε	deformation or strain of a spring
σ	applied stress
k	spring constant
G'	the storage modulus (defines the energy stored in the specimen due to the applied strain)
G"	the loss modulus (defines the dissipation of energy)
G*	complex modulus (can be defined as the vector sum of G' and G")
M_n	number average molecular weight
M_w	weight average molecular weight
D	polydispersity (measure of the breadth of the molecular weight distribution)
DVB	divinylbenzene
ICP-AES	inductively coupled plasma atomic emission spectroscopy
pDADMAC	Polydiallyldimethylammonium chloride
m-DIB	meta-diisopropenylbenzene
BA	butylacrylate
AIBN	2,2'-azobisisobutyronitrile

Stellenbosch University http://scholar.sun.ac.za

CHAPTER 1

1 Introduction

1.1 Background

It has been the aim of chemists over the ages to be able to direct the characteristics of synthesised chemicals on a molecular level, so that they could perform specific functions because of their atomic architecture. Over the last few years chemists have focussed their efforts on directing their syntheses on a scale beyond that of single atoms and small molecules, i.e. they have been looking at synthesis on a supramolecular scale. This has been done in order to produce large assemblies of molecules with a specific molecular architecture, so-called mesostructures or mesoscopic materials (*meso* = sizes ranging from 1 to 500 nm), which have the ability to perform selected functions.

This has been achieved with inorganic polymers. Since 1992 it has been possible to direct the structure of assemblies of inorganic precursors into ordered inorganic polymers [1]. This discovery launched an entire new field of research which has now expanded beyond mesoscopic materials, to synthesis on a panoscopic scale (*pano* = of any sizes) [2].

Organic polymer syntheses have, however, not yet reached the same level of sophistication and control as is possible with the inorganic polymers. Attention was therefore given to organic polymers, and to the directed synthesis of organic polymer mesostructures. Literature reports no successful attempts to create discrete, nano-shaped polymeric structures on the same length scale as, or one to one copies of, templates, deformable templates or structure-directing hosts.

1.2 Colloids and Self-Assembly

The term colloid was coined in 1861 by Thomas Graham (from the Greek word meaning glue). The International Union of Pure and Applied Chemistry (IUPAC) defines a colloid as any material with at least one of its three dimensions between one and one thousand nanometers [3, 4].

Colloids were initially investigated as classical sols (Michael Faraday studied colloidal gold sols in the 1850s), but with the discovery of polymers and biopolymers, the study of colloids expanded and gave birth to the field of polymer science.

Association colloids, also sometimes referred to as complex fluids, is a branch of colloidal science. It involves the study of colloids formed by the association of amphiphilic compounds. An

Stellenbosch University http://scholar.sun.ac.za

amphiphilic compound or amphiphile can be defined as a molecule containing both hydrophilic (i.e. "water loving") and lyophilic ("oil loving") substructures, which differ greatly in their solubilities [5, 6].

James McBain [7] was the first to suggest that molecules of an amphiphilic nature would self-assemble into aggregates he called micelles (from the Latin word *micella*, meaning small bit). This suggestion was made after noting a drastic change in the osmotic pressure of an amphiphilic system. Hartley [8] suggested that these aggregates were spherical while McBain believed that they were of a lamellar nature.

Over the last two decades the self-assembly of molecular components into supramolecular arrays has become an area of great interest, as can be seen in the numerous publications on this topic (for example, see references 9 - 12 and the references cited therein). Self- assembly can be described, in a basic definition, as the spontaneous intermolecular association via non-covalent bonds (i.e. interactions such as electrostatic, hydrophobic and hydrogen bonds) resulting in thermodynamically stable, well-defined structures, with dimensions ranging from 10 nm to 10 μm [13, 14].

It is this self-assembly of amphiphilic molecules that forms the basis of membranes found in nature, of many industrial processes and products, and also of this study.

1.3 Motivation

The motivation for this project can be summarised by pointing towards the elegant self-assembly of amphiphilic compounds as found in nature. The astounding simplicity and ease with which such structures are formed, and the great difficulty we as scientists have in fully understanding such systems, is challenge enough. An even greater challenge, however, lies in the manipulation and application of these delicately structured molecular architectures to achieve the synthesis of designed molecular entities on a mesoscopic scale.

1.4 Objective

The objective of this study was to apply nature's self-assembled structures as hosts or templates for the directed synthesis of discrete polymeric structures on the same length scale as, and preferably a direct one to one copy of, the original host or template.

Stellenbosch University http://scholar.sun.ac.za

1.5 Tasks and Layout of Thesis

This objective was approached in the following way. Firstly, current literature concerning self-assembly and polymerisation in organised media was studied. An overview of this is presented in Chapter 2. It is shown that, to date, the objective of this study had not been described in any other published work.

A short description of analytical techniques used during this study, with specific reference to techniques suitable for use with mesostructured systems, is presented in Chapter 3.

Meaningful advances had been made by Beck et al [1] in the field of the structure directing of inorganic polymers (i.e. silicate polymeric structures) by using surfactant solutions below the liquid crystalline phase regions. High concentration surfactant phases as hosts for the structure-directed synthesis of crosslinked and non-crosslinked polystyrene polymers were therefore used, as described in Chapter 4.

A new type of mesostructured material that could serve as a structure-directing host, polyelectrolyte-surfactant complexes, is introduced in Chapter 5. The synthesis and characterisation of a series of alkyl sulphate surfactants complexed with polydiallyldimethyl-ammonium chloride is discussed.

In Chapter 6, one of these polyelectrolyte-surfactant complexes, namely polydiallyldimethyl-ammonium chloride – sodium dodecyl sulphate, was identified as a structure-directing host. This was due to its availability, low cost and defined phase structure. It was then utilised as a host in order to ascertain if the added mechanical stabilisation of a high molecular weight polyelectrolyte backbone might provide the necessary stability and deformability needed to direct the structure of an included guest polymer.

Firstly, the stability of the host after inclusion of various monomers (styrene, butylacrylate, m-DIB and ethyleneglycoldimethacrylate (EGDMA)) was investigated and, secondly, the effects of polymerisation and the presence of the various amounts of guest polymer on the host were investigated. Finally, guest polymer morphology was investigated to ascertain whether the objective of this study, i.e. to produce discreet polymeric particles on the same length scale as, or preferable a direct one to one copy of, the original host, was indeed achieved.

Conclusions to this proof-of-principle study and recommendations for future studies are given in Chapter 7.

Stellenbosch University http://scholar.sun.ac.za

1.6 References

1. Kresge C.T., Leonowicz, M.E., Roth W.J., Vartuli J.C., Beck J.S. Nature 1992, **359**, 710

2. Ozin G.A. Chem. Commun. 2000, **1**, 419-432

3. Vold R.D., Vold M. J. Colloid and Interface Chemistry, Addison-Wesley Publishing Company, 1983.

4. Evans D.F., Wennerström H. The Colloidal Domain, Wiley-VCH, 1994

5. Winsor P.A. Chem. Rev., 1968, **68**, 1-39

6. Wennerström H., Lindman B. Phys. Rep. (Phys. Lett.) 1979, **52**, 1

7. McBain J.W. Trans. Faraday Soc. 1913, **9**, 99

8. Hartley G.S. Aqueous solutions of paraffin chain salts, Hermann, Paris, 1936

9. Lehn J.M. Supramolecular Chemistry, VCH, Weinheim, 1995

10. Cates M.E., Safran S.A. Curr. Opin. Colloid Interface Sci. 1996, **1**, 327

11. Ringsdorf H., Schlarb B., Venzmer J. Angew. Chem. Int. Ed. Engl. 1988, **27**, 113

12. Fuhrhop J-H., Helfrich W. Chem. Rev. 1993, **93**, 1565

13. Lehn J. Angew. Chem. Int. Ed. Engl. 1988, **27**, 90

14. Lehn J. Angew. Chem. Int. Ed. Engl. 1990, **29**, 1304

Stellenbosch University http://scholar.sun.ac.za

CHAPTER 2

2 Theoretical and Historical Background

As was discussed in the introduction, there is a gap in knowledge in polymer chemistry that concerns creating nano-shaped organic polymeric particles by either a template, deformed template or structure-directing host.

In order to address this problem, which has been chosen as the goal of this work, it is necessary and often enlightening to review all newly published attempts to create structured or ordered nano-particles (whether they are organopolymer by nature, or rather only self-assembled surface active materials, oligomers and polymers such as block copolymers with surface active properties). Also to be included are the known templated structures of inorganic materials.

One of the newest areas of surfactant self-assembly concerns polyelectrolyte-surfactant complexes. These are highlighted and will be referred to during the discussions and results in the following chapters.

2.1 Theoretical Background

2.1.1 Amphiphiles and Micelle Formation

2.1.1.1 Classification of amphiphiles

Amphiphilic compounds can be defined as molecules containing both hydrophilic (i.e. "water loving") and lyophilic ("oil loving") substructures, which differ greatly in their solubilities [1]. Amphiphiles, for which the term surfactant – i.e. surface-active agent – is also used, can be described and classified according to the charge (or absence of) carried by the hydrophilic part. A general classification for small molecules or telomers would therefore include anionic, cationic, non-ionic, amphoteric / zwitter-ionic, bolaform and higher star compounds (the bolaform compounds will be discussed in section 2.1.1.4). Some examples of compounds in the various classes of amphiphiles are given below in Table 2.1. This section will not discuss oligomeric or polymeric surfactants.

Stellenbosch University http://scholar.sun.ac.za

Classification of types of amphiphiles	Specific examples of compounds
Anionic	Sulphonate, sulphate, carboxylate, phosphates eg. Sodium dodecylsulphate (SDS). Can be combined onto a non-ionic polyethylene oxide spacer.
Cationic	Alkylamine (primary, secondary, tertiary, quaternary forms) e.g. Cetyltrimethylammoniumbromide (CTAB)
Non-ionic	Polyethylene oxide hydrophiles
Zwitter-ionic	Phosphatidylcholine
Bolaform	Glc-NC-(n)CN-Glc (n = 6 – 16)

Table 2-1 Some specific examples of compounds in the various classes of amphiphiles

In 1949 Griffin devised an empirical scale, the HLB scale (hydrophilic-lipophilic balance) to describe nonionic surfactants [2]. This has found wide use for selection of surfactants for emulsification processes. A broad classification of applications of non-ionic and ionic surfactants according to their assigned HLB values is given in Table 2.2 below [3, 4]

Range of HLB Values	Application of Surfactants within the given HLB range
3-6	Water in oil emulsifier
7-9	Wetting agent
8-15	Oil in water emulsifier
13-15	Detergent
15-18	Solubilizer

Table 2-2 General classification of uses of surfactants according to their HLB values [Taken from ref 3, pg 10]

Stellenbosch University http://scholar.sun.ac.za

2.1.1.2 Micelle formation

Changes occurring on a nano-structural level as the concentration of an amphiphile in an aqueous solution increases, can be discussed in terms of changes in various properties of the solution, e.g. surface tension, conductivity, viscosity etc. The approach followed in this section is to explain (in a simplified way) changes on the molecular level in terms of changes in the surface tension of a model surfactant system, such as sodium dodecylsulphate. Other experimental techniques frequently applied to follow changes occurring on this nano-structural level include conductivity and viscosity measurements, solubilisation studies, and scattering (light, laser, x-rays, neutron) studies.

At low concentrations, surfactant molecules will arrange themselves at the air-water interface, with their hydrocarbon tails directed away from the water, and charged headgroups interacting with the water molecules. The presence of the molecules at the interface will lower the surface tension (an air-water interface has a higher surface tension than an air-hydrocarbon interface), which will decrease further with increasing surfactant concentration. Some of the amphiphilic molecules will also be present as free "monomer" in the solution.

At a very specific concentration (called the critical micelle concentration or CMC, 8.1×10^{-3} mol/l in the case of SDS [5a]), a sudden change will be observed in the surface activity of the solution. After this point, the surface tension will remain constant over a wide concentration range. On a nano-structural level, this sudden change in the observed properties is characterised by a large change in the rearrangement of the amphiphile molecules. The "free monomeric" amphiphiles in solution aggregate, above the CMC, into spherical-like aggregates termed micelles (after McBain). It is assumed that no micelles are formed before the CMC is reached (although this assumption remains a controversial one - it falls beyond the scope of this study).

As the concentration of the amphiphile is increased, more micelles are formed in the solution, but the concentration of the amphiphilic molecules present at the surface will remain constant (as the surface tension maintains a constant value). The number of molecules combining to form such a micelle is called the aggregation number; for SDS it is approximately 63. This stays constant as the amphiphile concentration is increased.

The size, shape and structure of micelles have been investigated by various means, including various scattering techniques, electron spin resonance spectroscopy (ESR) and nuclear magnetic resonance spectroscopy (NMR). Using techniques such as NMR and fluorescent probes it has been

Stellenbosch University http://scholar.sun.ac.za

established that the core of the micelles is fluid-like (e.g. pure hydrocarbon), with some penetration by the surrounding water molecules into the so-called Stern-layer surrounding the micelle [5b].

2.1.1.3 Self-assembly

2.1.1.3.1 General Concepts

Before the self-assembly of amphiphilic molecules is discussed in detail, some general concepts concerning surfactants and their properties will first be given. As a general approximation, an increase in the chain length of an amphiphilic molecule will lead to a decrease in the CMC. An increase in the chain length by 2 methylene units results in a decrease in the CMC of ionic surfactants by a factor of 4, and in the case of non-ionic surfactants by a factor of 10 [5c]. This can be explained in terms of higher / more unfavourable interactions between the longer hydrocarbon chains and the aqueous environment (the introduction of polar groups increases the CMC for exactly the opposite reason). This trend is valid for chain lengths of up to 16 carbon atoms. For systems with more than 16 carbon atoms, the reduction is less rapid (probably due to coiling of the chains) [5c].

2.1.1.3.2 Self-assembly of amphiphiles into micelles

There are two main forces governing the self-assembly of amphiphilic molecules into micelles, namely, thermodynamic aspects of self-assembly, and intra-aggregate forces (between amphiphilic molecules within aggregates). This is true for dilute and semi-dilute systems. With an increase in concentration however, inter-aggregate forces also come into play in determining equilibrium structures [6].

Rather than approaching amphiphilic micelle formation from a thermodynamic point of view, molecular packing considerations and, in particular, the so-called packing parameter (P) or shape factor [6, 7] will be used to discuss which structures are formed. Another approached that will be discussed briefly, is that based on the spontaneous curvature of the surfactant layer at the interface between the surfactant and the surrounding medium.

Packing parameter $P = v_{hc}/a_0 l_c$ Eq. 2.1

where

v_{hc} = volume of hydrocarbon chain (nm^3)

a_0 = effective area per headgroup (nm^2)

l_c = critical length (nm) of an extended saturated hydrocarbon chain

Stellenbosch University http://scholar.sun.ac.za

Tanford [8] provided the following equations for the determination of the critical length (l_c) of an extended saturated hydrocarbon chain with n carbon atoms:

$$l_c <= l_{max} = (0.154 + 0.1265\ n)\ nm \qquad \text{Eq. 2.2}$$

where

n = number of carbon atoms

l_{max} = maximum length possible for an extended saturated hydrocarbon chain

nm = nanometers

and also provided the equation for the determination of the volume of a hydrocarbon chain (v_{hc})

$$v_{hc} = (27.4 + 26.9\ n) \times 10^{-3}\ nm^3 \qquad \text{Eq. 2.3}$$

The effective headgroup area is determined by the interaction of two opposing forces: the hydrophobic attractive interactions below the hydrocarbon-water interface (which induces the molecules to associate) and repulsive contributions consisting of hydrophilic, ionic or steric components (above the hydrocarbon-water interface). With these two opposing forces working in on the formation of equilibrium structures, the system will reach a position of an optimal area per headgroup when the total interaction energy per molecule in the aggregate is at a minimum. This optimal area is strongly influenced by parameters such as counterion concentration and pH (buffered solutions allow control).

The effective area per headgroup can be calculated by equation 2.4, once the mean aggregation number (for that specific amphiphilic system) and the radius of the micellar aggregates (eg spherical) are known. Aggregation numbers can be determined by any of the following techniques: light scattering, diffusion studies, sedimentation by ultracentrifugation, X-ray and neutron scattering and fluorescence probes.

Stellenbosch University http://scholar.sun.ac.za

$$M = 4 \pi R^2 / a_0 \qquad \text{Eq. 2.4}$$

where

M = mean aggregation number

R = radius of the micelle

a_0 = effective area per headgroup (nm^2)

It has been determined by Israelachvili [6, 7] that for certain critical values of the packing parameter (the critical packing parameter), the amphiphilic molecules will have certain packing shapes (the critical packing shape), and micellar aggregates will adopt certain shapes / structures. See Table 2.3.

Surfactant	Critical Packing Parameter	Critical Packing Shape	Structure of Micelle
Single-chain surfactants with large headgroup areas	< 1/3	Cone	Spherical in aqueous media
Single-chained surfactants with small headgroup areas	1/3 - ½	Truncated Cone	Cylindrical in aqueous media
Double-chained surfactants/lipids with large head-group areas, flexible chains	½ - 1	Truncated Cone	Bilayers / vesicles in aqueous media
Double-chained surfactants/lipids with small head-group areas, fluid chains,	~ 1	Cylinder	Bilayers / vesicles in aqueous media
Double-chained surfactants/lipids with small head-group areas, fluid chains	> 1	Inverted Truncated Cone or Wedge	Reverse micelles in nonpolar media

Table 2-3 Critical Packing Parameters and Associated Shapes [from 6, 9]

Stellenbosch University http://scholar.sun.ac.za

Factors causing changes from one micellar structure to another can be summarised as follow:

- Factors affecting headgroup area
- Factors affecting chain packing
- Change in temperature
- Mixtures of surfactants

The second system that can also be used to describe surfactant self-assembly is based on the spontaneous curvature of the surfactant layer on the interface [9]. Here the critical factor is the preferred mean curvature of a surfactant film.

The mean curvature (H) at a point on the surface of a micellar aggregate is defined by the following equation:

$$H = \tfrac{1}{2}\,(1/R_1 + 1/R_2) \qquad \text{Eq 2.5}$$

where

R_1, R_2 = the radii of curvature in two perpendicular directions

This can be represented graphically as shown in Figure 2.1-1 below.

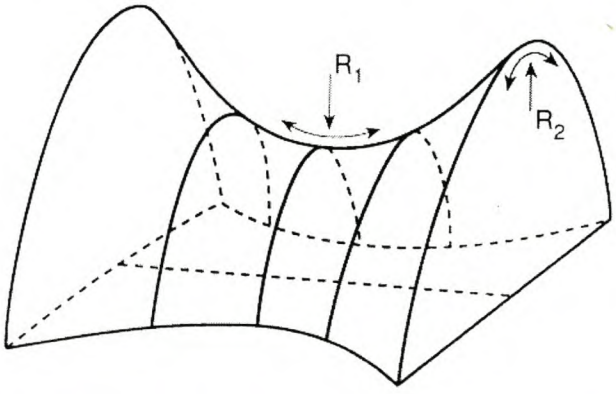

Figure 2.1-1 Graphical representation to define the mean curvature H at a point on the surface of a micellar aggregate [from reference 9, pg 16]

A sign can be assigned to the radii of curvature by defining a normal direction $\vec{n}$ for the surface. $\vec{n}$ is defined to be positive, pointing in the direction of the polar region. The curvature of inverted structures will therefore be negative.

Stellenbosch University http://scholar.sun.ac.za

Table 2.4 summarises the different shapes, R values and consequent H values of the different micellar aggregates

Shape of aggregate	R values	H values
Sphere	$R_1 = R_2 = R$	1/R
Cylinder	$R_1 = R$, $R_2 = \infty$	1/2R
Planar bilayer	$R_1 = R_2 = 0$	0*
Inverted structures	Negative values	Negative values

* in the case of a saddle shaped surface with $R_1 = -R_2$, H will also be = 0

Table 2-4 Preferred mean curvature of surfactant films and associated shapes [from ref. 9]

2.1.1.4 Self-assembly of bolaamphiphiles

A special case of Self-assembly is associated with the so-called bolaform amphiphiles. These amphiphiles contain hydrophilic moieties at the two ends of a short (6 – 16 C atoms) hydrocarbon spacer molecule. The name bola refers to the weapon used by South American indigenous peoples, consisting of two balls at the end of a piece of rope.

The noncovalent interactions possible between the hydrophilic / charged groups at the ends, combined with the hydrophobic interactions of the hydrocarbon spacers, leads to the Self-assembly of these bolaamphiphiles into monolayered sheets. These sheets interact to form multilayered helical fibers. Further, intermolecular hydrogen bonds and hydrophobic interactions also lead to the formation of solid-like supramolecular fibrous and tubular structures of several hundreds of micrometers in length [10]. Other interesting Self-assembly phenomena have been observed; during the supramolecular construction of bolaamphiphilic microtubes, vesicles are incorporated into the microtubules [11]. Further manipulation of the self-assembled structures can be performed by structural modifications (eg protonation) of the hydrophilic moieties [12].

Stellenbosch University http://scholar.sun.ac.za

2.1.2 Self-Assembly into Mesomorphic Phases

2.1.2.1 Liquid crystals, liquid crystalline - and mesomorphic phases

Liquid crystals were discovered in 1888 by Reinitzer, an Austrian botanist [13]. Lehman was the first to describe the properties of liquid crystallinity in 1889. He initially named them flowing crystals and finally, in 1900, used the name liquid crystals [14].

Liquid crystalline phases, mesomorphic phases or mesophases can be explained in terms of what they are not. It refers to a state of matter where the degree of order is between that of a solid crystal and that of an isotropic (or amorphous) liquid (see Figure 2.1-2 a). In solid crystals the degrees of long-range positional and orientational order is almost perfect, whereas in the liquid, or a gas, long-range order can be more accurately described as long-range disorder. In a mesophase there is a degree of order, but perfect long-range order does not exist [15]. Mesogens, the molecular moieties or groups that give rise to mesophases, can be classified as amphiphilic or non-amphiphilic (usually a rod- or disc-shaped geometry). A discussion of liquid crystalline polymers and block-co-polymer systems exhibiting mesoscopic behaviour will follow.

2.1.2.2 Classification of mesomorphic phases

Mesomorphic phases (as generated by mesogens) can be classified into three groups, according to their mechanism of formation. 1) **Thermotropic** mesophases are induced by a change in temperature, while 2) **lyotropic** mesophases are induced by addition of a solvent. 3) **Amphotropic** mesophases are induced by either a change in temperature, by addition of a solvent, or by both [15, 16, 18].

Thermotropic mesogens exhibit a range of mesophases, including nematic (see Figure 2.1-2 b), smectic (see Figure 2.1-2 c) and tilted smectic (smectic C, see Figure 2.1-2 c) phases.

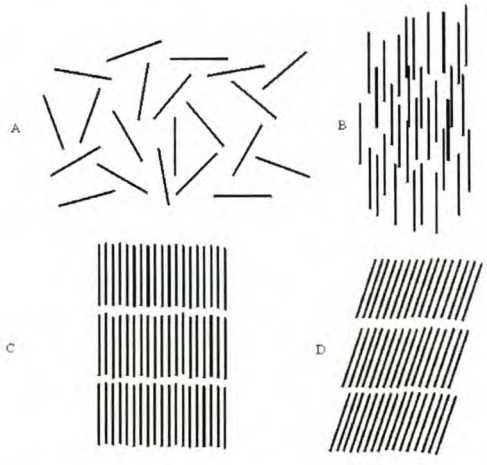

Figure 2.1-2 Molecular arrangement in various mesomorphic phases [Adapted from ref 15, pg. 5]

Stellenbosch University http://scholar.sun.ac.za

Binary systems (water / amphiphile) can generate various mesomorphic phases with either an increase in the concentration of water or amphiphile, i.e. the composition of the system must change, or a change in the temperature. For many single chain ionic amphiphiles a variation in concentration / composition is the most important way to induce phase changes [17]. As can be seen below in Figure 2.1-3, the phase boundaries are therefore almost vertical.

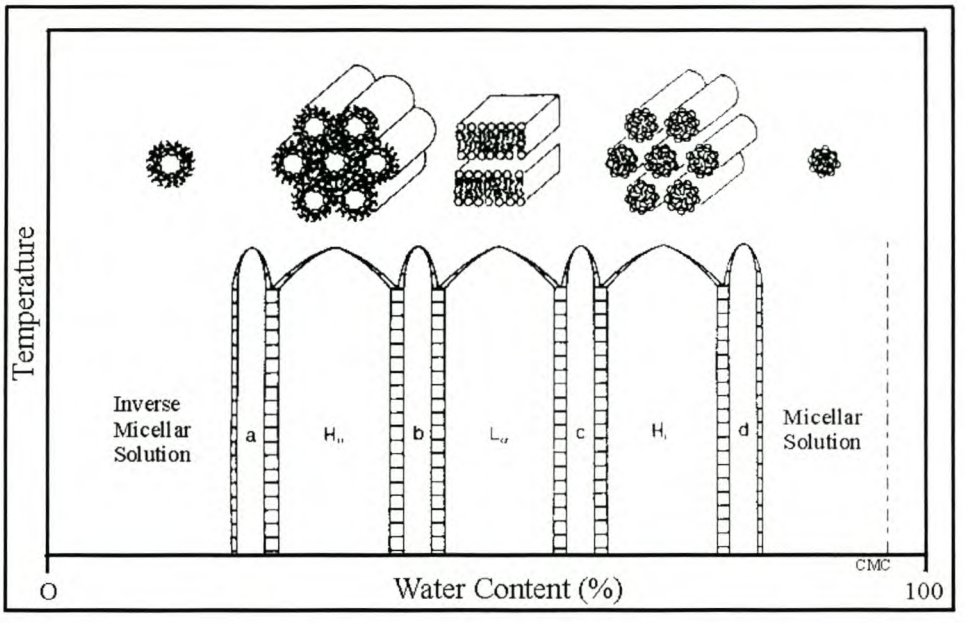

Figure 2.1-3 Schematic representation of the occurrence of various lyotropic mesophases [Figure taken from ref 17, pg. 9]

Some of the mesophases found in water / amphiphile systems (starting with the isotropic and micellar phases) are as follows:

- Cubic phase (also called "viscous isotropic phases" in earlier studies):

  I-phase, consists of micelles packed in a cubic array, occurring between micellar and hexagonal phases;

  Other cubic phases also exist, forming bicontinuous structures, occurring in the transition between hexagonal and lamellar phases (if formed at all by the particular surfactant system);

- Hexagonal array of rod-like structures, also called the "middle soap" phase:

  H_I-phase consists of rod-shaped micelles of indefinite length packed in a hexagonal array, and separated by a continuous water region;

- Lamellar phase (also known as the "neat soap" phase):

  L_α-phase, consists of surfactant molecules arranged in bilayers separated by water layers;

Stellenbosch University http://scholar.sun.ac.za

- Inverse hexagonal array of rod-like structures

  H_{II}-phase, the hydrocarbon chains occupy the spaces between the hexagonally packed cylinders of water (also of indefinite length).

Figure 2.1-3 gives only a general outline. Depending on the specific type of amphiphilic compound, such solutions could contain these (and other) mesophases.

Amphiphilic mesogens self-assemble into these structures. The basis of such self-assembly is similar to that of micelle formation. Unfavourable interactions of the amphiphilic groups with the solvent as well as favourable hydrophobic interactions drive the process of mesophase formation [19]. These mesophases are thermodynamically stable, and the phase found depends on the amphiphilic/mesogenic component concentration. Generally the order in a mesophase increases with increase in the amphiphile concentration.

As the mesogenic component concentration is increased, phase transitions will occur. Kekicheff and co-workers showed [20-23] that even in the case of a very simple amphiphilic compound such as sodium dodecyl sulphate (SDS) a number of intermediate mesophases exist in the concentration region situated between the ordered hexagonal and lamellar phases. These structures, which include a tetragonal phase, a cubic phase, a rhombohedral phase and a two-dimensional monoclinic phase, occurring over very narrow concentration ranges (< 1 %), are suggested to be necessary for the system to change from a system of high curvature (cylinders) to that of zero curvature (bilayers).

The observed transitional / intermediate states occur through the deformation of cylinders (the hexagonal phase) into ribbons (two dimensional monoclinic phase), which then merge (side and length wise - rhombohedral phase). Continual deformation leads to a cubic phase, which finally produces the lamellar phase (which initially still contains some defects). These changes were ascribed to a constant change in the mean curvature of the interfaces.

Certain polymers also exhibit liquid crystalline behaviour due to mesogenic groups present in either the main chain of the polymer, the side chain or both. The mesogens can be disc-shaped, rod-like or amphiphilic in nature. Poly (hydroxynapthoic acid) is a good example of a rigid rod-like main chain, non-amphiphilic liquid crystalline polymer [24].

Block copolymers phase separate on a mesoscopic length scale due to unfavourable interactions, providing the basis for the formation of mesomorphic phases [25].

Stellenbosch University http://scholar.sun.ac.za

2.1.3 Emulsions and Microemulsions

The two types of emulsions that are relevant to the present study can be differentiated on a thermodynamic basis.

Macroemulsions (commonly known as emulsions) can be defined as thermodynamically metastable or unstable, turbid systems, containing oil (apolar) and water (polar) components, and a surface-active agent / emulsifier (stabilising the interface between the two phases) which could be monomeric or polymeric in nature, or even particles adsorbed on the interface. Usually the emulsifier concentration is very low (< 1%). The formation of a macroemulsion requires either chemical or mechanical energy. Due to its unstable state, the final fate of a macroemulsion is separation into two separate equilibrium phases [26, 9].

Microemulsions can be defined as thermodynamically stable, isotropic, colloidal dispersions containing large amounts of oil (apolar) and water (polar) components. These two components are thermodynamically stabilised by an amphiphilic component. The presence of the amphiphilic component in various concentrations will cause the system to form any of the following microemulsion structures spontaneously: oil in water (O/W), water in oil (W/O) or bicontinuous [27, 28, 9].

Microemulsions usually also contain a so-called co-surfactant, usually a short chain aliphatic alcohol such as butanol, pentanol or hexanol. Co-surfactants are, as a rule, always present in microemulsions containing anionic surfactants, but not necessarily in microemulsions containing more hydrophobic non-ionic amphiphiles. The purpose of the co-surfactant is to increase the effective surfactant number in the interface (with their hydrocarbon tails contributing to the hydrocarbon volume) while the alcohol group displaces apolar groups at the polar-apolar interface. This will affect the spontaneous curvature of the interface, and therefore also the stability and the structures formed in a microemulsion system.

Microemulsions form various equilibrium phases, as described by Winsor in 1948 [29]. He described the following

Type I: in equilibrium with excess oil

Type II: in equilibrium with excess water

Stellenbosch University http://scholar.sun.ac.za

Type III: in equilibrium with both water and oil excess phases

Type IV: single phase containing no excess / free oil or water layers

These four equilibrium phases are schematically represented in Figure 2.1-4.

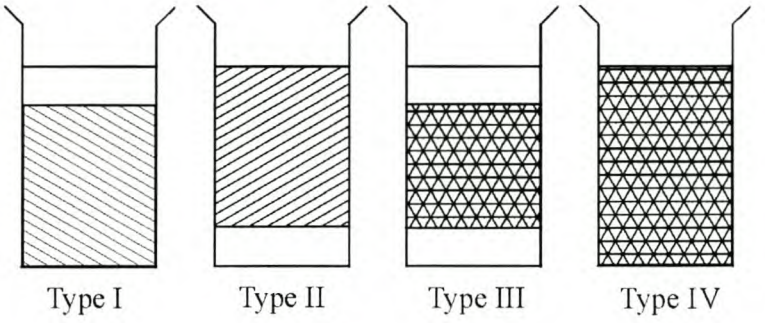

Figure 2.1-4 Winsor equilibrium phases for microemulsions [Taken from Ref 28, pg. 218].

2.1.4 Polyelectrolyte-Surfactant Complexes

2.1.4.1 Polyelectrolyte-surfactant complexes in solution

The aggregation and formation of complexes from polyelectrolytes and surfactants have been known for some time [30, 31, 32]. The first systems to be studied were probably the interactions between proteins and surfactants in the 1930's [30]. Since then, research has focused on two broad areas of interest, namely interactions between uncharged polyelectrolytes and charged surfactants and the interactions between charged polyelectrolytes and surfactants of opposite charge. In certain cases micelles of mixed nature, i.e. consisting of charged and uncharged surfactants, were also utilised [33]). Attention in this work will be devoted mainly to the field of interactions between oppositely charged species.

The combination of polyelectrolytes and surfactants of opposite charge might lead to soluble or insoluble complexes, depending on the chosen charge balance and stoichiometry of the systems (polyelectrolytes and surfactants of like charge show only weak interaction). Once again, the association of surfactants with an oppositely charged polyelectrolyte can be discussed by making use of the surface tension of such a solution, as depicted in Figure 2.1-5. Since the surfactant is very active at the air-water interface, and the polyelectrolyte fairly inactive, making use of surface tension should provide information on the new species formed in solution.

Stellenbosch University http://scholar.sun.ac.za

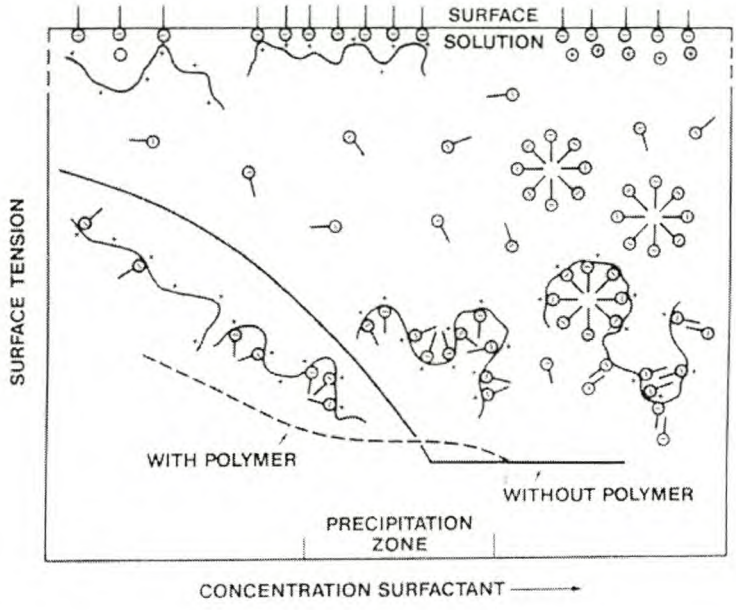

Figure 2.1-5 Conditions in bulk and surface of a solution containing a polyelectrolyte (fixed concentration) and surfactant [taken from ref. 34, pg 175].

The influence of the presence of the polyelectrolyte can already be seen at very low concentrations of surfactant. The surface tension of the solution is much lower than would be the case for surfactant only, indicating the formation of a very active surface species. This species is depicted on the far left side of Figure 2.1-5, where the polyelectrolyte shows some interaction with the surfactant molecules at the air-water interface. As the surfactant concentration is increased, at the air-water interface as well as in the solution, higher / more interaction is seen with the polyelectrolyte. The surface tension is still lower than for the surfactant-only system. As the reaction system approaches 1:1 stoichiometry the polyelectrolyte-surfactant complex will start to precipitate, first seen as turbidity in the solution. A further lowering of the surface tension is also observed. The surface tension now begins to approach values similar as those found in a surfactant-only system after the CMC. As the surfactant concentration is increased beyond the point of charge neutralisation, the surface tension has the same values as found for a surfactant-only system. This would indicate that all polyelectrolyte molecules are to be found in the solution in interactions with surfactants, and none at the air-water interface. The excess surfactant can now be found at the air-water interface, behaving as surfactants in a solution with a concentration higher than that of the CMC. With a further increase in the surfactant concentration, the precipitation zone is crossed, and the polyelectrolyte-surfactant complex precipitates are re-dissolved (according to the "beads-on-a-string" model as discussed below). The surface tension values now correspond to those of a surfactant-only system.

In general, most of the investigations concerning the surfactant binding to polymers were performed at low polymer concentrations, while phase equilibria of such systems were studied at higher

Stellenbosch University http://scholar.sun.ac.za

concentrations [35]. Investigations into the binding process were performed by Shinoda in the early 1970's [32], followed by a series of studies by Kwak et al. from 1980 to 1985 [36-39]. Results showed that the aggregation process is a highly cooperative process, i.e. the process takes place over a very narrow surfactant concentration range and is driven not only by electrostatic interactions, but also by the interactions of the hydrophobic alkyl tails of the surfactant associating. The degree of binding ß (ß corresponds to the fraction of available charges on the polyelectrolyte neutralised by the binding of surfactant ions) increases very sharply, and levels off at values close to one. Furthermore, it was confirmed that the process commenced at concentrations much lower than the critical micelle concentration (CMC) of the surfactant, at the so-called critical aggregation concentration (CAC). The CAC can be defined as the concentration where the aggregation of surfactant and polyelectrolyte can first be detected. This concept was initially described by Jones in two papers in the late 1960's [40, 41]. The addition of salt to a reaction system decreases the CAC, indicating higher shielding by the added ions and reduced interaction between the polyelectrolyte and surfactant [4]. A later study by Ohbu showed that for cationic cellulose / SDS systems, binding already occurred at very low SDS concentrations and that ß at SDS concentrations of only 5 % the value of the CMC was already 0.5 [42].

Factors affecting complex formation differ for polyelectrolytes and surfactants [43].

Properties of the polyelectrolyte which affect complex formation are:

- Linear charge density E (generally an increase in E causes stronger interactions)
- Hydrophobicity of the polymer (interaction enhanced with increasing hydrophobicity)
- Flexibility of the polyelectrolyte backbone
- Length of the polyelectrolyte chain

A study by Shirahama and co-workers [44] focussing on the effect of the size of the polyelectrolyte on the binding process indicated that both the CAC and the cooperativity of the binding process are influenced by the molecular weight of the polyelectrolyte. The CAC increases, while the cooperativity decreases. This was attributed to the effect of a change in the number of binding sites (charges) due to a change in the length of the polyelectrolyte.

Stellenbosch University http://scholar.sun.ac.za

Properties of the surfactant that affect the complexation process are:

- Geometry of the surfactant
- Alkyl chain length (i.e. hydrophobicity)
- Nature of the counterion
- Concentration of the surfactant (above or below the CMC)

Precipitation of the complex is observed at a ß-value of 1, since the binding of the surfactant would remove all charges responsible for the stabilisation / solvation of the polyelectrolyte. The solid state properties of these one to one complexes will be discussed in more detail below. As the surfactant concentration is increased, the complex is re-solubilised. This takes place at ß-values much higher than unity (3 in the case of the Ohbu study [42]), and probably takes place following the so-called "beads-on-a-string" model of polyelectrolyte-surfactant interaction. This model for such systems in solution was already proposed in 1974 by Shirahama [45]. Here the excess surfactant will interact with the bound surfactant, forming micelle-like structures in close association with the polyelectrolyte (resembling the beads on a string), causing the total aggregate to be solubilised again. The whole complex is therefore actually converted into a polyelectrolyte of opposite charge (compared to the original polyelectrolyte). In a later study, Cao et al [46] showed that interactions of a hydrophobically modified cationic polyelectrolyte with SDS at molar ratios above 1 influenced the viscosity of the solutions drastically. They found that at molar ratios of approximately 2.2 to 2.3 there was a sharp increase in the viscosity, probably indicating intermolecular aggregation of polymer chains via hydrophobic interactions of SDS molecules.

Currently investigations into polyelectrolyte-surfactant interactions in solution focus on such factors as chemical structures and concentrations of the polyelectrolyte and surfactant, ionic strength and temperature of the reaction solutions. The techniques used to investigate these can be divided into classical physical methods and spectroscopical methods. Physical methods would include conductance and potentiometry, surface tension, viscometry and calorimetry, amongst others. Spectroscopic methods include techniques such as nuclear magnetic resonance spectroscopy (NMR), electron spin resonance spectroscopy (ESR), infra-red (IR) and Raman spectroscopy, light scattering, UV and fluorescence spectroscopy, microscopy and finally neutron and small angle X-ray scattering (SANS and SAXS) [43].

Current studies also include investigations of natural polyelectrolyte systems, and the interactions between surfactants and polysaccharides [47], polypeptides [48] and proteins [49].

Stellenbosch University http://scholar.sun.ac.za

The combination of polyelectrolytes and surfactants has been extensively used in a wide variety of applications, including the production of photographic film emulsions, cosmetics, pharmaceutical applications, paper manufacturing, mining applications, as rheology modifiers and various food science applications [50]. Other applications that have been investigated include the utilisation of complexes from lipids and polyelectrolytes as membrane mimicking agents [51]. New trends in similar systems, where electrostatic interactions between oppositely charged polyelectrolytes and other charged components (proteins/enzymes, charged particles) are utilised, are finding application in biochemical and biomedical research and possible drug targeting studies [52].

2.1.4.2 Polyelectrolyte-surfactant complexes as new mesoscopically organised materials

Probably the first investigation into the solid state structure of polyelectrolyte-surfactant complexes was performed by Harada and Nozakura in 1984 [53a]. They investigated the structure of dried, 1:1 stoichiometry complexes by means of TEM. Ujiie and co-workers investigated the formation of ion-surfactant and polyelectrolyte-surfactant complexes in the early 1990's, tentatively proposing structures for the formed complexes [53b]. Kunitake et al [51] and Okahata et al [54] investigated the synthesis and application of bilayered polyelectrolyte-lipid complexes as biological membrane mimicking systems.

It was only 10 years after the first investigations that the solid-state structure of such complexes was fully elucidated for the first time, by Antonietti and co-workers [55]. The field of solid polyelectrolyte-surfactant complexes and resulting morphologies from such materials is therefore still a fairly new area of research.

Various groups have investigated the structure and behaviour of crosslinked polyelectrolyte gels with surfactants [56, 57]. The phases formed within such crosslinked gels, as well as the influence of the surfactant concentration in the gel, were investigated by means of SAXS. As surfactant is removed from the gel (i.e. the concentration internally lowered) the gel undergoes collapse. The mechanism of collapse has been studied extensively. Evmenenko and co-workers [58] studied the formation of self-assembled structures in carrageenans (water-soluble sulfonated polysaccharides). Although these polyelectrolyte systems are not crosslinked, they induce gelation in solutions. Gelation of these naturally occurring polyelectrolytes in the presence of surfactants leads to the formation of Self-assembled structures in the gel (similar to micellization in solution).

Stellenbosch University http://scholar.sun.ac.za

In the case of uncrosslinked polyelectrolytes, complexes can be prepared from inexpensive or easily available starting materials, to yield mesoscopically ordered materials

Such complexes can be synthesised using either charge coupling or hydrogen bonding between the two components. Hydrogen bonding assisted complex formation has not been the subject of this work, and for further information the reader is referred to references 59 and 60 and the references within [59, 60].

In the case of charge coupling, the mechanism proposed for the facile production of highly ordered materials can be explained in terms of the high cooperativity seen in the behaviour and formation of complexes in solution. Electrostatic interactions between the charged moieties a well as hydrophobic interactions between the polymer backbones and alkyl tails of the surfactant are the main driving forces in the self-assembling formation of these well-defined complexes [61]. Figure 2.1-6 provides a schematic representation of the initial complex formation.

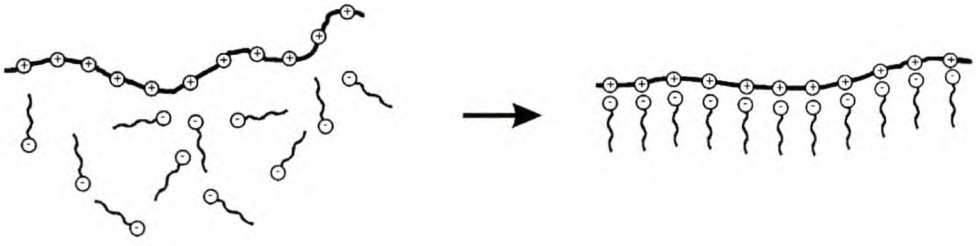

Figure 2.1-6 Schematic representation of the formation of polyelectrolyte-surfactant complex from oppositely charged components.

Once the complex has been synthesized, the system has no well-defined mesomorphic structure. It is only after solvent casting that a mesoscopically ordered structure is obtained. This is due to the very high glass transitions of the ionic layers, which inhibit organisation of the structures during formation of the complex [62]. After casting, depending on the components used, films obtained can be flexible, of high homogeneity, good optical quality and often have high mechanical stability.

Since the units of construction can be seen as a line of ion pairs (the one dimensional array of charges / binding sites on the polymeric backbone and the surfactant head groups) and a continuous hydrophobic alkyl tail section, it could be expected (in hindsight!) that demixing and micro - or rather nano in this case - phase separation would take place in the solid state, and a connected mesophase will form [63]. The characteristic length of these mesophases will be limited by the surfactant geometry. The lengthscale ξ of the phase separation cannot be more than twice the length of a fully stretched alkyl chain; it will be between 2 – 8 nm, depending on the nature of the surfactant [64].

Stellenbosch University http://scholar.sun.ac.za

These complexes have been investigated by various methods, including optical microscopy, thermal analyses [69], mechanical analyses [70], dielectric analyses [71], NMR analyses [64], and X-ray analyses [for example see references 57, 62 and 67] (both Wide Angle X-ray Scattering (WAXS) and Small Angle X-ray Scattering (SAXS)). The actual structure of the phase is dependent on a wide variety of factors, including the charge density of the polyelectrolyte, ratio of the volume fractions of the alkyl versus the ionic subphases, the absolute interface energy (as determined by the amount of surfactant molecules bound per unit volume) and the spontaneous curvature of the interface (as found in surfactant-only systems) [66, 63]. In the case of crosslinked polyelectrolyte gels, for example, it was found that with longer alkyl chains lengths, lower charge density and lower hydrophobicity of the polyelectrolyte chain is needed to form highly ordered structures [65]. Since these factors do not operate independently from each other, it is not possible at this stage to predict the specific phase structure that a complex will hold before analysis of the actual synthesised complex. The determination of the fine phase structure, making use of rigorous mathematical treatment of small angle X-ray data, is a separate field of study [65], and not discussed in this introduction to polyelectrolyte-surfactant complexes. These studies make use of routes of data evaluation originally developed by Perret and Ruland [73] for the structural analyses of mesostructured materials by means of x-ray analysis.

Phase structures that have been reported include hexagonally ordered cylindrical phases (including normal, reverse and undulating cylindrical phases [55]), cubic and lamellar (normal as well as so-called perforated layer (mattress) and egg-carton phases [63, 64, 67]).

Investigation of complexes by wide angle X-ray analyses shows that the complexes are non-crystalline on a local length scale, i.e. the surfactants side chains exhibit liquid or liquid crystalline type arrangements. If the surfactant chain length is increased to above 16 C atoms, this could lead to side chain crystallinity.

Antonietti and co-workers using the results of SAXS analysis combined with mathematical treatment (a rather tedious and skilled technique) of the data showed that the various complexes form a variety of phases. A study performed by Antonietti and co-workers [68] on the effect of changing (but not mixing) the surfactant tail lengths showed that due to mismatch of local surfactant geometry and the phase morphology, undulations develop on the mainly lamellar phase morphology [68, 63]. When the surfactant chain length is increased to 20, the proposed structure of this complex can be described as a perforated layer phase, where the ionic layer is regularly pierced by the alkyl layer. Similar frustration effects were also observed in the case of an hexagonal phase, yielding an ionic phase consisting of undulating cylinders [55]. Such mismatching could be

Stellenbosch University http://scholar.sun.ac.za

removed to a large extent, as was shown in the case of the addition of cholesterol to a biomembrane analogue complex (naturally occurring soybean lecithin complexed with polydiallyldimethyl-ammoniumchloride) [69]. The added cholesterol has an ordering influence on the original undulating bilayer structure, causing the undulation to almost disappear at 10 weight % cholesterol. At higher cholesterol concentrations (30 weight %) the system demixes on a macroscopic scale.

Further insight into the physical properties, molecular dynamics and relaxation processes of various polyelectrolyte-surfactant complexes have been provided by mechanical and dielectrical analyses [70], conductivity measurements [71] and high resolution NMR investigations [64].

New approaches to and applications of polyelectrolyte-surfactant complexes include the use of conducting polyelectrolytes, using mesogenic surfactant molecules [61], making use of the ordering of the surfactant molecules for various electrical and electronic applications (e.g. to build oriented nanowires [72], fluorescent complexes [74, 75] and various drug targeting studies [76, 77]. Fluorinated surfactants have been combined with polyelectrolytes, to provide new materials with ultra low surface energies [e.g. 78, 79].

Reactions performed in polyelectrolyte-surfactant complexes are an area that is very relevant to this work, but have not received much attention from researchers. Crosslinked polyelectrolyte gels in combination with surfactant have also been applied for the production of metal colloidal particles within the organised structures formed [80]. In non-crosslinked polyelectrolyte systems, Dreja and Lennartz [81] have used a polymerisable surfactant to form a complex with a polyelectrolyte. During polymerisation with γ-radiation, degradation of the monomer (the surfactant) was assumed to be the preferred reaction pathway, rather than the formation of a polyelectrolyte-polyelectrolyte complex. In another study where reactions in polyelectrolyte-surfactant complexes were studied, Kwak et al described a system where phase separation could be induced photochemically [82]. Nuyken and co-workers used a photolabile diazosulfonate chromophore as surfactant in a later study to investigate the stability and structure of the formed polyelectrolyte-surfactant complexes [83]. They found that ultraviolet (UV) irradiation led to the loss of ionic interactions, with the degradation of the photolabile compound taking place.

This concludes the investigation into the theoretical background for this study. The next section will be devoted to a review of the history of structure-directing reactions.

Stellenbosch University http://scholar.sun.ac.za

2.2 Historical – Structure-directing Reactions

2.2.1 Background

Over the last three decades, a variety of experiments have been carried out to perform polymerization reactions in organized media [84]. One aim is to imprint the organized structure onto the polymer to be formed, preserving the shape imprint of the organized state after the removal of the surfactant / organised medium / template.

In principle, it is possible to imprint the organised structure into a polymeric structure, and has been achieved when covalently bonded structured materials (such as membranes and inorganic polymers) were used as templates (see Section 2.2.2).

In the case of more dynamic, non-covalently bonded templates (i.e. templates that are mesoscopically ordered and rely on the principle of Self-assembly to form), this proved to be a more difficult task. In 1992 it was already possible to imprint the organised structure of a labile template into an inorganic polymer (see Section 2.2.3.1). Up to date, it has not been possible to polymerise organic polymers in such "soft" organized phases and to preserve a 1 : 1 –copy of the template structure. This is due to the influence of the growing polymer chain on the liquid crystalline templating phase, causing disruption of the templating phase and consequent phase separation into a thermodynamic stable polymer particle and templating phase [85].

Another motivation to carry out polymerisation in organized media is to make "hybrids", where the embedded polymer significantly contributes to the performance of the overall system, e.g. via its ductility, the ability for stress dissipation or the stability lent by the polymer.

The main areas of structure-directing polymerisation (SDP) reactions have been divided as shown in Fig 2.2-1

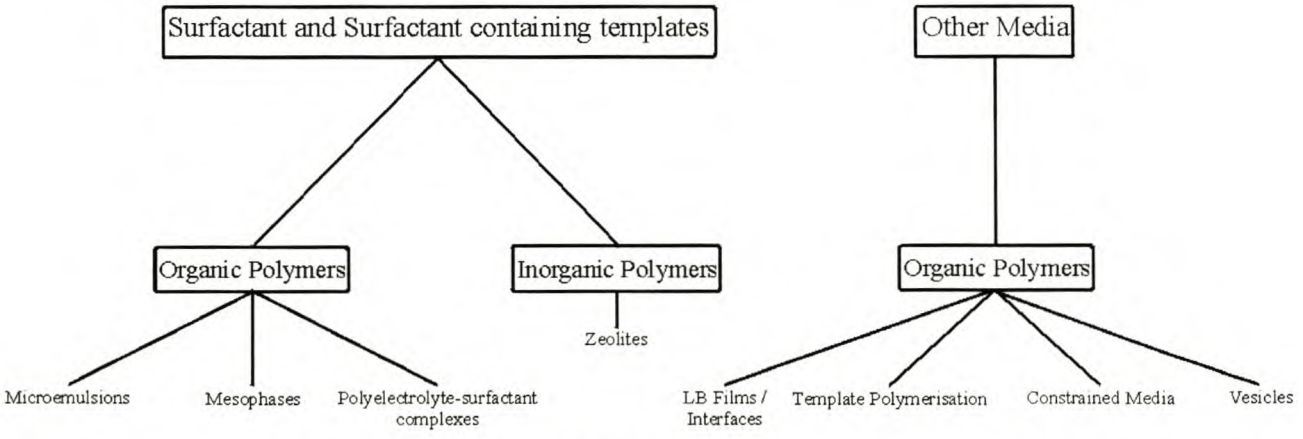

Figure 2.2-1 An overview of structure-directing polymerisation reaction – classification of the areas of study investigated

Stellenbosch University http://scholar.sun.ac.za

Earlier reaction schemes used in structure-directing polymerisation can be divided into two main areas of study as follows: 1) surfactant and surfactant-containing templates (SCT) and 2) other organic media. Since the focus of the present work is mainly on surfactant-containing templates (SCT), only a brief mention will be made of the latter.

2.2.2 Structure-directing Polymerisation Reactions in Other Media

This section contains very brief summaries of some areas of research in which other media (than surfactants) are used to direct the structure of organic polymers during synthesis.

2.2.2.1 Polymerisation at interfaces

The preparation of ultrathin polymer films with controlled thickness and molecular orientation can be achieved by any of the following techniques: Langmuir-Blodgett deposition, vacuum deposition and self-assembly of monomers [86-88]. A further approach that has been utilised to form a polymer at an interface was the production of polypyrrole on the interface between an aqueous solution and lipid self-assembled tubules [89]. Discrete strings of polymer were formed, following very exactly the sharp edge interface of the twisted lipid structure.

2.2.2.2 Polymerisation in Constrained Media

In this field of directed synthesis the molecular architecture and dimensionality of the space in which polymerisation reactions may take place are taken into account, rather than only the nature of the reactive species [90].

Low dimensional inclusion polymerisation includes polymerisation in organic hosts (as first performed by Clasen in 1956 in channels of thiourea [91]) as well as in inorganic hosts, such as MCM 41 [92, 93]. Two-dimensional inclusion polymerisation can take place within either layered inorganic structures (such as clays) [94] or layered organic structures (e.g. lamellar membrane structures) [95].

2.2.2.3 Template Polymerisation

This process is well known and characterised in biological systems, where the formation of DNA and RNA is regulated by an enzymatic template polymerisation process. Here one string of the

Stellenbosch University http://scholar.sun.ac.za

DNA molecule acts as a template onto which monomer units are fitted (by hydrogen bonding matching) before they are joined to form a daughter molecule, a RNA molecule. Template polymerisation can therefore be defined as the process of the conversion of monomers into a complementary / daughter macromolecule in the vicinity of the original polymer, which acts as a macromolecular template or so-called parent molecule. The template will affect the formation of the daughter in respect to kinetics of formation, and structural aspects (such as molecular weight distribution and stereoregularity).

Most recently, template polymerisation has been used to polymerise various acrylate monomers [96, 97] in the presence of templates such as poly(allylamine) hydrochloride and poly (N-vinylpyrrolidone). In a biomimetic approach, the polymerisation of complementary 5'-acryloyladenosine (in the presence of non-complementary 5'-acryloyluridine) using poly(5'-acryloyluridine) as template was achieved [98].

2.2.2.4 Polymerisation in Vesicles

Initial investigations into polymerisation in vesicles concentrated on the formation of bilayered vesicles with polymerisable amphiphiles / vesicle forming monomers [99]. Recent work by German and co-workers [100, 101] has shown that polymerisation of monomers within bilayers of vesicles yields interesting parachute-like vesicle-polymer hybrid particles. This morphology was ascribed to phase separation of the polymer from the vesicle, but with the polymeric particle still attached to the parental templating bilayered vesicle.

2.2.3 Structure-directing Polymerisations in Surfactant Media

This aspect of structure-directing polymerisations can be divided into two main areas, namely organic and inorganic polymerisations. The latter will be discussed first, since the success in the area of inorganic polymerisation was partly the motivation for the original investigation undertaken for this work.

2.2.3.1 Structure-directing Polymerisations in Surfactant Media for Inorganic Polymers

The meaningful advance in the field of inorganic template synthesis came in 1992, with the publication of two papers by Kresge et al, describing the synthesis and characterisation of a novel

Stellenbosch University http://scholar.sun.ac.za

synthetic, inorganic, structured compound, MCM-41 [102, 103] for which they proposed a surfactant liquid crystal templating mechanism.

This synthetic compound, with regular, well defined channel systems, gave uniform mesopores in the 1.5 nm - >10 nm range. Since zeolites find wide application in, amongst other processes, catalysis, the production of materials with zeolite-like catalytic performances but with pore sizes larger than the previously attainable 1.3 nm made this development very attractive to a variety of industries.

At this stage it is considered appropriate to introduce an outline / framework, similar to that used by Göltner and Antonietti [104], for the production of mesoporous inorganic solids. The synthesis conditions used for the production of mesoporous inorganic materials can be divided into two distinct types:

- Low concentration surfactant templating
- True liquid crystalline templating

The initial results obtained by Kresge et al [102, 103] were obtained by making use of low concentration surfactant-assisted hydrothermal synthesis.

Three major pathways / routes for the synthesis of mesoporous inorganic solids can be described:

- electrostatic charge-density matching (between the inorganic polymer P^- and the surfactant S^+)
- reverse charge matching (P^+ and S^-)
- counterion mediated synthesis ($S^+ X^- P^+$ with X^- = halide ion or $S^- M^+ P^-$ with M^+ = metal ion)

In the low concentration surfactant templating pathway the surfactant (at low concentration, above the CMC but below the transition to a liquid crystalline phase), together with organic auxiliary hydrocarbon reagents (such as alkylated benzenes) provide the correct relative volumes, interface area and spontaneous curvature of the interface, to form the sought after phase in the final product. Syntheses of modified mesostructures were undertaken, yielding functionalised, and even bi-functionalised (for catalysis and separation concurrently), mesoporous inorganic compounds [105].

Stellenbosch University http://scholar.sun.ac.za

In another, more recent approach to the templating of inorganic porous materials, inverse emulsions were used as templates [106]. Here the emulsion droplets serve as a template. The size of the templating droplets can be varied to provide macroporous inorganic materials with pore sizes ranging from 50 nm to several micrometers.

In the case of true liquid crystalline templating for the production of regular mesoporous inorganic structures, Attard et al [107] performed syntheses in bulk lyotropic liquid crystalline phases of non-ionic surfactants. The inorganic precursors were contained within the aqueous domains of the mesophase, and led to the retention of the original mesophase in the final inorganic product. The degree of order is directly related to that found in the original surfactant mesophase, yielding a true 1 : 1 copy of the original.

Other systems producing lyotropic phases, such as amphiphilic block copolymers, were recently used to produce templated inorganic mesoporous solids [108, 109]. With this direct templating route, the only requirement is that the template has the ability to form stable, pre-organised aggregates, in the presence of the reactants [66].

2.2.3.2 Structure-directing Polymerisations in Surfactant Media for Organic Polymers

2.2.3.2.1 Polymerisation in Microemulsion

In 1980 Stoffer and Bone performed a series of polymerisations in water-in-oil microemulsions [110-112]. This initiated a considerable research effort in this field. These polymerisations were carried out using methyl acrylate and methyl methacrylate (continuous phase with the co-surfactant pentanol), and resulting structures were investigated by means of scanning electron microscopy (SEM).

Jayakrishnan and Shah performed a thorough investigation of oil-in-water microemulsion polymerisations using vinyl monomers [113]. Atik and Thomas carried out such a study in 1981, but performed the polymerisation using styrene as the monomer close to the region of existence of normal emulsions [114]. Already in these early studies the structures obtained from the microemulsions were of interest.

Candau and co-workers were the first to publish a report on polymerisation in an inverse microemulsion. This was done with toluene as the continuous phase, and water / acrylamide mixtures the dispersed inverse phase [115, 116]. Here polymers of high molecular weight (> than

Stellenbosch University http://scholar.sun.ac.za

10^6) and small particle size (< 20 nm) were produced. As the microemulsion was stable, no co-surfactant was used. The monomer probably acted as co-surfactant.

The instability of certain systems became an early point of discussion and study. It was found that the presence of, for instance, polystyrene, or even short oligomers, had a significant effect on styrene microemulsions [117]. The instability and consequent demixing was described by Gan and Chew in 1984 as follows: " the microemulsion instability must be referred to the complex effect of entropic increase in free energy due to the conformation limitations and / or the limited solubilities of polymer / water and polymer / co-surfactant." [118].

Various other studies were performed, investigating various factors of the microemulsion systems (stability, electrolyte influence etc. [119]), kinetics of polymerisation in a microemulsion [120, 121], and size control of the obtained latices [122]. It was only in 1988 that Haque and Qutubuddin published a paper showing that it was possible to obtain novel three-dimensionally organised materials from one-step microemulsion polymerisations [123]. This was in the same year that Strey and co-workers, using freeze fracture electron microscopy [27], established the microstructure of various microemulsion systems. In 1989 Qutubuddin et al reported on an extensive study of the polymerisation of styrene in a bicontinuous microemulsion [26] to produce extended porous materials.

Menger and co-workers prepared continuous structured polymeric materials from microemulsions, and characterised the materials in terms of morphology and surface area [124]. They made use of the term "water pools" to describe the porous regions produced in the materials due to the influence of the parental microemulsion.

Cheung and co-workers then produced a series of papers [125-128] describing the results of investigations into the formation of microporous materials produced from microemulsion polymerisations. (Note: According to reference 154, the IUPAC definitions for micropores, mesopores and macropores are: micropores –smaller than 2 nm; mesopores – between 2 and 100 nm; macropores – larger than 100 nm. The term most often used (albeit incorrectly) in literature is microporous, usually referring to macroporous systems, and this has also been applied in this work.)

Photopolymerisation was used to produce these microporous materials, since Haque et al reported difficulties with phase separation during thermal polymerisation. Since photopolymerisation can be carried out at low temperatures, no problems were encountered with attaining assembled structural equilibrium prior to polymerisation. Photopolymerisation also proceeded more rapidly than thermal polymerisation, which allowed polymerisation to proceed beyond the point where phase separation

Stellenbosch University http://scholar.sun.ac.za

would significantly alter the microstructure of the formed polymeric material. They obtained microporous [126] and fibrous structures [125] in Winsor IV microemulsions. Various investigations were then carried out in Winsor IV microemulsion systems with a variety of monomers (eg methyl methacrylate (MMA), acrylic acid (AA), ethyleneglycoldimethacrylate (EGDMA)). Results of this route of synthesis indicated that it would be possible to form microporous membranes, with the possibility, under certain circumstances, to move to surfactant-free systems. In reference 128 they produced polymeric microporous membranes from both surfactant-containing and surfactant-free microemulsions. It was evident that the structure of the resulting materials was directed by the composition of the microemulsions, with the microemulsions serving as a rudimentary template for the reactions.

Gan, Chew and co-workers published their first paper on the production of microporous polymeric solids from bicontinuous microemulsions in 1994 [129]. From the monomers methyl methacrylate MMA, EGDMA, 2-hydroxyethylmethacrylate (HEMA) and a reactive surfactant sodium-11-(N-acrylamido)-undecanoate, they produced open-celled three dimensional microporous structures of transparent polymeric solids. This indicated that the microemulsion directed the structure of the polymeric material produced. They showed in later publications that the morphology of the materials produced was strongly dependent on the composition of the microemulsion, i.e. the water content, ratio of monomers [130] surfactant content [131], chain length [132], ratio of chain lengths of the surfactants [133] and mixtures of non-polymerisable and polymerisable surfactants [134]. The morphology of the microporous materials from the bicontinuous microemulsions seemed to consist of incompletely coalesced spherical aggregates [135]. Since there was a marked difference in the morphology of samples obtained from various locations in the reaction vessels (e.g. top or bottom) during most of their studies, this indicated that the structures obtained were not the results of a thermodynamic equilibrium state in the reaction system, but rather of a kinetic state frozen in by polymerisation [136].

Antonietti and Hentze showed conclusively that a direct copy of the microemulsion templating phase could not be obtained using microemulsion polymerisation [137]. Making use of optical microscopy, rheology and electron microscopy they showed that the polymer chains form spherical aggregates already in the early stages of the reaction, which lead to the formation of multilamellar vesicles. As the reaction consumes monomer, and changes the composition of the microemulsion in terms of monomer and polymer content, lyotropic phases appear. The final structure, and connectivity in the microporous systems, was indirectly influenced by the presence of these phases. The presence of the growing polymer chain had the further effect of thermodynamically

Stellenbosch University http://scholar.sun.ac.za

destabilising the template / structured liquid wherein it is formed [66], causing the structural balance in the microphase separated microemulsion template to be modified [104].

Antonietti and Hentze then investigated the influence of the surfactant counterion used in microemulsion formation, and the influence this variation had on the final morphological features of the obtained polymeric products [137]. This idea was further developed in the polymerisation in lyotropic phases, and will be discussed in Section 2.2.3.2.2.

Cheung and co-workers summarised polymerisations in microemulsions as follow: "The results of this study indicate the possibility of forming porous polymeric solids having specifically tailored morphology and microstructure by the polymerisation of monomer containing microemulsions." [138]. It was, however, not possible to produce a one to one copy of the microemulsion template.

Other non-templating applications have been developed. Gan and co-workers showed that ion-containing membranes could be prepared by microemulsion polymerisation [139]. Other interesting applications include the production of very long inorganic nanowires ($CaSO_4$ > 100 μm) from water-in-oil microemulsions [140]. Pileni and co-workers have also shown that, through the use of colloidal assemblies, it is possible to control the shape of metallic nanoparticles [141, 142].

2.2.3.2.2 Polymerisations in Lyotropic Mesophases

In general, all work in this area of polymerisations can be classified into the three following areas (as discussed in [143]):

- Polymerisation of lyotropic structures / aggregates of polymerisable surfactants
- Polymerisation of organic monomers in lyotropic structures / aggregates of non-polymerisable surfactants
- Co-polymerisation of organic monomers with lyotropic structures / aggregates of polymerisable surfactants

In earlier investigations [eg. 144] only SAXS and microscopy analyses were used to describe so-called successful polymerisation of acrylamide in lyotropic mesophases with retention of the lyotropic order. Burban, He and Cussler showed, with detailed analytical investigations, that the formed polymeric phase demixes to form a non-ordered polymer subphase, while the lyotropic (sub)phase shows similar high order to that it had before the polymerisation reaction [145]. This

Stellenbosch University http://scholar.sun.ac.za

retention of high order, as detected by SAXS before and after the reaction, was then used as only evidence in claiming successful retention of the order, and therefore successful templating. After the removal of the ordered surfactant phase however, it was shown that the system had lost all order [145, 146].

McGrath and co-workers performed an extensive study on the polymerisation of polymerisable surfactants in their isotropic and lyotropic states [147-150]. In the case of allyldodecyldimethylammonium bromide (ADAB) [147] the polymerisations did not proceed to conversions higher than 30 %. The formed polymer chain was described as being incorporated into the monomer lyotropic matrix by interweaving between the surfactant aggregates. Polymerisation of the lyotropic phases induced no phase change or phase separation, but the newly incorporated polymer chain rather increased the stability of the lyotropic phases.

During a study of the polymerisable surfactant sodium-undecenoate [149], the following conclusions of importance to obtaining copies of the liquid crystalline template were reached. They found that the surfactant geometry was maintained in micellar and hexagonal phases after polymerisation. In these cases the phases were maintained. In the case of lamellar mesophases the alkyl chain order was lowered during polymerisation, leading to phase transitions.

Another approach in the polymerisation of polymerisable surfactants was used by Wegner and co-worker. They photo-crosslinked lyotropic phases generated by amphiphilic triblock copolymers, with retention of lyotropic order [151]. This system was not highly crosslinked, and could be destroyed by swelling in organic solvents. Hentze et al showed the crosslinking of lyotropic phases generated by amphiphilic diblock copolymers by means of γ radiation [152]. This was achieved with retention of the lyotropic order. The *d*-spacings (repeat unit length) in these systems decreased by 5-10% after crosslinking, but retained all other lyotropic features. The system remained crosslinked, even after extraction with organic solvents.

In general, polymerisation of organic monomers in lyotropic mesophases follow the same route as found above for the lamellar phases of sodium undecenoate, as well as was found in the case of polymerisation in microemulsions. The thermodynamic influence of the growing polymer chain (i.e. the entropy loss of a growing polymer chain in a confined geometry) causes loss of order on a nanometer scale.

The structures obtained from such disrupted templates are, nevertheless, interesting, with directing of the structure evident from the morphologies obtained. Antonietti and co-workers showed that with the use of counterion-coupled gemini surfactants, also known as cocogems, i.e. two surfactants

Stellenbosch University http://scholar.sun.ac.za

coupled via a tartrate ion, a bi-functional counterion, they could afford extra stability to mesophasic templates [146]. This led to the formation of polymer gels with micrometer-sized, layer-like architectures. Even though the cocogem stabilised lyotropic template was not free from changes during the formation of the guest polymer (crosslinked polyacrylamide), it allowed some preservation of long range order. In a further systematic study by Antonietti and co-workers, they showed that, even without obtaining a direct copy of the template, they were still able to vary and control the structure of the resulting three dimensional polymeric gel [153].

Göltner and Antonietti can be quoted to summarise this section, as well as efforts in general in the area of templating research.

"Progress in understanding the mechanism of the templating process gives reason to hope that a direct templating, at least with the aid of liquid crystalline phases, is within reach by the use of kinetically more stable templates and thermodynamic adjustment of template and monomer." [66].

2.3 References

1. Winsor P.A. Chem. Rev., 1968, **68**, 1-39.

2. Griffin W.C. J. Soc. Cosmet. Chem. 1949, **1**, 311

3. Ananthapadmanabhan K.P. in "Interactions of Surfactants with Polymers and Proteins" (Ed. E.D. Goddard & K.P. Ananthapadmanabhan) CRC Press, Boca Raton, 1994

4. Goddard E.D. Colloids Surf. 1986, **19**, 301

5a. Mukerjee P., Mysels K.J., CMC of Aqueous Surfactant Systems, National Standard Reference Data Service, US National Bureau of Standards, 1971

5b. Chevalier Y., Chachaty C. J. Phys. Chem. 1985, **89**, 880

5c. Rosen M.J. Surfactants and Interfacial Phenomena, John Wiley & Sons, New York, 1989

6. Israelachvili J.N. Intermolecular and Surface Forces, Academic Press, 1992.

7. Israelachvili J.N., Mitchell D.J., Ninham B.W. J.Chem. Soc Faraday Trans. I, 1976, **72**, 1525

8. Tanford C. The Hydrophobic Effect, Wiley, New York, 1980

Stellenbosch University http://scholar.sun.ac.za

9. Evans D.F. Wennerström H. The Colloidal Domain, Wiley-VCH, New York, 1994

10. Shimizu T., Masuda M. J.Am. Chem Soc. 1997, **119**, 2812

11. Shimizu T., Kogiso M., Masuda M. Nature 1996, **383**, 487

12. Shimizu T., Kogiso M., Masuda M. J.Am. Chem Soc. 1997, **119**, 6209

13. Reinitzer F. Liq Cryst. 1989, **5**, 7 (English translation of the original paper: Reinitzer F. Monatsh. Chem. 1888, **9**, 421)

14. As cited in Brown, G.H., Shaw W.G. Chem. Rev. 1957, **51**, 1049

15. Percec V., Jonsson H., Tomazos D. in "Polymerization in Organised Media" (Ed. C. M. Paleos) Gordon and Breach Science Publishers, Philadelphia 1994.

16. Tiddy G.J.T. Phys. Rep. 1980, **57**, 1

17. Seddon J.M. Biochimica et Biophysica Acta 1990, **131**, 1

18. Ringsdorf H., Schlarb B., Venzmer J. Angew. Chem. Int. Ed. Engl. 1988, **27**, 113

19. Cates M.E., Safran S.A. Curr. Opin. Colloid Interface Sci. 1996, **1**, 327

20. Kekicheff P., Cabane B. J. Phys (France) 1987, **48**, 1571

21. Kekicheff P., Grabielle-Madelmont C., Ollivon M. J. Colloid Interface Sci. 1989, **131**, 112

22. Kekicheff P. J. Colloid Interface Sci. 1989, **131**, 133

23. McGrath K.M., Kekicheff P., Kleman M. J. Phys. II (France) 1993, **3**, 903

24. Blumstein A. (Ed.) Liquid Crystalline Order in Polymers, Academic Press, New York, 1978

25. Förster S., Antonietti M. Adv. Mater. 1998, **10**, 195

26. Qutubuddin S., Haque E., Benton W.J., Fendler E.J. in "Polymer Association Structures – Microemulsions and Liquid Crystals" (Ed. M.A. El-Nokaly), American Chemical Society, 1989

27. Jahn W., Strey R. J. Phys. Chem. 1988, **92**, 2294

Stellenbosch University http://scholar.sun.ac.za

28. Candau F., in "Polymer Association Structures – Microemulsions and Liquid Crystals" (Ed. M.A. El-Nokaly), ACS Symposium Series 384, American Chemical Society, Washington DC, 1989

29. Winsor P.A. Trans. Faraday Soc. 1948, **33**, 376

30. Bull H.B., Neurath H. J. Biol. Chem. 1937, **118**, 163

31. Anson M.L. Science 1939, **90**, 256

32. Arai H., Murata M., Shinoda K. J. Colloid Interface Sci. 1971, **37**, 223

33. Li Y., Dubin P.L., Dautezenberg H., Lück U, Hartmann J., Tuzar Z. Macromolecules 1995, **28**, 6795

34. Goddard E.D. in "Interactions of Surfactants with Polymers and Proteins" (Ed. E.D. Goddard & K.P. Ananthapadmanabhan) CRC Press, Boca Raton, 1994

35. Rodenhiser A.P., Kwak. J.C.T. Polymer Surfactant Systems: Introduction and Overview in "Surfactant Science Series Volume 77: Polymer –Surfactant System" (Ed J.C.T. Kwak) Marcel Dekker Inc., New York, 1998

36. Hayagawa K., Kwak J.C. J. Phys. Chem. 1982, **86**, 3866

37. Hayagawa K., Ayub A.L., Kwak J.C. Colloids Surfaces 1982, **4**, 389

38. Hayagawa K., Santerre J.P., Kwak J.C. Macromolecules 1983, **16**, 1642

39. Hayagawa K., Kwak J.C. J. Phys. Chem. 1983, **87**, 506

40. Jones M.N. J. Colloid Interface Sci. 1967, **23**, 36

41. Jones M.N. J. Colloid Interface Sci. 1968, **26**, 532

42. Ohbu K., Hiraishi O., Kashiwa I. J. Am. Oil Chem. Soc. 1982, **59**, 108

43. Li Y., Dubin P.L. in "Structure and Flow in Surfactant Solutions" (Ed. C.A. Herb & R.K. Prud'homme) ACS Symposium Series 578, American Chemical Society, Washington DC, 1994

44. Liu J., Takisawa N., Shirhahma K., Abe H., Sakamoto K. J. Phys. Chem. B 1997, **101**, 7520

Stellenbosch University http://scholar.sun.ac.za

45. Shirahama K., Tsujii K., Takagi T. J. Biochem. 1974, **75**, 309

46. Zheng X-L, Cao W-X. Pol. Int. 1998, **46**, 285

47. Thalberg K., Lindman B. in Surfactants in Solution, Vol 11 (Eds. K.L. Mittal., D. Shah), Plenum Press, New York, 1991.

48. MacKnight W.J., Ponomarenko E.A., Tirrell D.A. Acc. Chem. Res.,1998, **31**, 781

49. Ciferri A. Macromol. Chem. Phys. 1994, **195**, 457

50. Goddard E.D., Ananthapdmanabhan K.P. Applications of Polymer-Surfactant Systems in "Surfactant Science Series Volume 77: Polymer –Surfactant System" (Ed J.C.T. Kwak) Marcel Dekker Inc., New York, 1998

51. Uchida, M.; Kunitake, T.; Kajiyama, T. New Polymeric Materials 1994, **4**, 199

52. Caruso F., Trau D., Möhwald H., Renneberg R. Langmuir; 2000; **16**, 1485

53a. Harada, A., Nozakura S. Polym Bull. 1984, **11**, 175

53b. Ujiie S., Iimura K. Macromolecules 1992, **25**, 3174

54. Okahata Y., Enna G., Taguchi K., Seki T. J. Am. Chem. Soc. 1985, **107**, 5300

55. Antonietti M., Conrad J., Angew. Chem. Int. Ed. Engl. 1994, **33**, 1869

56. Mironov A.V., Starodoutsev S.G., Khoklov A.R., Dembo A.T., Yakunin A.N. Macromolecules 1998, **31**, 7698

57. Zhou S., Yeh F., Burger C., Chu B. J. Polymer Sci B, 1999, **37**, 2165

58. Shtykova E., Dembo A., Makhaeva E., Khoklov A., Evmenenko G., Reynaers H. Langmuir 2000, **16**, 5284

59. Ikkala O., Ruokolainen J., Torkkeli M., Tanner J., Serimaa R., ten Brinke G. Coll.Surf.A. 1999**, 147**, 241

60. Luyten M.C., van Ekenstein G., Wildeman J, ten Brinke G, Ruokolainen J, Ikkala O, Torkkeli M, Serimaa R. Macromolecules 1998, **31**, 9160

61. Ober C.K., Wegner G. Adv. Mater. 1997, **9**, 17

Stellenbosch University http://scholar.sun.ac.za

62. Antonietti M., Maskos M. Macromolecules 1996, **29**, 4199

63. Antonietti M., Burger C., Effing J. Adv. Mater. 1995, **7**, 751

64. Antonietti M., Radloff D., Wiesner U., Spiess H.W. Macromol. Chem. Phys. 1996, **197**, 2713

65. Zhou S., Burger C., Yeh F., Chu B. Macromolecules 1998, **31**, 8157

66. Antonietti M., Göltner C. Angew. Chem. Int. Ed. Engl. 1997, **36**, 910

67. Antonietti M., Wenzel A., Thünemann A. Langmuir 1996, **12**, 2111

68. Antonietti M., Conrad J., Thünemann A. Macromolecules 1994, **27**, 6007

69. Antonietti M., Wenzel A. Colloids Surf A: Phys Eng Asp 1998, **135**, 141

70. Antonietti M., Neese M., Blum G., Kremer F. Langmuir, 1996, **12**, 4436

71. Antonietti M., Maskos M., Kremer F., Blum G. Acta Polym. 1996, **47**, 460

72. Thünemann A.F., Ruppelt D., Ito S., Müllen K. J. Mater. Chem. 1999, **9**, 1055

73. Perret R., Ruland W. Kolloid Z. 1971, **247**, 835

74. Thünemann A.F., Ruppelt D. Langmuir 2000, **16**, 3221

75. Thünemann A.F., Ruppelt D., Schnablegger H., Blaul J. Macromolecules 2000, **33**, 2124

76. Thünemann A.F., Beyermann J., Langmuir 2000, **16**, 850

77. General S., Max Planck Institute for Colloids and Interfaces, Personal Communication, 2000

78. Antonietti, M., Henke S., Thünemann A. Adv. Mater. 1996, **8**, 41

79. Thünemann A.F., Kubowicz S., Pietsch U. Langmuir 2000, ASAP Article

80. Bronstein L.M., Platonova O.A., Yakunin A.N., Yanovskaya I.M., Valetsky P.M., Dembo A.T., Obolonkova E.S., Makhaeva E.E., Mironov A.V., Khokhlov A.R. Colloids Surf. A, 1999, **147**, 221

81. Dreja M., Lennartz W. Macromolecule 1999, **32**, 3528

82. Effing J.J., Kwak J.C.T. Angew. Chem. Int. Ed. Engl. 1995, **34**, 88

Stellenbosch University http://scholar.sun.ac.za

83. Antonietti M., Kublickas R., Nuyken O., Voit B. Macromol. Rapid Commun. 1997, **18**, 287

84. Candau F., in "Polymerization in Organised Media" (Ed. C. M. Paleos) Gordon Breach Science Publishers, Philadelphia, 1994.

85. Faul C.F.J., Antonietti M., Sanderson R.D., Hentze H-P, accepted for publication in Langmuir

86. Organic Thin Films, Adv. Mater. 1991, **3**, 1

87. Richardson T. Chem. Britain 1989, **25**, 1218

88. Tieke B. in "Polymerization in Organised Media" (Ed. C. M. Paleos) Gordon Breach Science Publishers, Philadelphia, 1994.

89. Goren M., Qi Z., Lennox R.B. Chem. Mater. 2000, **12**, 1222

90. Miyata M. in "Polymerization in Organised Media" (Ed. C. M. Paleos) Gordon Breach Science Publishers, Philadelphia, 1994.

91. Clasen H. Z. Elektrochem. 1956, **60**, 982

92. MacLachlan M.J., Aroca P., Coombs N., Manners I., Ozin G.A. Adv. Mater. 1998, **10**, 114

93. Wu C-G., Bein T. Science 1994, **266**, 1013

94. Giannelis E.P., Krishnamoorti R., Manias E. Adv. Polym. Sci. 1999, **138**, 107

95. Lamparski H.G., Oblinger E., O'Brien D.F. Macromolecules 1999, **32**, 5450

96. Rainaldi I., Cristallini C., Ciardelli G., Giusti P. Polymer International 2000, **49**, 63

97. Cristallini C., Ciardelli G., Polacco G., Villani A., Lazzeri L., Giusti P. Polymer International 1999, **48**, 1251

98. Khan A., Haddleton D.M., Hannon M.J., Kukuli D., Marsh A. Macromolecules 1999, **332**, 6560

99. Regen S.L., Czech B., Singh M. J. Am. Chem. Soc. 1980, **102**, 6638

100. Jung M., Hubert D.H.W., Bomans P.H.H., Frederik P.M., Meuldijk J., van Herk A.M., Fischer H., German A.L. Langmuir 1997, **13**, 6877

Stellenbosch University http://scholar.sun.ac.za

101. Jung M., Hubert D.H.W., Frederik P.M., Bomans P.H.H., van Herk A.M., German A.L. Adv. Mater. 2000, **12**, 210

102. Kresge C.T., Leonowicz, M.E., Roth W.J., Vartuli J.C., Beck J.S. Nature 1992, **359**, 710

103. Beck J.S., Vartuli J.C., Roth W.J., Leonowicz M.E., Kresge C.T., Scmitt K.D., Chu C.T-W., Olson D.H., Sheppard E.W., McCullen S.B., Higgins J.B., Schlenker J.L. J. Am.Chem.Soc, 1992, **114**, 10834

104. Göltner C.G., Antonietti M. Adv. Mater 1997, **9**, 431

105. Hall S.R., Fowler C.E., Lebeau B., Mann S., Chemical Communications 1999, **2**, 201

106. Imhof A., Pine D.J. Nature 1997, **389**, 948

107. Attard G.S., Glyde J.C., Göltner C.G. Nature 1995, **378**, 366

108. Göltner C.G., Henke S., Weissenberger M.C., Antonietti M. Angew. Chemie Int. Ed. Engl 1998, **37**, 613

109. Hentze H-P., Krämer E., Berton B., Förster S., Antonietti M., Dreja M. Macromlecules 1999, **32**, 5803

110. Stoffer J.O., Bone T., J. Polymer Sci. Polym. Chem Ed. 1980, **18**, 2641

111. Stoffer J.O., Bone T. J. Dispersion Sci. Technol. 1980, **1**, 37

112. Stoffer J.O., Bone T. J. Dispersion Sci. Technol. 1980, **4**, 393

113. Jayakrishnan A., Shah D.O. J. Polym Sci. Polym. Lett Ed 1984, **22**, 31

114. Atik S.S., Thomas J.K. J. Am. Chem. Soc. 1981, **103**, 4279

115. Leong Y.S., Candau F. J. Phys. Chem., 1982, **86**, 2269

116. Candau F., Leong Y.S., Pouyet G., Candau S. J. Colloid. Interface Sci. 1984, **101**, 167

117. Gan L.M., Chew C.H., Friberg S.E., Higashimura T., J. Polymer Sci. Polym. Chem Ed. 1981, **19**, 1585

118. Gan L.M., Chew C.H. J. Dispersion Sci. Technol. 1984, **5**, 179

119. Holtzscherer C., Candau F. J. Colloid Interface Sci. 1988, **125**, 97

Stellenbosch University http://scholar.sun.ac.za

120. Guo J.S., El-Aasser M.S., Vanderhoff J.W. J. Polymer Sci. Polymer Chem Ed. 1989, **27**, 691

121. Feng L., Ng K.Y.S. Macromolecules 1990, **23**, 1048

122. Antonietti M., Bremser W., Müschenborn D., Rosenauer C., Schupp B. Macromolecules 1991, **24**, 6636

123. Haque E., Qutubuddin S., J. Polymer Sci Polymer Lett. Ed. 1988, **26**, 429

124. Menger F.M., Tsuno T., Hammond G.S. J. Am. Chem. Soc. 1990, **112**, 1263

125. Sasthav M., Cheung H.M. Langmuir 1991, **7**, 1378

126. Raj P.W.R., Sasthav M., Cheung H.M. Langmuir 1991, **7**, 2586

127. Raj P.W.R., Sasthav M., Cheung H.M. Langmuir 1992, **8**, 1931

128. Raj P.W.R., Sasthav M., Cheung H.M. Polymer 1993, **34**, 3305

129. Gan L.M., Chieng T.H., Chew C.H., Ng S.C. Langmuir 1994, **10**, 4022

130. Chieng T.H., Gan L.M., Chew C.H., Ng S.C. Polymer 1995, **36**, 1941

131. Chieng T.H., Gan L.M., Chew C.H., Lee L., Ng S.C., Pey K.L., Grant D. Langmuir 1995, **11**, 3321

132. Chieng T.H., Gan L.M., Chew C.H., Ng S.C., Pey K.L. Polymer 1996, **37**, 2801

133. Chieng T.H., Gan L.M., Chew C.H., Ng S.C., Pey K.L. Polymer 1996, **37**, 4823

134. Chieng T.H., Gan L.M., Chew C.H., Ng S.C., Pey K.L. Langmuir 1996, **12**, 319

135. Chieng T.H., Gan L.M., Chew C.H., Ng S.C., Pey K.L. J. Appl. Polym. Sci. 1996, **60**, 1561

136. Antonietti M., Hentze H-P. Colloid Polym. Sci. 1996, **274**, 696

137. Antonietti M., Hentze H-P. Adv. Mater. 1996, **8**, 840

138. Raj P.W.R., Sasthav M., Cheung H.M. J. Appl. Polym. Sci. 1993, **47**, 499

139. Chow P.Y., Chew C.H., Ong C.L., Wang J., Xu G., Gan L.M. Langmuir 1999, **15**, 3202

140. Rees G.D., Evans-Gowings R., Hammond S.J., Robinson B.H. Langmuir 1999, **15**, 1993

Stellenbosch University http://scholar.sun.ac.za

141. Tanori J., Pileni M.P. Langmuir 1997, **13**, 639

142. Lisieki I., Pileni M.P. J. Am. Chem. Soc. 1993, **115**, 3887

143. Hentze H-P. Ph.D. Dissertation, University of Potsdam, Cuvillier Publishers, Göttingen, 1997

144. Laversanne R. Macromolecules 1992, **25**, 489

145. Burban J.H., He M., Cussler E. AIChe J. 1995, **41**, 907

146. Antonietti M., Göltner C., Hentze H-P. Langmuir 1998, **14**, 2670

147. McGrath K.M., Drummond C.J. Colloid Polym. Sci. 1996, **274**, 316

148. McGrath K.M. Colloid Polym. Sci. 1996, **274**, 399

149. McGrath K.M. Colloid Polym. Sci. 1996, **274**, 499

150. McGrath K.M., Drummond C.J. Colloid Polym. Sci. 1996, **274**, 612

151. Yang J., Wegner G. Macromolecules 1992, **25**, 1791

152. Hentze H-P., Krämer E., Berton B., Förster S., Antonietti M. Macromolecules 1999, **32**, 5803

153. Antonietti M., Caruso R.A., Göltner C., Weissenberger M.C. Macromolecules 1999, **32**, 1383

154. Sing K.S.W., EverettD.H., Haul R.A.W., Moscou L., Pierotti R.A., Rouquerol J., Siemieniewska T. Pure Appl. Chem. 1985, **57**,603

Stellenbosch University http://scholar.sun.ac.za

CHAPTER 3

3 Characterisation and Analysis of Polymer and Mesophase Morphology

3.1 Introduction

In the study of the morphology and characteristics of mesophases and mesostructured systems x-ray diffraction, namely small angle x-ray scattering (SAXS) and wide angle x-ray scattering (WAXS), and polarised light microscopy are the most basic of analytical techniques needed. The thermal and mechanical properties, or in the case of mesostructured systems the nanomechanical properties, of mesophase and mesostructured materials are closely related to the phase morphology, and are therefore important aspects to be investigated in the full characterisation of such systems.

Since the production of polymer particles with specific morphologies and molecular characteristics within mesostructured templates is the aim of this study, mesophase structure, polymer characterisation, and more important characterisation of the morphology of polymeric particles, forms an invaluable part of this study. Electron microscopy, both scanning electron microscopy (SEM) and transmission electron microscopy (TEM), are therefore used extensively.

This section will provide the specific theoretical background to experimental techniques that applied to this investigation. Techniques are listed in priority in terms of frequency of use and importance. References to more detailed descriptions of these techniques are provided.

All SAXS, WAXS and DMA studies were performed at the Max Planck Institute for Colloids and Interface, Golm, Germany.

3.2 Analytical techniques

3.2.1 X-ray Scattering

In order to investigate morphologies and gain structural information of an ordered system by means of a scattering technique, it is imperative that the wavelength of the waves being scattered be of about the same length as the distance between the scattering centers.

Stellenbosch University http://scholar.sun.ac.za

In the investigation of ordering at an atomic and molecular level (as is found in the case of crystalline and liquid crystalline mesophases), X-ray and neutrons satisfy the above mentioned criteria, and have been used extensively in structural investigations of mesostructured systems.

In this work extensive use was made of X-ray scattering, with X-rays from Cu Kα radiation with a wavelength $\lambda = 0.154$ nm, which is more than suitable to provide the necessary information on the mesostructured system.

X-rays show interaction with the electrons of constituent atoms as they pass through matter. Through these interactions the X-rays will undergo scattering in all directions, with coherent scattering (where all scattered rays have the same wavelength as the original incoming X-ray) being most important. It can be assumed that atoms (including the contributions of all electrons and the nucleus) act as point sources of scattered radiation.

The scattered coherent radiation will interfere either destructively or constructively (giving rise to a scattered beam). When scattering takes place from a three-dimensional array of atoms / scattering centers, characteristic scattering images will result from the constructive and destructive interference of the scattered beams.

This forms the basis of scattering experiments, where the variation of the intensity of the scattered beam is measured in dependence of the scattering angle, 2θ.

Wide Angle X-ray Scattering (WAXS) can be used to resolve structure (spacing between scattering layers) at an interatomic level (~0.1 nm). Here the scattering intensity is measured from approximately 5 ° to 180 °. Bragg's Law is used to describe conditions where constructive interference will take place, and can be described by the following equation:

$$n\lambda = 2d \sin\theta \qquad \text{Eq. 3.1}$$

where

n = integral number of wavelengths

λ = wavelength

d = spacing between layers of scattering centers

θ = half the scattering angle

Stellenbosch University http://scholar.sun.ac.za

In the case of mesostructured / colloidal systems, structural elements are usually in the range of 2 to 200 nm. The characterisation of such systems can be performed by making use of Small Angle X-ray Scattering (SAXS), with angles of measurement of the scattered intensity from close to 0 to 5 °.

Scattering vector s can be described from Bragg's law

$$1/d = (2 \sin \theta) / \lambda \equiv |\vec{s}| \, (\mathrm{nm}^{-1}) \qquad \text{Eq. 3.2}$$

In an effort to describe the relation between s in reciprocal space and the scattering angle 2 θ, the following construction can be made. If an imaginary sphere is constructed with diameter 2/λ, and the point where the beam leaving the sample intersects the circle is the origin of the reciprocal space, the scattering vector s can described as shown in the figure below.

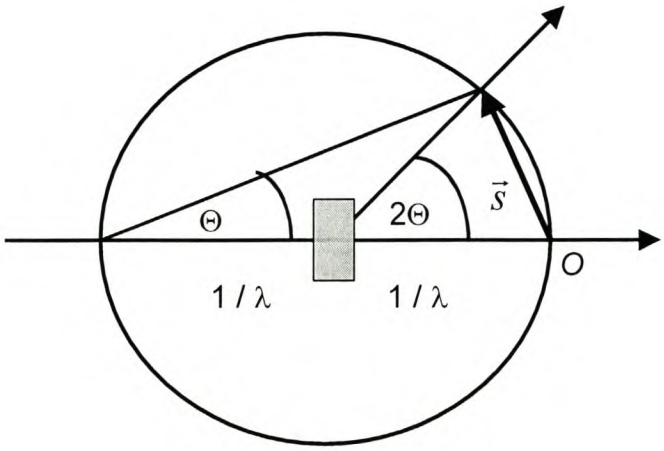

Figure 3.2-1 Schematic representation of the relationship between $|\vec{s}|$ in reciprocal space and the scattering angle 2θ

The relationship of the detected scattering intensity I($\vec{s}$) and the electron distribution function $\rho(\vec{r})$ (from which structural information of the system investigated can be extracted) can be visualised by the following representation:

$$\begin{array}{lccc} & \rho(\vec{r}) & \overset{\Im}{\Leftrightarrow} & A(\vec{s}) \\ \text{Real space} & \Downarrow {}^{*2} & & \Downarrow \; |\,|^2 \quad \text{Reciprocal space} \\ & P(\vec{r}) & \overset{\Im}{\Leftrightarrow} & I(\vec{s}) \end{array}$$

Figure 3.2-2 Relationship between I($\vec{s}$) and $\rho(\vec{r})$

Stellenbosch University http://scholar.sun.ac.za

If the primary beam of X-rays is scattered by two point scattering centers (Figure 3.2.3 below), it results in a phase shift in the scattered beam.

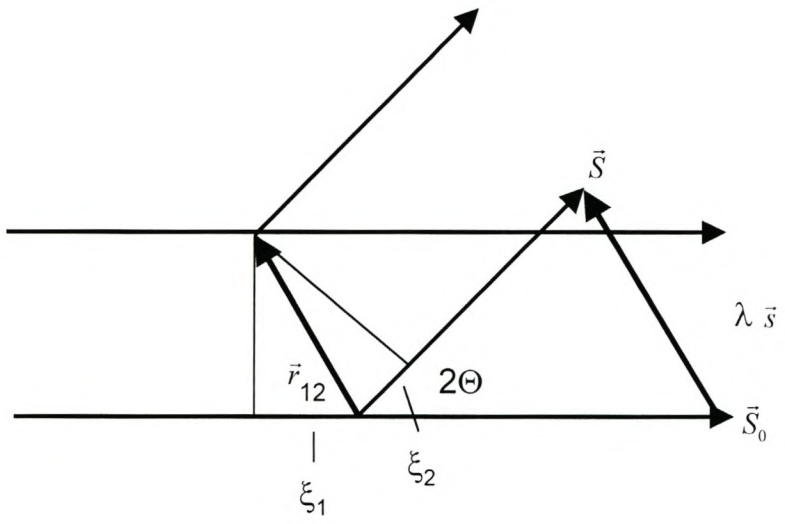

Figure 3.2-3 Scattering at two point scattering centers

Firstly, the path difference ξ between the scattered beams can be described by the following equation:

$$\xi = \xi_1 + \xi_2 = -\vec{r}_{12} \cdot \vec{S}_0 + \vec{r}_{12} \cdot \vec{S} = \vec{r}_{12} \cdot \left(\vec{S} - \vec{S}_0\right) \qquad \text{Eq. 3.3}$$

With $\vec{S}$ and $\vec{S}_0$ the vectors of the incoming/primary and scattered beam.

The phase shift between the incoming and scattered beam is described by the following equation:

$$2\pi \frac{\xi}{\lambda} = 2\pi\ \vec{r}_{12} \cdot \frac{\vec{S} - \vec{S}_0}{\lambda} = 2\pi\ \vec{r}_{12} \cdot (\vec{s}) \qquad \text{Eq 3.4}$$

Now, it can be shown that complex scattering amplitude A($\vec{s}$) for N point scatter centres (of differing scattering power) is equal to

$$\mathrm{A}(\vec{s}) = \sum_{k=1}^{N} n_k \exp(2\pi i \vec{r}_k \vec{s}) \qquad \text{Eq. 3.5}$$

Stellenbosch University http://scholar.sun.ac.za

If $A(\vec{s})$ is calculated for a continuous electron density distribution $\rho(\vec{r})$ (as found in experimental systems) rather than for point sources of scattering , the resulting function where integration is performed over the whole volume is found to be the Fourier Transform of $\rho(\vec{r})$

$$A(\vec{s}) = \int \exp(2\pi i \vec{r}\vec{s})\rho(\vec{r})d^3\vec{r} = \Im\rho(\vec{r}) \qquad \text{Eq. 3.6}$$

Now, scattering intensity $I(\vec{s})$ in terms of s can be calculated from $A(\vec{s})$ by the following equation:

$$I(\vec{s}) = |A(\vec{s})|^2 = A^+(\vec{s})A(\vec{s}) \qquad \text{Eq. 3.7}$$

This calculation, unlike the Fourier transform in the previous equation, is not reversible (see Figure 3.2-2 above).

Furthermore, $I(\vec{s})$ is the Fourier transform of $P(\vec{r})$, the so-called Patterson function. This function is the autocorrelation function of the electron density distribution $\rho(\vec{r})$, and can also be calculated directly from $\rho(\vec{r})$ via the following operation:

$$P(\vec{r}) \equiv \rho^{*2}(\vec{r}) \equiv \rho(\vec{r}) * \rho(-\vec{r}) \qquad \text{Eq. 3.8}$$

The conclusion from this is when you have the electron density distribution $\rho(\vec{r})$, you can calculate the scattering intensity. In practice however, you would acquire the scattering intensity. Ideally one would be able to get the electron density distribution $\rho(\vec{r})$, and therefore structural information from this data via a structure factor. This is not possible due to the non-reversible nature of some of the calculations (as represented in Figure 3.2-2). Therefore, from calculations from $\rho(\vec{r})$ functions it is possible to predict structures and intensity distributions, which in conjunction with other complimentary analysis methods can be used pinpoint structures of mesoscopically structured experimental systems.

In the case of this study, the data obtained fitted known structures from previously investigated generic systems and structural analyses, and could be used in a quantitative way to judge changes taking place within such structured systems such as changing of *s*, and therefore changes in *d*.

Stellenbosch University http://scholar.sun.ac.za

3.2.2 Dynamic Mechanical Analysis (DMA)

In order to investigate the mechanical properties of a sample, a force must be applied to the sample. Materials can be regarded as being viscoelastic, thereby possessing the combined properties of two independent particular types of ideal materials, namely the elastic solid and the viscous liquid. An elastic solid has a definite shape and is deformed by external forces into a new equilibrium shape. On the removal of these forces, it will return to its original shape. A viscous liquid has no definite shape, and will flow irreversibly when an external force is applied to it. For the case of elastic solids, Hooke's law applies. It states that the deformation or strain (ε) of a spring is linearly related to applied stress (σ) by a constant specific to that spring. In equation form this can be written as

$$\sigma = k * \varepsilon \qquad \text{Eq. 3.9}$$

where

k = spring constant

The relationship of stress to strain (from k) is an indication of the material's stiffness, the modulus (E). We can now write the modulus as

$$E = d\sigma / d\varepsilon \qquad \text{Eq. 3.10}$$

In the case of viscous liquids and liquid-like flow (called the Newtonian model), there is no elasticity or stiffness that can be measured; but rather the tendency to resist flow is measured as viscosity (η). As stress is applied to a liquid, it is related to the rate of strain (or shear rate) by means of the viscosity. This is analogous to Hooke's law for elastic solids.

$$\sigma = \eta * \gamma = \eta (\partial\varepsilon / \partial t) \qquad \text{Eq. 3.11}$$

where

η = viscosity

$\gamma = \partial\varepsilon / \partial t$ = shear rate

In the case of a viscoelastic material, one that shows the combined behaviour of both the ideal elastic and viscous materials, the response to an applied dynamic force is an intermediate between that of the ideal cases. The difference between the applied stress and the resulting strain is an angle

Stellenbosch University http://scholar.sun.ac.za

δ, and must be added to the above equations to obtain equations for the behaviour of a viscoelastic material.

If a dynamic force is applied to a sample, e.g. sinusoidally oscillating the applied stress, the sample will deform sinusoidally. The strain will lag behind the stress, and can be written as follows:

Strain: $\varepsilon(t) = \varepsilon_0 \sin(\omega t)$ Eq. 3.12

Stress: $\sigma(t) = \sigma_0 \sin(\omega t + \delta)$ Eq. 3.13

where

$\varepsilon(t)$ = strain at time t and ε_0 = maximum strain

$\sigma(t)$ = applied stress at time t and σ_0 = maximum stress

ω = angular frequency of the oscillation

t = time

δ = phase lag

If we expand the equation for the stress

$\sigma(t) = \sigma_0 \sin(\omega t) \cos\delta + \sigma_0 \cos(\omega t) \sin\delta$ Eq. 3.13

the stress can be considered to consist of two components. The two components are

G', in phase with the strain with magnitude $\sigma_0 \cos\delta$

G", out of phase with the strain with magnitude $\sigma_0 \sin\delta$

The equation for the stress can therefore be re-written to yield the following equation

$\sigma(t) = \varepsilon_0 G' \sin(\omega t) + \varepsilon_0 G'' \cos(\omega t)$ Eq. 3.14

$= \varepsilon_0 |G^*| \sin(\omega t + \delta)$

With

$G' = \sigma_0 / \varepsilon_0 \cos\delta$, the storage modulus

defines the energy stored in the specimen due to the applied strain

Stellenbosch University http://scholar.sun.ac.za

$G'' = \sigma_0 / \varepsilon_0 \sin \delta$, the loss modulus

defines the dissipation of energy ($\pi/2$ out of phase with the strain)

$G^* =$ complex modulus

can be defined as the vector sum of G' and G"

$$G^* = G' + iG'' \qquad \text{Eq. 3.16}$$

In the case of mesostructured materials, and more specifically polyelectrolyte-surfactant complexes, the storage modulus G' gives an indication of the mobility of the alkyl chains at temperatures below 50 °C. Any further interactions of the surfactant alkyl chains with included guest polymer can therefore be easily observed in this low temperature region.

For further detailed studies of rheology and dynamic mechanical analyses, the reader is referred to references [4, 5 and 6].

3.2.3 Microscopy

3.2.3.1 Polarised Light Microscopy

All non-opaque substances can be divided into two groups according to their behaviour when examined between crossed polars, namely isotropic and anisotropic materials. Isotropic materials have optical properties that are the same in all directions, and allow light to travel through them with the same velocity in all directions. Anisotropic materials, such as non-cubic crystals, liquid crystals, certain drawn polymers and natural fibres, have optical (and physical) properties that are a function of direction. These materials are birefringent and will interact with the incident light by altering its plane of polarisation. These materials can therefore be investigated and characterised by polarised light microscopy.

The interaction of polarised light with an optically anisotropic material can be described as follows: (also see Fig 3.2-4) when polarised light interacts with an anisotropic oriented sample, it can be considered as broken into two wave components. These components (one polarised parallel to the long axis of an oriented material, and the other polarised parallel to the short axis) will show different interactions with the material, will therefore travel through the material with different velocities and exhibit different refractive indices ($n_{\parallel}$ and $n_{\perp}$). They will therefore emerge from the material with an optical path difference (o.p.d.). When these components enter the second

Stellenbosch University http://scholar.sun.ac.za

polarising filter, only the components vibrating in the vibration axis of this second filter will be allowed to pass.

These components that have passed through the filter, will be able to interact / interfere with each other. Some light will therefore pass (unless the o.p.d. is equal to zero), and the anisotropic material will appear bright against a dark background. Since anisotropic materials allow polarised light to travel through at two different velocities and therefore exhibit two different refractive indices ($n_{\parallel}$ and $n_{\perp}$), such materials are classified as birefringent.

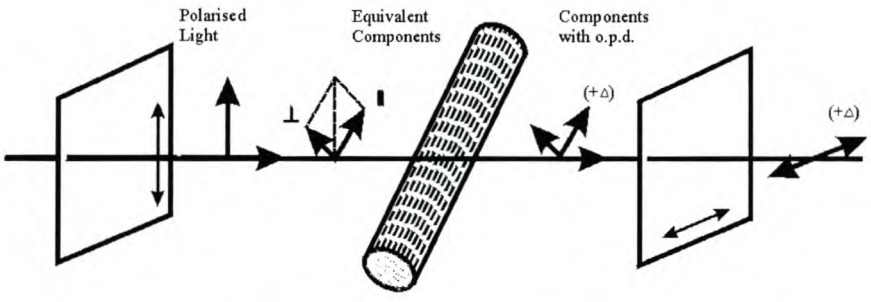

Figure 3.2-4 Interaction of polarised light with an anisotropic material [taken from 9].

If one of the two axes of the material investigated lies parallel to the first polarising filter, one of the component vectors will have zero amplitude. The remaining component will be blocked by the second polarising filter, providing one of four positions (two each for the two axes) of extinction found with well-organised materials.

Anisotropic materials will exhibit different textures due to the presence of different phases in the materials. Through the use of polarised light microscopy it is generally therefore possible to identify various phases of oriented samples. H_1 phases generally show a texture under cross polars that can be described as fan-like. L_α phases generally show a streaky texture [11, 12].

3.2.3.2 Electron Microscopy

It was only after de Broglie proposed that electrons can be viewed as waves of very short wave length, that it was considered to apply electrons to microscopy. With the use of magnetic fields as electron "lenses", the first electron microscopy to exceed the resolving power of an optical microscope was produced by Knoll and Ruska.

Stellenbosch University http://scholar.sun.ac.za

The main advantage of electron microscopy over conventional optical microscopy is the fact that electrons have a much shorter wavelength, which increases the resolving power of the electron microscope.

The wavelength of an electron can be written as

$$\lambda = h / m_e v \qquad \text{Eq. 3.18}$$

where

h = Planck's constant

m_e = rest mass of an electron

v = velocity

The kinetic energy of an electron, charge e and rest mass m_e, when accelerated by a potential difference V (as in an electron microscope) can be written as

$$\tfrac{1}{2} m_e v^2 = Ve \qquad \text{Eq. 3.19}$$

Therefore, the wavelength λ of an electron can now be written as

$$\lambda = h / (2 m_e V e)^{1/2} \qquad \text{Eq. 3.20}$$

A good approximation for the wavelength of an electron in an electron microscope can therefore be written as

$$\lambda = (1{,}5 / V)^{1/2} \text{ nm}$$

In the case of a 100kV acceleration, the wavelength of an electron would be therefore be 0,0037 nm. With this value, one would expect the limit of resolution of an electron microscope to be better than required to resolve individual atoms. Unfortunately that is not the case.

The limit of resolution δ (i.e. the smallest separation between two elements where the elements can still be resolved), as defined by Abbe in 1874, can be expressed by the following equation:

$$\delta = \lambda / (n \sin \theta) \qquad \text{Eq. 3.21}$$

where

λ = wavelength of the light used

Stellenbosch University http://scholar.sun.ac.za

n = refractive index of the medium in the object space

2θ = angular aperture

Abbe called $n \sin \theta$ the numerical aperture of the lens. From this expression it can be seen that there are three possible ways to improve the resolution limit; by using shorter wavelength light, by increasing the refractive index, or by increasing $\sin \theta$ (increasing the numerical aperture in the last two instances). Objects smaller than 500 nm cannot be resolved with an optical microscope, which therefore excludes direct imaging of mesostructured materials from being examined.

It is therefore with an electron microscope with much shorter wavelength, and higher resolution limits that mesostructured materials can be investigated. Unfortunately, even with the wavelength of an electron 10^5 times shorter than that of visible light, the resolution limit is not improved by the same factor. The practical resolution limit of an electron microscope would therefore be approximately 0.2 nm, several orders of magnitude higher than that of an optical microscope. It is therefore suitable to use in the investigation of mesostructured materials.

An electron microscope is built on the same principles as an optical microscope, but has some specific modification necessary for the use of electrons. To ensure that an electron microscope functions properly, the pathway of the electrons from the source (usually a hot filament), providing a constant stream of electrons, to the specimen must be clear of any obstructions. Any collisions with gas molecules will cause the electrons to deviate from their pathway, and the system is therefore kept under high vacuum. For the focussing of the electron beam, magnetic "lenses" are utilised. These lenses operate by making use of magnetic fields to concentrate and focus the electron beam as needed.

Two types of electron microscopes are available for analyses. Both will be discussed briefly. References are provided for further reading.

3.2.3.2.1 Transmission Electron Microscope (TEM)

The TEM operates very analogous to the transmission optical microscope. Imaging radiation is passed through a thin sample or specimen, and is then focused (in the case of the TEM by magnetic lenses) to obtain a magnified image. The beam of electrons has various interactions with the specimen. It is the radiation leaving the specimen that is of importance, and will be responsible for image formation.

Stellenbosch University http://scholar.sun.ac.za

In order to ensure that the image contrast is sufficiently high to provide an image, various techniques can be used to enhance the natural contrast of a specimen. This can include such techniques as vapour deposition, imbedding and staining with heavy metals, microtoming to provide thin sections (< 200 nm), and a variety of special techniques for biological samples. Sample preparation is of the utmost importance, since this can introduce artefacts in the specimen. Furthermore, care should be taken during the investigation of the specimen, that electron beams of high intensity (in order to obtain better contrast and brightness) do not damage the sample.

3.2.3.2.2 Scanning Electron Microscopy

In the case of a scanning electron microscope, the magnetic lenses are not used to focus the beam to provide a magnified image. In this case the electron beam is focussed ("squeezed") to give a beam of small diameter (10 – 20 nm), which is then scanned across the surface of the specimen. Secondary electrons scattered from the surface are collected, amplified and used to form a point-by-point image of the specimen surface.

The resolution limit is mainly defined by the size of the spot. With too small a spot size the chance exists that the signal intensity of scattered electrons become too low to be detected.

Since the specimen is bombarded by negatively charged electrons, the sample is made conductive (if not already) by coating with a thin layer of metal or carbon. The resulting charge build-up is then removed via conductive bridges from the specimen to the holder.

This technique is suitable for use with polymer structures, as long as care is taken not to destroy the specimen by the high-energy interactions with the electron beam.

3.2.4 Gel Permeation Chromatography (GPC)

Gel permeation chromatography (GPC) or Size Exclusion Chromatography (SEC) is an analytical technique developed initially for the fractionation of macromolecules according to their molecular size. It has developed into one of the most useful methods for quick and routine determinations of average molecular weights and molecular weight distributions of polymers. These terms can be defined by the following equations:

Stellenbosch University http://scholar.sun.ac.za

M_n = number average molecular weight

= number of molecules (N_i) of a particular size (M_i)

$= \Sigma N_i M_i / \Sigma N_i$ Eq 3.22

M_w = weight average molecular weight

= weight fractions (w_i) of molecules of a given mass (M_i)

$= \Sigma w_i N_i / \Sigma w_i = \Sigma N_i M_i^2 / \Sigma N_i M_i$ Eq 3.23

D = polydispersity

= measure of the breadth of the molecular weight distribution

$= M_w / M_n$ Eq. 3.24

The experimental set-up (very similar to that of a HPLC) and the basis on which separation takes place, can be described as follows. The separation process can be described as movement of polymer (in a suitable solvent) through a column containing tightly packed microporous gel particles with preferential penetration of the micropores by different size molecules. Larger molecules are excluded from the pore volumes, and will therefore move through the column faster (shorter elution times), while small molecules will penetrate the pores, and require longer elution times. Detection of the eluted polymers usually takes place by any of a variety of detectors, with the most common detectors using refractive index, UV/VIS absorption (either fixed wavelength or diode array providing a complete UV/VIS spectrum), light scattering and evaporative light scattering, although IR, NMR, mass spectrometry etc. amongst others have been used.

This technique provides separation according to the molecular sizes of the species, but gives no absolute values for the molecular weights. In order to obtain absolute values either scattering, and or a calibration with standards of known molecular weights (as determined by absolute methods such as light scattering, osmotic pressure measurements or by solution viscosity measurements) has

Stellenbosch University http://scholar.sun.ac.za

to be performed. A limited number of calibration standards are available (which is a major drawback for this technique), with polystyrene standards most commonly used.

Properties that can be determined by GPC analyses with suitable standards include determination of M_w, M_n and from that D (the polydispersity). In the case where the polymer and the standard differ from each other, a universal calibration method must be employed, where the hydrodynamic radius generally depends on the product of the intrinsic solution viscosity and the molar mass versus elution volume of the polymer solvent and temperature conditions. The product is a measure of the molar volume occupied by the polymer molecule under the prescribed conditions.

3.2.5 Differential Scanning Calorimetry (DSC)

In order to directly investigate the thermal properties (such as enthalpy or entropy) of a material, rather than monitoring a property with a change in the temperature as is the case with DMA, use is made of DSC. DSC is mainly used for studies of thermally induced physical transitions within materials, but degradation -, polymerisation - and other chemical reactions and interactions can also be studied.

In order to assess the thermal properties of a material, the heating and cooling rates are of the utmost importance during the investigation. With too high a rate, a thermal lag will exists, where with too low a rate, possible degradation of the specimen may take place.

In the case of DSC, a sample and reference are heated independently from each other, both maintained at the programmed temperature (T_p). The temperature of both the sample and reference are constantly measured and compared with the instantaneous value of T_p. Power in watts (W) delivered to the sample and reference via the individual heaters is dependent of the departure of the individual temperatures from the programmed temperature T_p, e.g. as would be the case for an endothermic transition (e.g. melting) taking place within a specimen, and can be written as:

Power delivered to the sample $= W_s(T_s - T_p)$ Eq. 3.25

Power delivered to the reference $= W_r(T_r - T_p)$ Eq. 3.26

The differential power requirement (ΔW) can be written as follows

$$\Delta W = [W_s(T_s - T_p) - W_r(T_r - T_p)] \quad \text{Eq 3.27}$$

and is the quantity that is usually plotted and represented as a function of T_p, T_r or T_s.

Stellenbosch University http://scholar.sun.ac.za

Further quantitative analyses can be performed in order to obtain enthalpy changes in samples and modulated temperature heating profiles can be applied, but falls beyond the scope of use in this investigation.

3.3 References

XRD

1. Hammond C. The Basics of Crystallography and Diffraction, International Union of Crystallography / Oxford University Press, Oxford, 1997

2. Burger C. Moderne Aspekte der Kolloidforschung: Röntgenstreuung an Polymeren und Kolloiden, MPI für Kolloid- und Grenzflächenforschung, Teltow-Seehof, 1996

3. Burger C. Neue Aspekte der Kolloidanalytik: Röntgenstreuung, MPI für Kolloid- und Grenzflächenforschung, Teltow-Seehof, 1998

DMA

4. Menard K.P. Dynamic Mechanical Analysis – A Practical Introduction, CRC Press, Boca Raton, 1999

5. Ward I.M., Hadley D.W. An Introduction to the Mechanical Properties of Solid Polymers, John Wiley & Sons, Chichester, 1993

6. Neilsen L.E. Mechanical Properties of Polymers and Composites (in two volumes), Marcel Dekker Inc., New York, 1974

Polarised Light Microscopy and Electron Microscopy

7. Bradbury S., Bracegirdle B. Introduction to Light Microscopy, Bios Scientific Publishers, Oxford, 1998

8. Southworth H.N. Introduction to Modern Microscopy, Wykeham Publications Ltd., London, 1975

Stellenbosch University http://scholar.sun.ac.za

9. Spencer M. Fundamentals of Light Microscopy, Cambridge University Press, Cambridge, 1982

10. Goldstein J.I., Newbury D.E Echlin P., Joy D.C., Fiori C., Lifshin E. Scanning Electron Microscopy and X-ray Microanalysis – a text for biologists, materials scientists and geologists, Plenum Press, New York, 1981

11. Rosevear F.B. J. Am. Oil. Chem. Soc. 1954, **31**, 628

12. Winsor P.A. Chem. Rev. 1968, **68**, 1

13. Collings P.J. Liquid Crystals – Nature's Delicate Phase of Matter, Princeton University Press, Princeton, 1990

Gel Permeation Chromatography

14. Pasch H., Trathnigg B. HPLC of Polymers, Springer Verlag, Berlin, 1998

15. Campbell D., White J.R. Polymer Characterization – physical techniques, Chapman & Hall, London, 1989

16. Barth H. G., Mays J.W. (Eds.) Modern Methods of Polymer Characterization, John Wiley & Sons, New York, 1991

Differential Scanning Calorimetry

17. Utschick H., Methods of Thermal Analysis, Ecomed Verlagsgesellschaft AG, Landsberg, 1999

18. Campbell D., White J.R. Polymer Characterization – physical techniques, Chapman & Hall, London, 1989

19. Chiu J. (Ed.) Polymer Characterization by Thermal Methods of Analysis, Marcel Dekker Inc., New York, 1974

Stellenbosch University http://scholar.sun.ac.za

CHAPTER 4

4 Polymerisation in high SDS concentration solutions

4.1 Introduction

The idea at the onset of this research project was to try and mimic successes found with inorganic systems in the production of the family of M41S and other inorganic mesoporous materials [1-4]. The goal was therefore, through the application of a reaction system containing high concentration of a surfactant (but below the concentration where a lyotropic mesophase would form), to direct the structure of an organic polymer to possibly yield mesostructured organic polymers.

Since this was an introductory study into template directed polymerisations, it was decided to keep the reaction solutions to three components only (water, surfactant and monomer), rather than add a fourth, the co-surfactant (after reference 5). It was also decided to concentrate on the low monomer concentration region of such a ternary system, to try and avoid phase disruption and separation. Combined with the use of low monomer concentration, quiescent conditions were employed.

4.2 Experimental

4.2.1 Materials

Sodium dodecyl sulphate (SDS) was obtained from Unilab/Saarchem (90 % SDS, containing various other chain lengths sulphate surfactants) and used as received. Styrene and methylmethacrylate (MMA) were distilled prior to use. Cross-linking agents divinylbenzene (DVB) and ethyleneglycoldimethacrylate (EGDMA) were obtained from Sigma/Aldrich and were used as received. UV initiator phenylacetophenone (Benzoin) was obtained from Sigma/Aldrich (95 % purity) and used as received. Chemical initiators $Na_2S_2O_3$ and $(NH_4)_2S_2O_8$ were obtained from Merck Chemical Co and used as received. NaCl was obtained from Saarchem (99 % purity) and used as received. Ethanol (Analar grade) was obtained from Merck and Saarchem and used as received.

Samples were filtered using a syringe filter system, onto polyvinilidenefluoride (PVDF – resistant to organic solvents) filters, pore size 0.25 μm from Millipore.

Stellenbosch University http://scholar.sun.ac.za

UV lamps employed for UV initiation were 15 W Philips Germicidal UV lamps. γ-irradiation of samples were achieved by exposure to a ^{60}Co source located at Infruitec Research Insittute, Agricultural Research Council, Stellenbosch.

Wide Angle X-ray Scattering (WAXS) analyses were performed on a Brucker Advance D8 X-ray Diffractometer (operating conditions: 40 kV, 40 mA), National Accelerator Centre, Faure, South Africa.

Atomic emission spectroscopy (AES) analyses were performed on a Varian Liberty II ICP-AES (operating power 1.2 kW), Physics Department, University of Stellenbosch.

4.2.2 Experimental Protocol:

In order to investigate the influences of changing the concentration and type of monomer, and the concentration of the surfactant, the following approach was used. A batch reaction system (12 reactions) was developed, with reactions performed in open reaction vessels (volume 25 ml), under nitrogen atmosphere in a closed environment. Temperature was regulated and kept at 25 °C. Ultraviolet (UV) initiation was utilised (2 x UV lamps, 14 W), with phenylacetophenone as UV initiator.

In order to narrow the field of investigation down, the following general formulations were used. The percentage of styrene monomer (always including 5 % divinylbenzene (DVB) as cross-linking agent and 0.5 % phenylacetophenone as UV initiator) present in the reaction system was restricted to three values only, i.e. 9.1 %, 4.75 % and 1 %. The concentration of SDS (in terms of percentage values) was restricted to the following values: 20, 25, 30 and 35 % (weight percentage in terms of the combined weight of the water and monomer). A typical formulation would consist of the following, with the concentration of the SDS stock solution typically 60 % by weight:

SDS (x ml of the stock solution, to provide the sought after concentration) H_20 (14 – x ml), styrene (1,4 g / 0,7 g / 0,14 g). Photoinitiator concentration 0.5 %. Cross-linking density 5 %. A typical reaction scheme is shown below in Table 4.2-1.

After careful mixing of the components, and allowing the reaction solutions to equilibrate for 4 hours, the series of reaction vessels (12) was irradiated for 4 hours under quiescent conditions. Variations of the above reactions conditions were also investigated to evaluate the reaction system under different conditions. This included the variation of the initiation mechanism to include chemical (redox) initiation and nuclear (γ-irradiation) initiation. During chemical initiation of the reactions, a redox initiator system (ammonium persulphate / sodium thiosulphate) was utilised.

Stellenbosch University http://scholar.sun.ac.za

When γ-irradiation was used to initiate the reactions, no other initiator was included in the reaction solutions.

Planning: Exp J, K							
		J = Sty					
Styrene = Styrene + 5%		K = DVB					
Scale Factor	7.143						
15 % SDS		**ml Sty**	**H2O + Sty**	**g SDS**	**SDS Sol**	**DI H2O**	Sample
H2O:	14.000		g	15 %	ml	ml	
Styrene:							
10g	1.400	1.538	15.400	2.310	5.133	8.867	**1**
5 g	0.700	0.769	14.700	2.205	4.900	9.100	**2**
1 g	0.140	0.154	14.140	2.121	4.713	9.287	**3**
20 % SDS		**ml Sty**	**H2O + Sty**	**g SDS**	**SDS Sol**	**DI H2O**	
H2O:	14.000		g	20 %	ml	ml	
Styrene:							
10g	1.400	1.538	15.400	3.080	6.844	7.156	**4**
5 g	0.700	0.769	14.700	2.940	6.533	7.467	**5**
1 g	0.140	0.154	14.140	2.828	6.284	7.716	**6**
25 % SDS							
			H2O + Sty	**g SDS**	**SDS Sol**	**DI H2O**	
H2O:	14.000		g	25 %	ml	ml	
Styrene:							
10g	1.400	1.538	15.400	3.850	8.556	5.444	**7**
5 g	0.700	0.769	14.700	3.675	8.167	5.833	**8**
1 g	0.140	0.154	14.140	3.535	7.856	6.144	**9**
30 % SDS							
			H2O + Sty	**g SDS**	**SDS Sol**	**DI H2O**	
H2O:	14.000		g	30 %	ml	ml	
Styrene:							
10g	1.400	1.538	15.400	4.620	10.267	3.733	**10**
5 g	0.700	0.769	14.700	4.410	9.800	4.200	**11**
1 g	0.140	0.154	14.140	4.242	9.427	4.573	**12**
35 % SDS							
			H2O + Sty	**g SDS**	**SDS Sol**	**DI H2O**	
H2O:	14.000		g	35 %	ml	ml	
Styrene:							
10g	1.400	1.538	15.400	5.390	11.978	2.022	**13**
5 g	0.700	0.769	14.700	5.145	11.433	2.567	**14**
1 g	0.140	0.154	14.140	4.949	10.998	3.002	**15**

Table 4-1 Typical reaction scheme

In order to remove the excess surfactant for analysis, 1 ml of the solution was washed with ethanol, the precipitate centrifuged and the supernatant discarded (after Chieng [6]). This process was repeated three times. The remaining precipitate was then filtered through a removable syringe filter. These sample-covered filter papers were mounted on SEM stubs for further coating and investigation.

Another cleaning procedure was also utilised for SEM analyses. THF was added to the reaction solutions after reaction, until a white precipitate formed. This would then be carefully filtered, the

Stellenbosch University http://scholar.sun.ac.za

precipitate removed and suspended in water. This cycle would be repeated a total of three times to ensure that all surfactant would be separated from the polymeric precipitate.

Sample preparation for TEM was performed by dialysis of the samples against deionised water for 96 hours, using a molecular weight cut-off membrane of 10 000. Once the conductivity of the samples were comparable to that of deionised water, the samples were diluted and dripped onto carbon-coated copper grids and left in air to dry before TEM investigation.

4.3 Results and Discussion

After UV irradiation of a typical reaction series, precipitation from ethanol was utilised as cleaning procedure. Results obtained from SEM investigations from series of reactions of styrene (cross-linked with 5 % DVB) and pure DVB yielded an array of shapes not commonly found in the polymerisation of styrene under normal emulsion polymerisation conditions. These reactions were repeated for other initiation mechanisms (chemical and γ-irradiation) and yielded similar SEM results for each repetition.

Irregular shaped particles (best described as "cornflake-like" particles) were produced in most cases. In addition to these, two different types of shaped particles were formed. Firstly, particles of approximately needle-like, plank-like and cigar-like shapes were found, with typical dimensions in the order of 2 μm high, 5 μm wide and 30 to 40 μm in length. In addition to these shaped particles, some particles that could best be described as ribbon-like structures were also present in some samples. The dimensions of these very large structures were 2 μm height, 5 μm in width and longer than 300 μm. Figures 4.3-1 a, b, c and d show some typical results obtained.

The composition of these particles was investigated, since their size and regularity indicated crystallinity, so that they could probably be from surfactant origin. Light microscopy showed that no particles of this size were present in the reaction solutions. This was confirmed by analyses performed using ultra-centrifugation and dynamic light scattering. Both these techniques indicated that the samples contained a polydisperse mixture of particles of sizes 500 nm and smaller.

Stellenbosch University http://scholar.sun.ac.za

a) Needle-like particles found

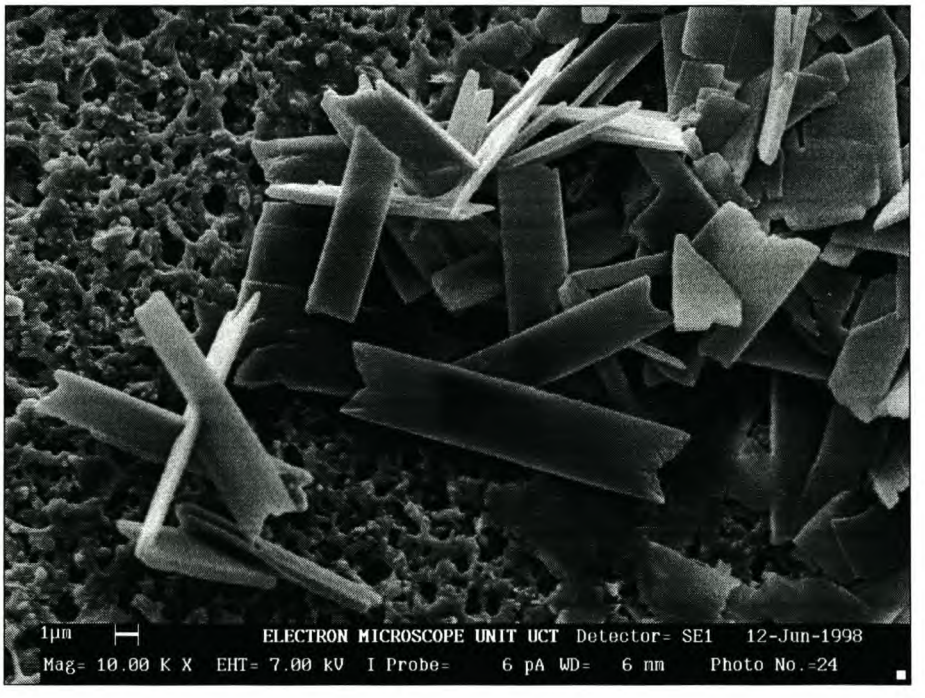

b) Plank-like particles found

Figure 4.3-1 a, b Typical results from the styrene polymerisations

Stellenbosch University http://scholar.sun.ac.za

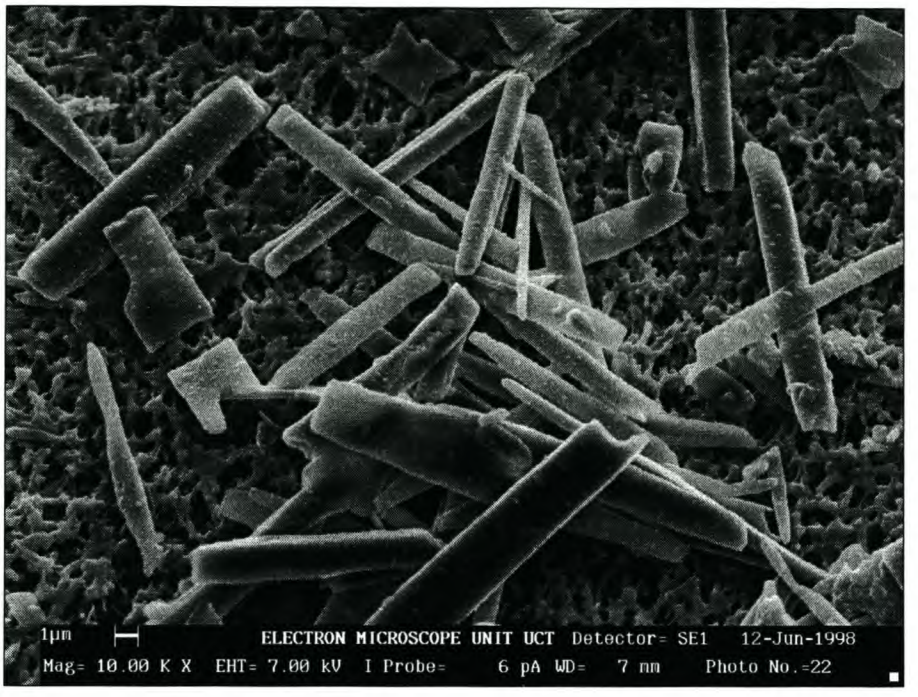

c) Cigar-shaped particles found

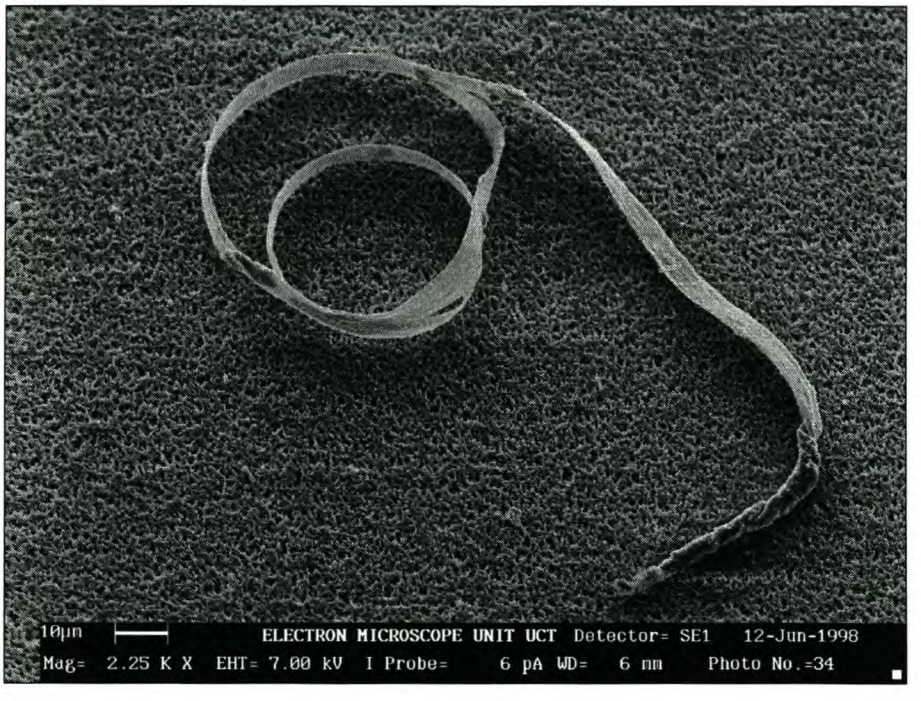

d) Ribbon-like particles found

Figure 4.3-1 c, d. Typical results from the styrene polymerisations

This confirmed the ideas that the shaped particles were not of polymeric nature. Samples were then prepared for TEM and SEM investigation using precipitation from THF as cleaning procedure. These investigations confirmed that the shaped particles were not polymeric in nature. The

Stellenbosch University http://scholar.sun.ac.za

particles that were found (see Figure 4.3-2 a (SEM) and 4.2 b (TEM)) were spherically shaped, and corresponded to the sizes found with light scattering and ultracentrifugation.

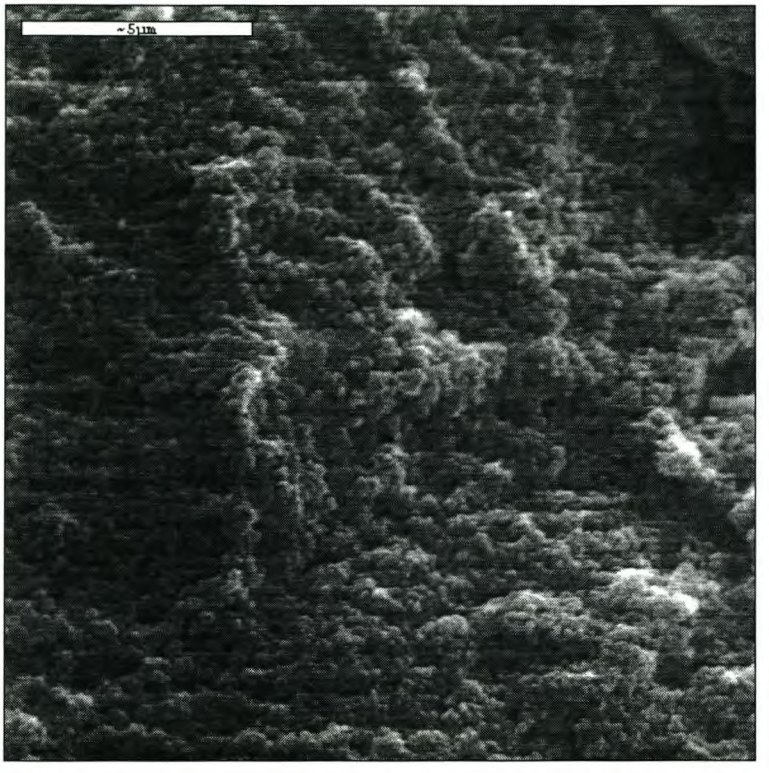

a) SEM Micrograph - spherical polystyrene particles after precipitation from THF

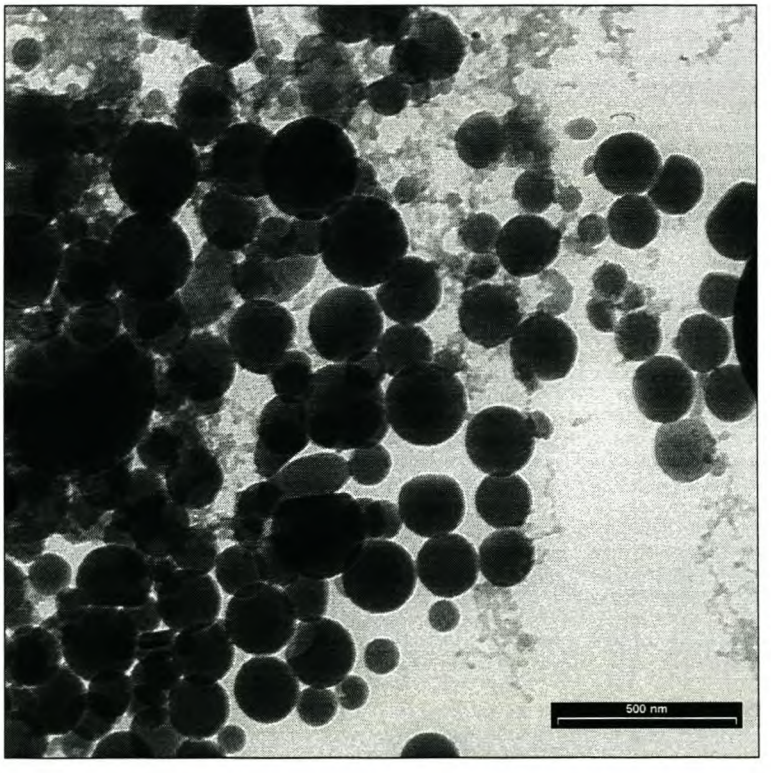

b) TEM Micrograph – Polydisperse mixture of spherical particles found after dialysis

Figure 4.3-2 a and b SEM and TEM investigation of the morphology of polymeric particles.

Stellenbosch University http://scholar.sun.ac.za

These findings can be explained from the fact that the system was not in a lyotropic mesophase during the polymerisation reaction. Other than the case found in the formation of mesostructured inorganic polymers where cooperative self-assembly of an ionic surfactant with silica precursors form a combined mesophase [7, 8], organic polymers precursors (monomers or oligomers) do not have the ability to form organised pre-aggregates (by charge-density matching or multi-dentate binding [9]). This would therefore indicate that the monomer was, from the onset of the reaction, absorbed in micellar (templating) aggregates. The large distribution of sizes found would indicate that control of the reactions was minimal.

In many cases, phase separation occurred during the reaction. This could be explained from and matches predictions and results from the literature [10, 11]. It was suggested that the thermodynamic influence of a growing polymer chain on a reaction solution would lead to the disruption of the template phase and cause demixing of the polymer phase on a micro and even macro scale. This seemed to have taken place here, with the formation of the spherical particles, rather than the formation / templating of micro- or nano-shaped particles as was the initial aim.

The formed polymeric particles seem to have been embedded into the larger, shaped particles (as can be seen on Figure 4.3-3) during the formation of these particles.

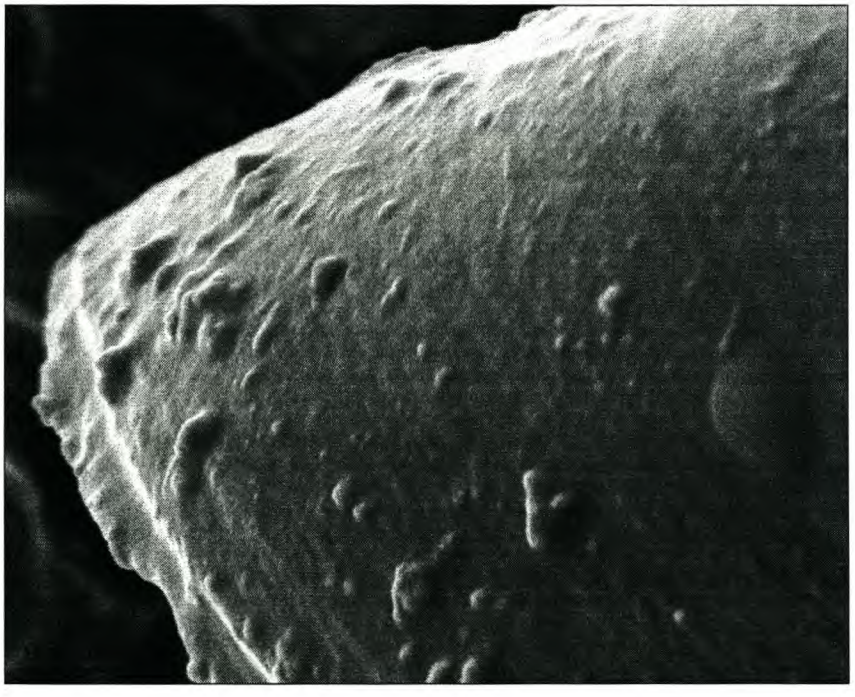

Figure 4.3-3 Polymeric particles embedded within surfactant crystalline structures

The origin of the shaped particles was of a more puzzling nature, and it was decided to pursue and elucidate the reasons for this unexpected occurrence of shaped particles. The motivation for this further investigation into the origin of the shaped particles was the following. McLeary

Stellenbosch University http://scholar.sun.ac.za

investigated the effect of polymerising in lyotropic phases of polymerisable surfactants [12]. The aim would therefore be to combine the formation of such regularly shaped particles with the polymerisation of polymerisable surfactants, in order to freeze in the solid-state structure and obtain a copy of the formed particles. This could be classified as a kind of solid-state templating procedure. This is currently part of an investigation carried out by a co-worker [13].

When high purity SDS was submitted to a similar set of treatments (i.e. the precipitation in ethanol and consequent centrifugation) no shaped particles were found. Only when the composition of the surfactant used in all the initial investigations was investigated more closely, was it realised that impurities in the form of electrolytes (concentration and type) were playing the defining role in the formation of the shaped particles.

The concentration and type of electrolytic impurities were determined by conductivity measurements and inductively coupled plasma atomic emission spectroscopy (ICP-AES). It was shown that sodium cation concentration (i.e. including the sodium bound to the surfactant) varied widely from sample to sample. This indicated, together with lower values of other common cations analysed for, that sodium cations were involved in the formation of the shaped surfactant particles. In the case of the surfactants where shaped particles were found, the Na^+ concentration was 20 ppm higher than could be expected if only sodium bound to the surfactant was calculated for. Common anions analysed for showed no such clear trend. It was therefore decided to calculate the amount of sodium needed from this data for various electrolyte pairs (Na_2SO_4, NaOH and NaCl). Investigations with these ion pairs showed that only SO_4^{2-} counter ions (at a concentration of 0,034 g Na_2SO_4 / g SDS) yielded shaped particles under controlled addition conditions.

Once the composition of the surfactant solutions was established, it was utilised to produce shaped particles from high purity SDS and the addition of electrolytes (in the form of Na_2SO_4). It was also found that the formation was highly specific to the solvent in which the precipitation took place. Methanol yielded irregularly shaped particles under the same conditions as found with ethanol. It was also clear that the presence of other organic components (such as hydrophobic styrene or MMA) would also influence the shape of the formed particles.

One factor that was established by means of WAXS analyses was that the precipitated shaped particles were not composed of either pure crystalline electrolytes or pure surfactant. Comparisons of WAXS data of crystalline Na_2SO_4, pure SDS, and precipitated crystalline structures indicate that the crystalline shaped particles contained structural elements from both the electrolyte and surfactant.

Stellenbosch University http://scholar.sun.ac.za

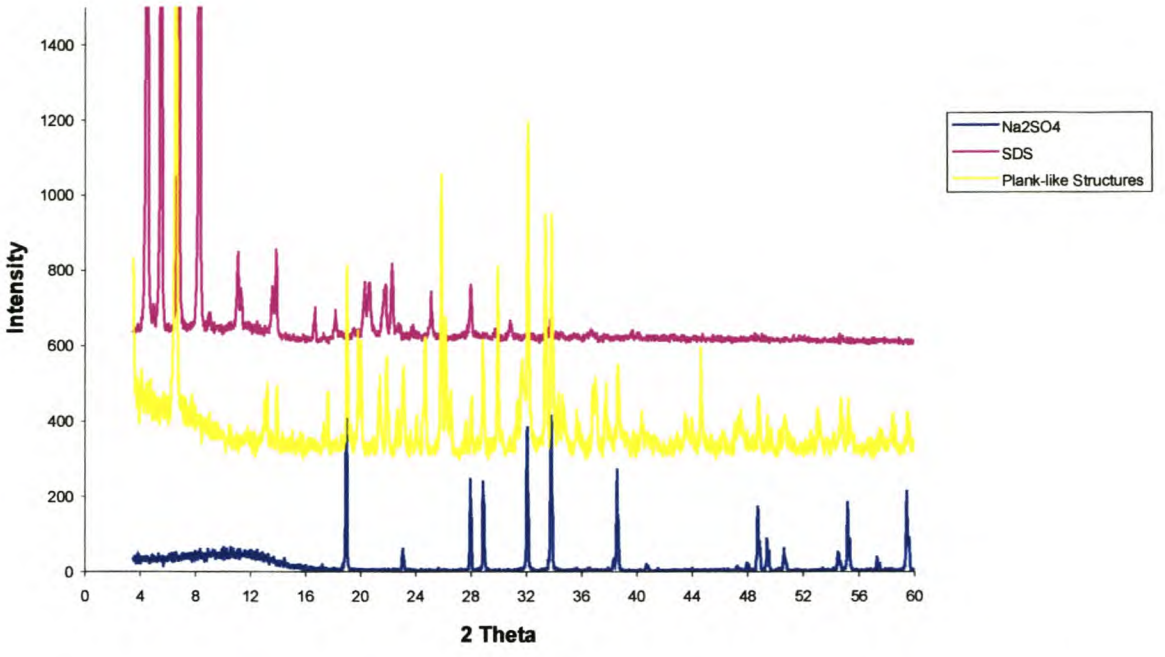

Figure 4.3-4 Comparison of WAXS analyses of pure Na2SO4, pure SDS and crystalline, plank-like structures.

An explanation for the formation of these specific structures can only be tentatively proposed. What was clear from the investigation was that the formation of these particles depends on a variety of factors, namely the type of electrolytes present, the concentration of electrolyte and the specific use of ethanol to precipitate the structures. The structures obtained from precipitation from ethanol are of a different order of magnitude than any mesophasic or intermediate mesophasic structure (for example the distorted cylinders and ribbon-like structures as found by Kekicheff and Cabane for SDS [14]) can be.

It might be possible that these structures are formed within the environment of altered polarity as provided by the addition of the non-solvent ethanol, and would show crystalline growth and precipitation under the specific conditions and ionic strength as provided by the electrolyte. These conditions are similar in nature (addition of non-solvent and the sensitivity to added counterions) as were found with the formation of rod-like structures made of lipid bilayers [15]. Even though much smaller structures are usually found, conditions for the formation of structured particles (fibers, rods and helices produced from twisted ribbons) are similar. Here cooperative hydrogen bonding of the alkyl tails and neutralisation of excess surface charge are instrumental in the production of solid rod-like structures. A similar situation is found with the formation of large ribbons of varying width and shape from 12-hydroxystearic acid. The width and shape of the ribbons are determined by the presence of various alkali metal ions, and solvents (such as hydrocarbons or alcohols) [16].

Stellenbosch University http://scholar.sun.ac.za

There are many further examples from the literature where the self-assembly formation of specific surfactant structures, especially in the case of large (>1 μm) tubule-like structures formed from flat bilayer sheets [17-19]. One example that was found in the literature concerning the formation of rod-like particles in emulsions was in a study by El-Aasser and co-workers [20]. They found crystalline rod-like particles in the reaction mixtures containing styrene, hexadecyltrimethyl-ammonium bromide and cetyl alcohol prior to polymerisation. In a system containing no cetyl alcohol no rod-like particles were observed. They suggested that the hexadecyltrimethylammonium bromide and cetyl alcohol formed a crystalline complex that would be stable under certain conditions. No mention was made of the presence of any electrolytes.

The results of this investigation showed that it is therefore also possible and that conditions were favourable to form specifically shaped particles from SDS, under conditions of fast precipitation, cooperative hydrogen bonding of the alkyl chains of the surfactant, and neutralisation of excess charges on the surface of such crystalline structures by the addition of electrolyte.

4.4 Conclusions

From the above results it is clear that the attempt to template organic polymers using surfactant solutions below the concentration where lyotropic mesophases are formed, was unsuccessful. Results from TEM and SEM investigations showed without doubt that this study also followed the pathway as found in literature, i.e. demixing and consequent separation of the polymeric phase. In this specific case there was minimal structure-directing on any part of the template / reaction solution, and only spherical particles with a very wide distribution in sizes were found.

It was shown that SDS forms microshaped particles (plank-like, rod-like and ribbon-like) under specific conditions of addition of a non-solvent for SDS (specifically ethanol) and presence of Na_2SO_4 as electrolyte. This is probably due to the cooperative hydrogen bonding of the alkyl tails and neutralisation of excess surface charge by the added electrolytes. The microshaping of polymerisable surfactants is currently under investigation for the possible production of solid-state templated surfactant structures.

Stellenbosch University http://scholar.sun.ac.za

4.5 References

1. Beck J.S., Vartuli J.C., Roth W.J., Leonowicz M.E., Kresge C.T., Scmitt K.D., Chu C.T-W., Olson D.H., Sheppard E.W., McCullen S.B., Higgins J.B., Schlenker J.L. J. Am.Chem.Soc, 1992, **114**, 10834

2. Kresge C.T., Leonowicz, M.E., Roth W.J., Vartuli J.C., Beck J.S. Nature 1992, **359**, 710

3. Tanev P.T., Pinnavaia T.J. Science 1995, **267**, 865

4. Bagshaw S.A., Prouzet E., Pinnavaia T.J. Science 1995, **269**, 1242

5. Perez-Luna V.H., Puig J. E., Castano V.M., Rodriguez B.E., Murthy A.K., Kaler E.W. Langmuir 1990, **8**, 1040

6. Chieng L. University of Singapore, Personal communication 1997

7. Huo Q., Margolese D.I., Ciesla U., Feng P., Gier T.E., Sieger P., Rosa L., Petroff P.M., Schüth F., Stucky G.D. Nature 1994, **368**, 317

8. Cheng C-F., Luan Z., Klinowski J. Langmuir 1995, **11**,2815

9. Göltner C.G., Antonietti M. Adv. Mater 1997, **9**, 431

10. Antonietti M., Göltner C., Hentze H-P. Langmuir 1998, **14**, 2670

11. Antonietti M., Göltner C.G. Angew. Chemie Int. Ed. Engl. 1997, **36**, 910

12. McLeary, M.Sc. Thesis, University of Stellenbosch, 1999

13. Ganeva D., PhD Thesis in preparation, University of Stellenbosch.

14. Kekicheff P., Cabane B. J. Phys (France) 1987, **48**, 1571

15. Fuhrhop J-H., Helfrich W. Chem. Rev. 1993, **93**, 1565

16. Claussen T.M., Vinson P.K., Davis H.T., Talmon J., Miller W.G. J. Phys. Chem. 1992, **96**, 474

17. Fuhrhop J-H., Demoulin C., Rosenberg J., Boettcher C. J. Am. Chem. Soc. 1990, **112**, 8458

18. Sommerdijk N.A.J.M., Feiters M.C., Nolte R.J.M., Zwanenburg B. Recl. Trav. Chim. Pays-Bas 1994, **113**, 194

Stellenbosch University http://scholar.sun.ac.za

19. Frankel D.A., O'Brien D.F. J. Am. Chem. Soc. 1991, **113**, 7436

20. Chou Y.J., El-Aasser M.S., Vanderhoff J.W. in Polymer Colloids II (Ed. R.M. Fitel), Plenum Press, New York, 1980

Stellenbosch University http://scholar.sun.ac.za

CHAPTER 5

5 Polyelectrolyte-surfactant complexes – preparation and characterisation

5.1 Introduction

From the previous chapter it was clear that the attempts to polymerise within labile surfactant templates failed. Although other interesting avenues of research were initiated from that investigation, the goal of creating shaped organic polymer nanoparticles was not reached. The results obtained were in agreement with various other studies, where it was shown that it is impossible to produce a 1 : 1 copy of a labile template, and that the preferred route followed during the reaction is demixing and phase separation into the structure-directing phase and a polymer phase [1, 2, 3].

In the search for a stable structure-directing synthesis medium it was decided to investigate the use of polyelectrolyte-surfactant complexes. Various other surfactant systems have been applied as possible structure-directing media over the last two decades, but with no direct success in producing 1 : 1 copies [4].

Previous investigations have indicated that the addition of a charged surfactant to an oppositely charged polyelectrolyte leads to well-defined materials. These materials exhibit the varied phase morphology of surfactants, however within a solid-state viscoelastic material with interesting properties [5-9]. It was therefore decided to investigate the structure-directing properties of these mesomorphic materials for organic polymerisations.

Various polyelectrolyte-surfactant systems have been studied by variation of the surfactant chain length [8], by variation of the properties of the polyelectrolyte backbone [10, 11] or by variation of both [12]. In this study the phase morphology of various complexes were investigated (for the first time) in order to evaluate their possible structure-directing use.

Polydiallyldimethylammoniumchloride (pDADMAC) was used as the high molecular weight polyelectrolyte backbone of the complex and was kept constant throughout the investigation. pDADMAC was used because of its good charge distribution / charge density, good binding properties, easy of use and low cost [13]. In the sulphate surfactant series used for this investigation, the hydrocarbon tail lengths (and therefore the hydrocarbon volume of the resulting

Stellenbosch University http://scholar.sun.ac.za

complexes) were varied to include the following surfactants: sodium decylsulphate (C_{10}), sodium dodecylsulphate (C_{12}), sodium tetradecylsulphate (C_{14}) and sodium hexadecylsulphate (C_{16}).

The phase morphology of the resulting complexes is discussed at the hand of small angle X-ray scattering (SAXS) data. Mechanical properties of the complexes were investigated by means of isochronal dynamic mechanical analyses (DMA). Thermal properties were investigated by means of dynamic scanning calorimetry (DSC). These measurements were performed at the Max-Planck-Institute of Colloids and Interfaces.

5.2 Experimental

5.2.1 Materials

High molecular weight pDADMAC (M_w = 375 000 – 500 000) was obtained from Sigma Chemical Company as a 20 weight % solution, and used as received. Sodium decylsulphate and sodium hexadecylsulphate were obtained from Lancaster Chemical Company, UK, at 99 % purity and used as received. Sodium tetradecylsulphate (95 % purity) was obtained from Sigma Chemical Company and used as received. Sodium dodecylsulphate (SDS, 99 % purity) was obtained from Serva Feinbiochemica, Heidelberg, Germany and used without further purification.

5.2.2 Experimental Procedure

Complexes from C_{10} and C_{12} Surfactants

For complex formation 2 g of the surfactant were dissolved in 100 ml distilled water at room temperature. An equimolar amount of pDADMAC (in terms of charged repeat units) was dissolved in the appropriate amount of distilled water to give an approximately 2 % (w/w) solution, and added dropwise to the surfactant solution under stirring. The resulting crude polyelectrolyte-surfactant complex precipitated, and the excess counterions were removed by several cycles of washing with distilled water and centrifugation, as described in [14]. The resulting clean complex was dried at 60 °C. Thin films were made by re-dissolving the complex in hot methanol, casting the mixture in teflon coated foil receptacles, left to dry overnight in air at room temperature, and then dried further at 60 °C.

Stellenbosch University http://scholar.sun.ac.za

Complexes from C_{14} and C_{16} Surfactant

The same protocol was followed as above, but all solutions were heated to 70 °C. The resulting crude polyelectrolyte-surfactant complex precipitated, and the excess counterions were removed by several cycles of washing with hot distilled water and centrifugation, as described in [14]. The resulting clean complex was dried at 60 °C. Thin films were made by re-dissolving the complex in hot 2-propanol and casting the mixture in teflon coated foil receptacles, left to dry overnight in air at room temperature, and then dried further at 60 °C.

5.2.3 Instrumental Techniques

High resolution SAXS diffractograms were obtained with a camera constructed at the Max-Planck-Institute of Colloids and Interfaces. Cu Kα X-rays were generated by a rotating anode (Nonius, FR591, P = 4 kW, $\lambda = 0.154$ nm). Small-angle x-ray scattering measurements were carried out with a Nonius rotating anode (FR 591) using image plates as detector. With the images plates placed at a distance of 40 cm from the sample, a scattering vector range from s = 0.07 to 1.6 nm^{-1} was available ($s = (2/\lambda * \sin(\theta))$. 2D diffraction patterns were transformed into a 1D radial average. The data noise was calculated according to Poisson-statistics which are valid for scattering experiments.

All WAXS diffractograms were obtained on a Nonius PFS120 powder diffractometer in transmission geometry. A FR590 generator was used as the source of Cu Kα radiation.

The DMA measurements were performed on a Netsch Instruments DM242 system with a heating rate of 3 K / min, and a frequency of 1 Hz. The temperature range investigated was from –130 °C to 150 °C.

DSC measurements were performed on a DSC 200 (Netsch Instruments). The heating rate was 10 K/min, and a pre-heating cycle was used for quantitative evaluations.

5.3 Results and discussion

WAXS analyses of the pure C_{10} and C_{12} complex films showed the films to be non-crystalline, i.e. the surfactant side chains exhibit a liquid or liquid crystalline type arrangement. The C_{14} and C_{16} complex films showed some side chain crystallinity. Figure 5.3-1 show the WAXS diffractograms of the C_{12} and C_{14} complexes.

Stellenbosch University http://scholar.sun.ac.za

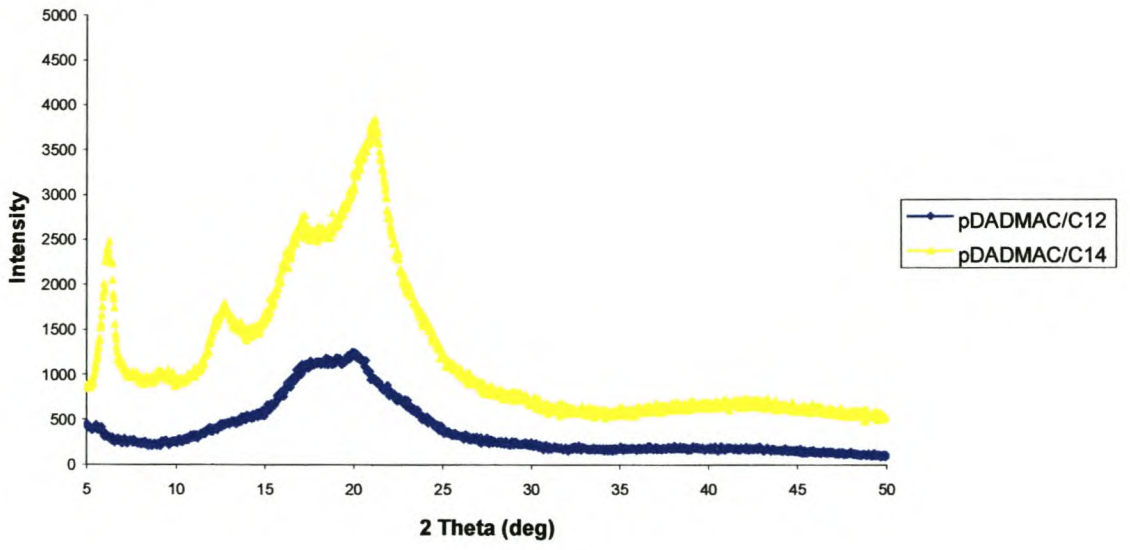

Figure 5.3-1 WAXS Diffractograms of pDADMAC-C_{12} and pDADMAC-C_{14} complex.

SAXS analyses of the purified complexes show a number of scattering peaks, indicating the existence of ordered mesophases. The positions of the peaks and proposed phase morphologies are summarised in Table 5.1 below.

Surfactant used	Peak positions s (nm^{-1})			*d*-spacing (nm)	Phase structure	Proposed fine structure
Decylsulphate	0.346	0.598	0.688	2.89 nm	Hexagonally packed cylinders	
Dodecylsulphate	0.324	0.556	0.646	3.08 nm	Hexagonally packed cylinders	Undulations of ionic cylinders
Tetradecylsulphate	0.354	0.723	1.146	2.82 nm	Lamellar	Tilted alkyl tails. Slightly interdigitated
Hexadecylsulphate	0.3474	0.693	Not detected	2.87 nm	Lamellar	Fully interdigitated alkyl tails

Table 5-1 Summary of data obtained from SAXS analyses of pure complexes.

Stellenbosch University http://scholar.sun.ac.za

In the case of the C_{10} and C_{12} complexes, the peak sequence of 1 : $\sqrt{3}$: 2 corresponds to reflections expected for a hexagonal mesostructure (hexagonally packed array of cylinders), which, when the respective volumes of the ionic and alkyl subphases are taken into account, can be considered to be inverse. See Figure 5.3.2 for the SAXS diffractograms of the C_{10} and C_{12} complexes.

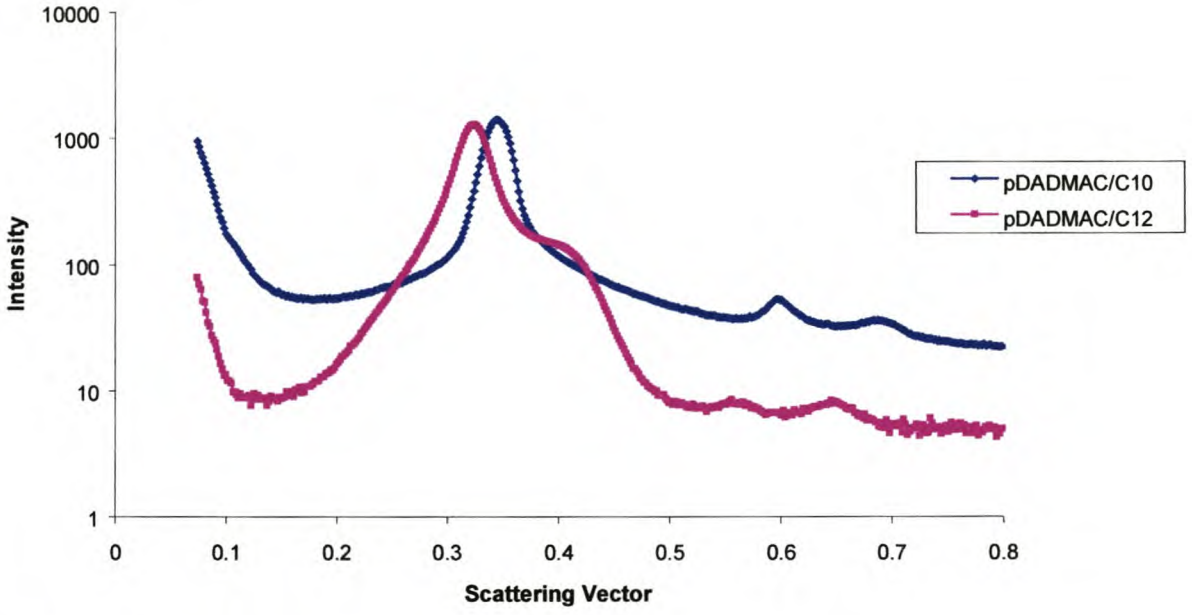

Figure 5.3-2 SAXS diffractograms of the C_{10} and C_{12} complexes.

The repeat unit distance in the pDADMAC-C_{10} complex is 2.89 nm. Since the length of a fully extended C_{10} hydrocarbon chain is 1.42 nm (calculated according to ref 15), it is expected that the alkyl phase is either minimally disordered or the alkyl tails from the ionic cylinders are only very slightly interdigitated.

The length of a fully extended C_{12} hydrocarbon chains is 1.67 nm, and the repeat unit distance in the C_{12} complex is 3.08 nm. It is therefore expected that the alkyl tails from the ionic cylinders interdigitated (much more than in the case of the C_{10} surfactant), or are tilted at an angle with some interdigitation. With the C_{12} complex however, it is interesting to note that there is also a pronounced additional peak at 1.23 times the primary peak. This was also found for the complexes between polyacrylic acid and dodecyltrimethylammonium counterions and was attributed to localized undulations of the cylinders due to frustration effects [9]. The excess surface area to accommodate these longer chains is therefore provided by the local undulations of the ionic cylinders. See Figure 5.3.3 below for a computer simulation of the undulating hexagonal phase. No such frustration effects were observed for the C_{10} complex.

Stellenbosch University http://scholar.sun.ac.za

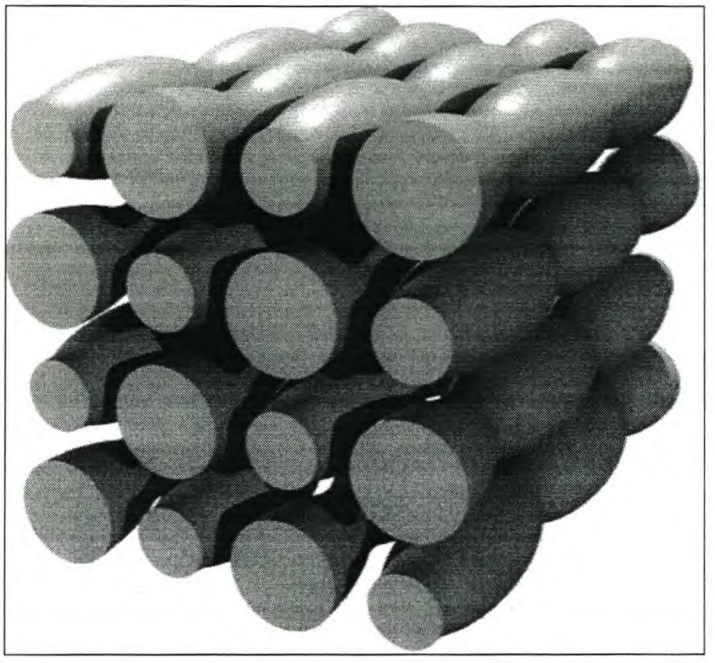

Figure 5.3-3 Undulating hexagonal phase proposed for the pDADMAC-C_{12} complex [with permission from M. Antonietti]. Continuous alkyl phase surrounding the ionic cylinders is omitted.

Different phase behaviour is evident for the complexes prepared from the C_{14} and C_{16} surfactants. A peak sequence of 1 : 2 and, in the case of the C_{14} complex the higher order reflection at approximately 4 times the scattering vector of the main peak, can be identified in both cases and are indicative of a lamellar morphology (see Figure 5.3-4 below). Since the lengths of fully extended C_{14} and C_{16} hydrocarbon chains are 1,93 nm and 2,18 nm respectively, the repeat distance found in these cases (2,82 and 2,87 nm respectively) can only be possible if the alkyl chains from two adjacent lamellae are interdigitated and tilted to a large extent. The exact phase structure (whether any undulations exist) can only be ascertained with a rigorous mathematical investigation of the scattering data [for examples see ref 10 and 11]. It is interesting to note that the higher order peak of the C_{16} complex is very broad (and any further higher order peaks are absent), indicating low long range order. This can be explained by the mechanics / mobility of the alkyl phase in terms of a high degree of interdigitation as mentioned above [11]. It is also known from other long chain surfactant complexes that, with higher degrees of side chain crystallinity (as was also found with the C_{14} and more so with the C_{16} complex) the order within the complex decreases [16].

Stellenbosch University http://scholar.sun.ac.za

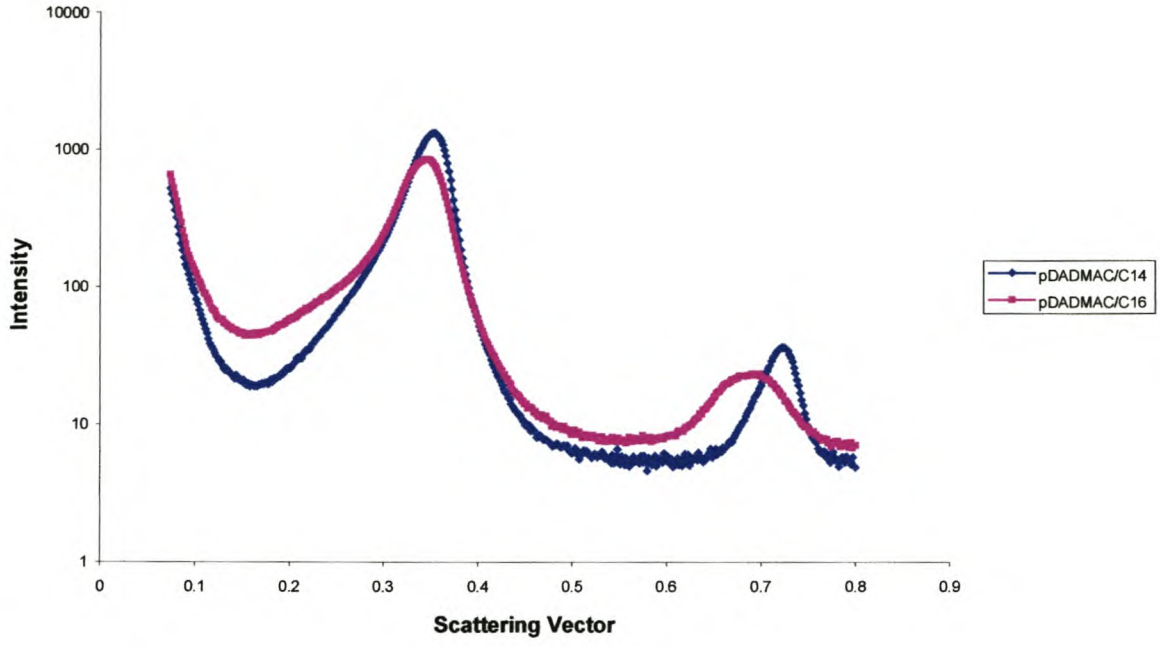

Figure 5.3-4 SAXS Diffractograms of C_{14} and C_{16} complexes

From DMA analyses data the general trends in terms of mechanical properties observed can be correlated to phase structures. Surface roughness (in terms of undulations) adds mechanical strength and stiffness to polyelectrolyte-surfactant complexes (more specifically bilayered structures) and can be seen as the nanomechanical analogue of corrugated iron [13].

It may be that undulations on cylinders would play a similar role in adding to the mechanical strength and stiffness under specific strains that need a structural shift. This can be seen in the DMA analyses of the series of complexes (see Figure 5.3-5 below). The C_{10} complex possesses the lowest shear modulus, while the undulating C_{12} complex shows a significant increase in the shear modulus G'. The C_{14} complex (where a transition from hexagonal to lamellar morphology was observed in the SAXS investigation) shows even higher mechanical strength, as can be expected for lamellar structures. If the C_{16} complex has undergone a simple increase in the undulations of the ionic layers, this trend is expected to continue, and the mechanical strength and stiffness of the complex ought to increase. This is however not the case, since there is a drop in shear modulus to below that of even the C_{12} complex.

Stellenbosch University http://scholar.sun.ac.za

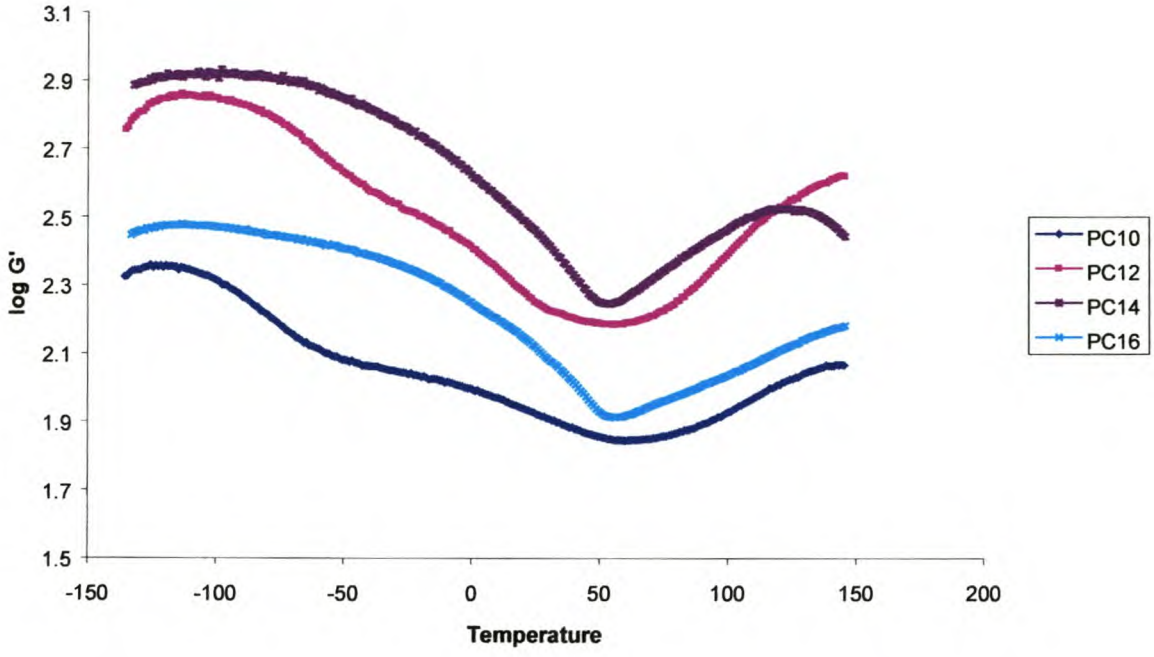

Figure 5.3-5 DMA analyses of various polyelectrolyte-surfactant complexes.

If this data is now evaluated in conjunction with the small increase in the repeat unit distance found for the C_{16} complex in comparison to that of the C_{14} complex, the following can be proposed. Trends observed can be correlated with the assumption that the C_{14} complex has an interdigitated lamellar phase structure. Undulations of the ionic layer are expected here, and would lend credence to this increase in stiffness. With the addition of two more carbons in the alkyl chain, the new complex dimensions derived from SAXS do not seem to accommodate the extra hydrocarbon volume by undulations on the ionic layers as is expected (as was seen in ref [8]). The small increase in the *d*-spacing correlates to a drop in the mechanical strength of the C_{16} complex. It is therefore proposed that the alkyl tail configurations have changed from slightly interdigitated and tilted (as found in the C_{14} complex) to where the extra two methylene units are simply accommodated in further interdigitation, including back folding, and so providing less resistance to interlamellar slip.

DSC evaluation of the films showed no transitions for the C_{10} and C_{12} complexes. This is similar to the results found for the complexes of polystyrene sulphonate and various alkyltrimethylammonium surfactants, where no glass transitions or phase transitions were observed [8]. In the case of the C_{14} and C_{16} complexes sharp endothermic transitions are observed at 40 °C and 49 °C respectively. These can be attributed to a crystalline melting transition within the alkyl layers, and was also observed in the DMA analyses of the films. This correlates to the WAXS analyses, which indicated some crystalline material to be present. A further exothermic transition was observed for both

Stellenbosch University http://scholar.sun.ac.za

complexes at high temperatures (182 °C and 186 °C respectively), an indication of chain flexibility occurring as ionic clusters allow "melt" translation of the groups in the ionic layers of the complexes.

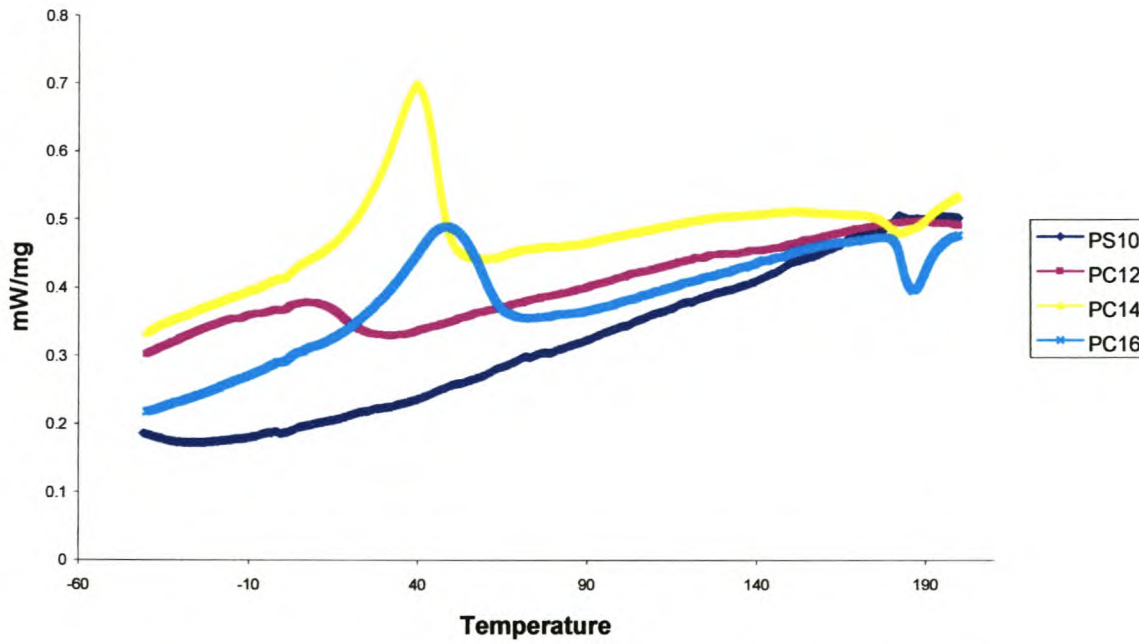

Figure 5.3-6 DSC Analyses of the series of polyelectrolyte-surfactant complexes

5.4 Conclusions

To expand the knowledge of self-assembled polyelectrolyte-surfactant complexes, a new series of complexes was synthesized using C_{10} to C_{16} linear alkyl sodium sulphates with polydiallyldimethylammonium chloride. Lyotropic behaviour was found in all cases (methanol used as solvent for the C_{10} and C_{12} complexes, and propanol for the C_{14} and C_{16} complexes). The C_{10} and C_{12} complexes decompose below 180 °C, whereas the C_{14} and C_{16} complexes exhibit a further aspect in addition to lyotropic behaviour in that they show a melting transition for the alkyl chains at 42 and 49 °C for C_{14} and C_{16} as well as transitions at 182 and 186 °C for the respective ionic areas. This is thought to be an ionic "glass" transition.

For the purpose of exploratory investigations into the structure-directing use of polyelectrolyte-surfactant complexes, well-defined systems are more desirable. From the above information, it seems that such simple complexes suitable for possible use would involve the C_{10} and C_{12} complexes. This decision is based on the fact that these complexes are easy to prepare, display easily defined phase morphologies and show no glass or phase transitions before losing stability at 180 °C.

Stellenbosch University http://scholar.sun.ac.za

From an economical point of view the C_{12} system is much more practical, since sodium dodecylsulphate is used widely in industry, and therefore affordable and easily obtainable. The system is well ordered, showing two higher order peaks which are attributed to scattering from a hexagonal array of ionic cylinders. The peak at 1.23 times the main scattering peak was attributed to undulations of the ionic cylinders.

In the case of the C_{14} and C_{16} complexes, the more complex phase morphologies and behaviour make these candidates for later investigations.

The application of the C_{12} complex as an ordered (due to the ordering of the surfactant alkyl phase) stable structure-directing host (due to the presence of a high molecular weight polyelectrolyte backbone) will be investigated in the next chapter.

5.5 References

1. Göltner C.G., Antonietti M. Adv. Mater 1997, **9**, 431

2. Antonietti M., Göltner C. Angew. Chem. Int. Ed. Engl. 1997, **36**, 910

3. Antonietti M., Göltner C., Hentze H-P. Langmuir 1998, **14**, 2670

4. Polymerization in Organised Media" (Ed. C. M. Paleos) Gordon and Breach Science Publishers, Philadelphia, 1994.

5. Ober C.K., Wegner G. Adv. Mater. 1997, **9**, 17

6. Antonietti M., Burger C., Effing J. Adv. Mater. 1995, **7**, 751

7. Antonietti M, Burger C, Thünemann A , Trends Polym Sci 1997, **5**, 262

8. Antonietti M., Conrad J., Thünemann A. Macromolecules 1994, **27**, 6007

9. Antonietti M., Conrad J. Angew. Chem. Int. Ed. Engl. 1994, **33**, 1869

10. Antonietti M., Maskos M. Macromolecules 1996, **29**, 4199

11. Antonietti M., Wenzel A. Colloids Surfaces A: Physicochem. Eng. Aspects 1998, **135**, 141

12. Kim B., Ishizawa M., Gong J., Osada Y. J. Polym. Sci. Polym. Chem. 1999, **37**, 635

Stellenbosch University http://scholar.sun.ac.za

13. Antonietti, M., Wenzel A., Thünemann A. Langmuir 1996, **12**, 2111

14. Thünemann A., Ruppelt D., Schnablegger H., Blaul J. Macromolecules 2000, **33**, 2124

15. Tanford C., The Hydrophobic Effect, Wiley, 1980

16. General, S. Max Planck Institute for Colloids and Interfaces, Personal Communication, 2000

Stellenbosch University http://scholar.sun.ac.za

CHAPTER 6

6 Structure-directed Synthesis of Polymer Mesostructures in Polyelectrolyte-Surfactant Films

6.1 Introduction

Over the last three decades, a variety of experiments were done to perform polymerisation reactions in organized media [1]. One motivation behind these efforts is to imprint the organized structure onto the polymer, and preserving the imprinted organised state of the guest after the removal of the structure-directing host. Another reason for polymerisation in organised media is to make "hybrids", where both polymer and structure-directing host contribute to the performance of the overall system, e.g. surface tensions, ductility, the ability for stress dissipation.

Polymerization reactions have been performed in zeolites [2, 3] in clays [4] or – more closely related to the present work - in ordered surfactant phases [5-12] and microemulsions [13-15]. Up to now, it was not possible to polymerise in such "soft" organized phases and to preserve a 1 : 1 copy of the structure-directing host structure. This is due to the influence of the growing polymer chain in the liquid crystalline phase, causing disruption of this ordered phase and consequent phase separation into a polymer phase and the original liquid crystalline structure-directing host phase.

Previous experiments to increase the stability or to decrease the dynamics of the surfactant ordered host made use of the variation of the counterions [16] or employed more stable, lyotropically ordered amphiphilic block copolymers as templates [17].

Here, we want to apply a new type of mesoscopically ordered polymer structure-directing host, which is also characterized by high host rigidity, but a flexible outside geometry, namely polyelectrolyte-surfactant complexes. In these systems, the addition of a charged surfactant to an oppositely charged polyelectrolyte leads to well defined materials with exhibit the rich phase morphology of surfactants, however within a solid state material with interesting properties [18-20]. Such complexes can also be made from polyelectrolyte gels [21] or using hydrogen bonding instead of charge coupling [22, 23]. Polyelectrolyte-surfactant complexes are formed by a very simple, though highly cooperative, process of charge neutralisation above a critical concentration, the so-called critical aggregation concentration (CAC), well below the critical micelle concentration (CMC) of the surfactant [24, 25]. The complexes are stabilized both by electrostatic interactions as well as hydrophobic interactions. Due to the low CAC (which also indicates low absolute exchange

Stellenbosch University http://scholar.sun.ac.za

rates), the polymeric nature of the counter ion, as well as the wide range of addressable morphologies, polyelectrolyte-surfactant complexes are regarded here as potentially interesting hosts for guest polymerisation reactions.

So far only the polymerisation of oppositely charged monomers associated with polyelectrolytes [26-28] and polymerizable surfactants within PE-Surf complexes is described in literature [29].

In the previous chapter the synthesis and characterisation of a series of polyelectrolyte-surfactant complexes were described. It was shown why the complex prepared from polyallyldimethylammonium-chloride and SDS was chosen as the structure-directing host. In the present work we will describe application of polyallyldimethylammonium-chloride (pDADMAC) and sodium dodecylsulfate (SDS) as hosts for the structure-directed polymerization of some vinyl guest monomers. This system was chosen since it combines high structural definition, appropriate charge density and good binding properties with a good solubility and swellability.

The swelling behaviour of the organised films with monomer and crosslinking agent is examined by weight uptake and small angle x-ray scattering (SAXS). The films after polymerisations, i.e. the hybrids between polymer and complexes, are examined by weight uptake, wide angle X-ray scattering (WAXS), SAXS, differential mechanical analysis (DMA) and transmission electron microscopy (TEM). In both cases, phase behaviour and the demixing were studied either by polarized light optical microscopy (POM) or by phase contrast microscopy (PCM).

6.2 Experimental

6.2.1 Sample Preparation

High molecular weight polydiallyldimethylammoniumchloride (pDADMAC, M_w 375 000 – 500 000) was purchased from Aldrich Chemical Co and used as received. Sodium dodecylsulfate (SDS) (99%, Serva Feinbiochemica, Heidelberg) was used without further purification.

For complex formation 4,00 g of the surfactant were dissolved in 200 ml distilled water. 2.24 g pDADMAC were dissolved in 100 ml distilled water and added drop-wise while stirring. The polyelectrolyte-surfactant complex precipitated, and the excess counterions were removed by several cycles of washing with distilled water and centrifugation, as described in [30]. The resulting clean complex was dried at 60 °C. Thin films were made by re-dissolving the complex in hot methanol, casting the mixture into Teflon coated foil receptacles, left to dry overnight in air at room temperature and then dried further at 60 °C.

Stellenbosch University http://scholar.sun.ac.za

Swelling with monomer was performed by bringing the weighed and dried films in contact with the appropriate amount of liquid monomer, and then left to swell in monomer to the following degrees (by weight): 3, 10, 15, 20 and 30 w%. Pure monomers were used; they were styrene (STY), m-diisopropenylbenzene (m-DIB), butylacrylate (BA) and ethyleneglycol-dimethacrylate (EGDMA).

For SAXS analyses films were swollen at room temperature in stabilised monomer. Films containing guest polymer after reaction were prepared by swelling the films in monomer and initiator (AIBN, recrystallised). Crosslinked guest polymer systems were prepared using the pure difunctional monomer and the same initiator. All polymerisation reactions were performed by heating the swollen films to ca. 70 ° C for at least 72 hours (120 hours in the case of m-DIB). For polymerisations, the monomer-swollen films were sealed in packages of non-oleophilic foil to ensure negligible loss of monomer throughout the thermal polymerisation process. After polymerisation, the films were removed from the sealed bags, dried in flowing air for 6 hours (to enable the removal of unreacted monomer) and then weighed to determine the weight after polymerisation.

6.2.2 Experimental techniques

SAXS curves were obtained with an Anton Paar compact Kratky camera using a Phillips PW1830 generator as the source of the Cu Kα incident radiation. Monochromatisation was accomplished using a nickel filter and pulse height discrimination. The measurements were performed in a s-range of 1.0×10^{-2} nm^{-1} < s < 9.0×10^{-1} nm^{-1} (the scattering vector s is defined as $s = 2/\lambda \sin \theta$ where 2θ is the angle between incident and scattered light). Peak positions and widths were determined by fitting smeared Lorentzian functions to the scattering curves.

High resolution SAXS diffractograms were obtained with a camera constructed at the Max-Planck-Institute of Colloids and Interfaces. Cu Kα X-rays were generated by a rotating anode (Nonius, FR591, P = 4 kW, λ = 0.154 nm). Small-angle x-ray scattering measurements were carried out with a Nonius rotating anode (FR 591) using image plates as detector. With the images plates placed at a distance of 40 cm from the sample, a scattering vector range from s = 0.07 to 1.6 nm^{-1} was available ($s = (2/\lambda * \sin(\theta))$). 2D diffraction patterns were transformed into a 1D radial average. The data noise was calculated according to Poisson-statistics which are valid for scattering experiments.

Monomer swelling studies were performed on films swollen in stabilised monomer, and wrapped in polyethyleneterephtalate films (transparent in this X-ray scattering region). Diffractograms were

Stellenbosch University http://scholar.sun.ac.za

recorded in air to avoid evaporation of monomer, which however results in loss of structure resolution due to parasitic scattering.

All WAXS diffractograms were obtained on a Nonius PFS120 powder diffractometer in transmission geometry. A FR590 generator was used as the source of Cu Kα radiation.

The DMA measurements were performed on a Netsch DM242 system with heating rate of 3 K / min, and frequency of 1 Hz. The temperature range investigated was from –130 °C to 150 °C.

The phase behaviour and the demixing were studied either by polarized light optical microscopy (POM) or by phase contrast microscopy using a Leica DM R optical microscope and a Linkam THM 600/S hotstage.

Samples of the guest polymer were prepared by dissolving the complex with hot methanol and separating the undissolved guest polymer by centrifugation. This cycle was repeated several times to ensure that all of the complex was removed from the remaining guest polymer fraction. GPC analyses were performed in THF with a set-up of Thermo Separation Products, using a P1000 pump and a UV1000 detector (λ = 260 nm), equipped with 5 μm, 8 × 300 mm SDV columns with 10^6, 10^5, 10^3 Å, from Polymer Standard Service, using a flow rate of 1 ml/min at 30 °C. The molecular weights were calculated with a calibration relative to PS standards.

Transmission electron microscopy was performed on a Zeiss 912Ω TEM at an accelerating voltage of 120 kV on the isolated cross-linked polymer casts, washed with hot methanol, and isolated by centrifugation. One washing cycle was also performed with distilled water, to ensure that no crystalline surfactant artefacts formed. The samples were then applied onto a carbon coated copper grids and dried in air.

6.3 Results and Discussion

6.3.1 Structural Investigation of the pDADMAC/SDS complex

A thorough investigation of the structure and physical properties of the pDADMAC/SDS complex was performed and described in Chapter 5.

6.3.2 Monomer Swollen films

The SAXS characterization was repeated after swelling the films with various amounts of monomer, with the data for EGDMA shown in Fig.6.3-1.

Stellenbosch University http://scholar.sun.ac.za

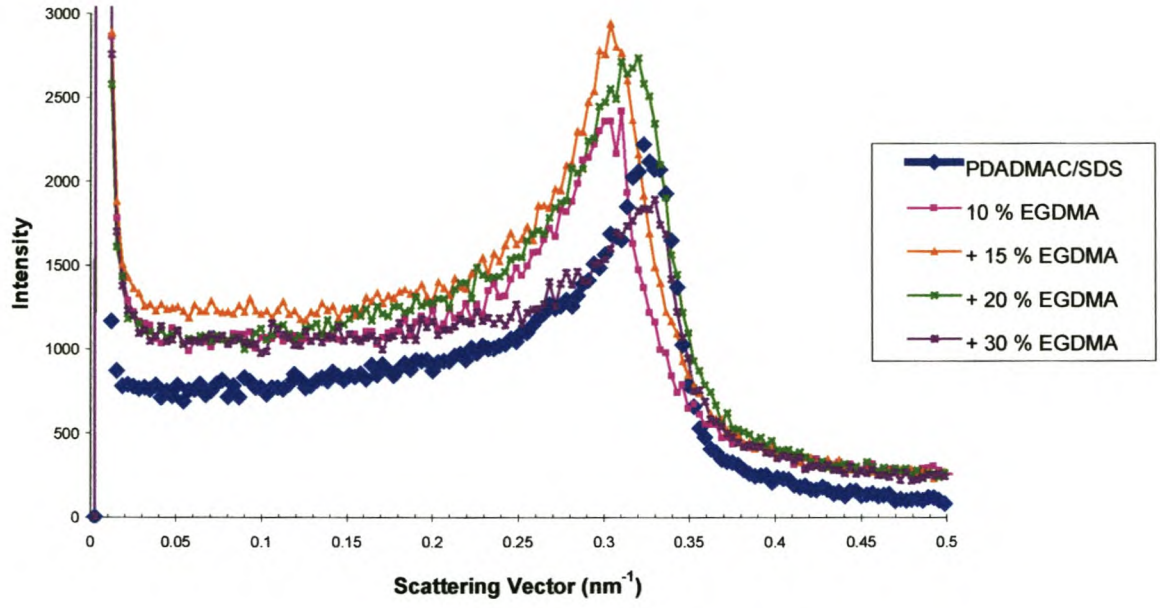

Figure 6.3-1 SAXS of complex films swollen with EGDMA

All data for other monomers used is presented below as a summary in Figure 6.3-2. The change in scattering vector S is plotted against the % monomer contained within the host complex film.

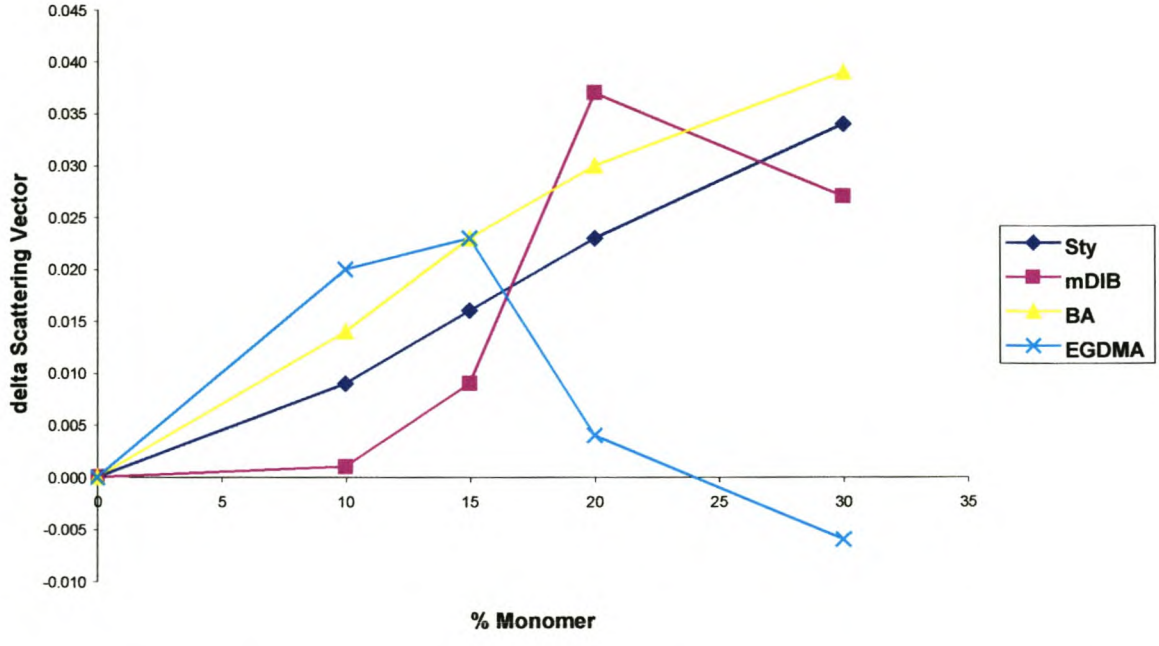

Figure 6.3-2 Summary of the swelling behaviour of pDADMAC/SDS films with various monomers.

It is seen that the peak intensity increases and is shifted to smaller scattering vectors (and therefore larger repeat units) up to the inclusion of 15 w% monomer, in accordance with our expectations.

Stellenbosch University http://scholar.sun.ac.za

For 20 w% EGDMA, the trend inverts; the curve shows a broader maximum with increasing s_{max}, indicating that the phase structure of the system is changing, and excessive swelling of one subphase does not occur under preservation of the order (see Figures 6.3-1 and 6.3-2). At 30 w% monomer present in the film, the scattering vector of the main peak is now larger than for the original host structure and very shallow and broad. We have to conclude that at this high loading, the local structure is essentially disrupted and not well organized.

Additional important information about the whereabouts of the monomer was obtained by DMA analyses of the complex with and without monomer (Fig.6.3-3). Here, the interest focuses on the low temperature range (from –140 °C to 50 °C), since in this region the mechanical response reflects the alkyl tail mobility.

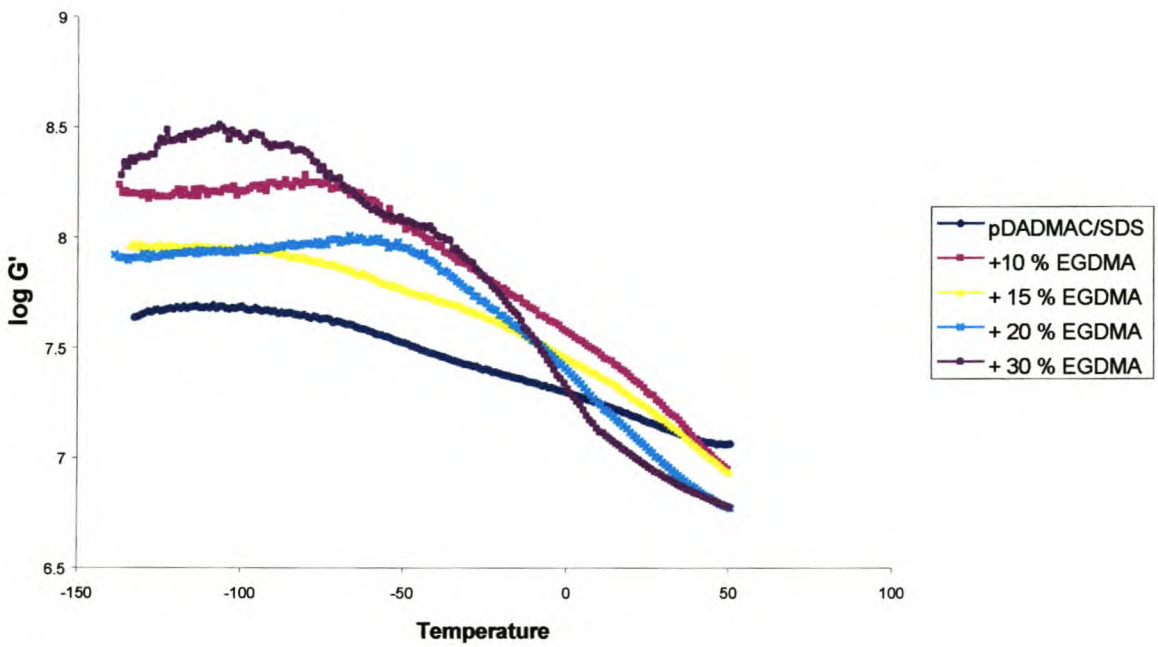

Figure 6.3-3 DMA of films with and without EGDMA monomer

The change in the properties of the alkyl phase is also seen in DMA analyses. The DMA analysis of a film without any monomer shows steady decrease in the alkyl chain mobility from a value of 7,65 for log G' at –130 °C, to 7,06 at 50 °C. This is typical softening behaviour of PE-Surf complexes coupled with the growing mobility of the alkyl tails [31]. Below – 60 ^{O}C, the alkyl tails essentially behave frozen, and the transition towards higher mobility is very broad, in good agreement with NMR measurements [32].

Swelling of the films with different amounts of EGDMA leads to a non-trivial result. In a systematic fashion, the modulus increases with increasing monomer content, while at higher

Stellenbosch University http://scholar.sun.ac.za

temperatures the modulus is decreased, as compared to the pure complex. The latter is the expected behaviour for a plasticised system where swelling reduces a modulus. The increase at lower temperatures is however not straightforward to explain, but certainly indicates phase disruption or the transformation of the hard ionic subphase in a branched, mechanically more resistant morphology. We conclude that EGDMA, presumably because of its bulkiness and partial polar character, is not an appropriate monomer for these types of experiments.

For swelling experiments with butylacrylate (BA), SAXS shows that only the peak attributed to the localized undulations vanishes, whereas the whole diffractogram shifts to smaller values of the scattering vector indicating respectively longer repeat distances (Figure 6.3-4). Plotting the *d*-spacing as calculated from the peak maximum against BA content, it is found that d increased from 3,08 nm (original film) to 3,52 nm in the case of the 30 % swollen system (Figure 6.3-5). This is, within experimental error, in good agreement with the expected square root swelling behaviour of a hexagonal mesophase.

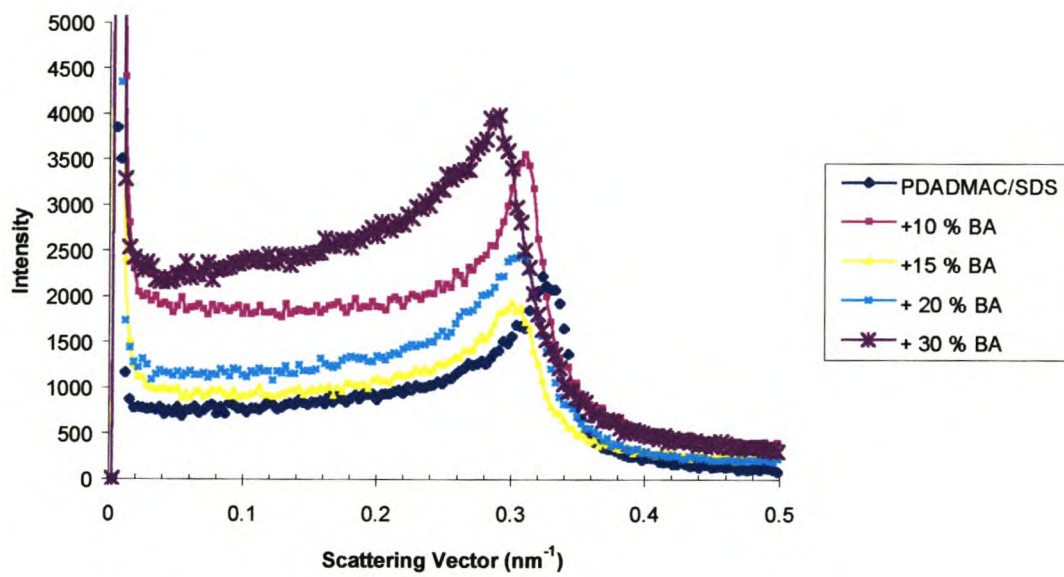

Figure 6.3-4 SAXS analyses complex films swollen with BA

Stellenbosch University http://scholar.sun.ac.za

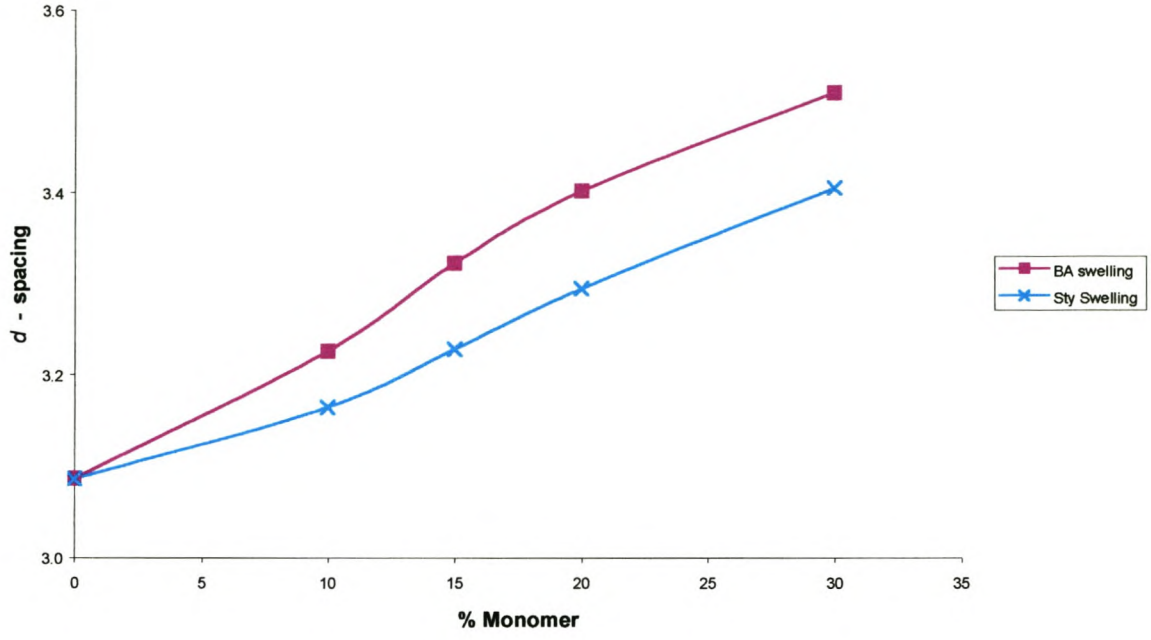

Figure 6.3-5 d-spacing versus monomer content of films swollen with BA and Sty

DMA analyses of the films swollen with BA show that the mechanical properties of the alkyl chain region of the host is affected (Figure 6.3-6). Increased mobility of the alkyl layer at low temperatures is found, showing that the monomer acts as plasticiser and is placed in the alkyl layer.

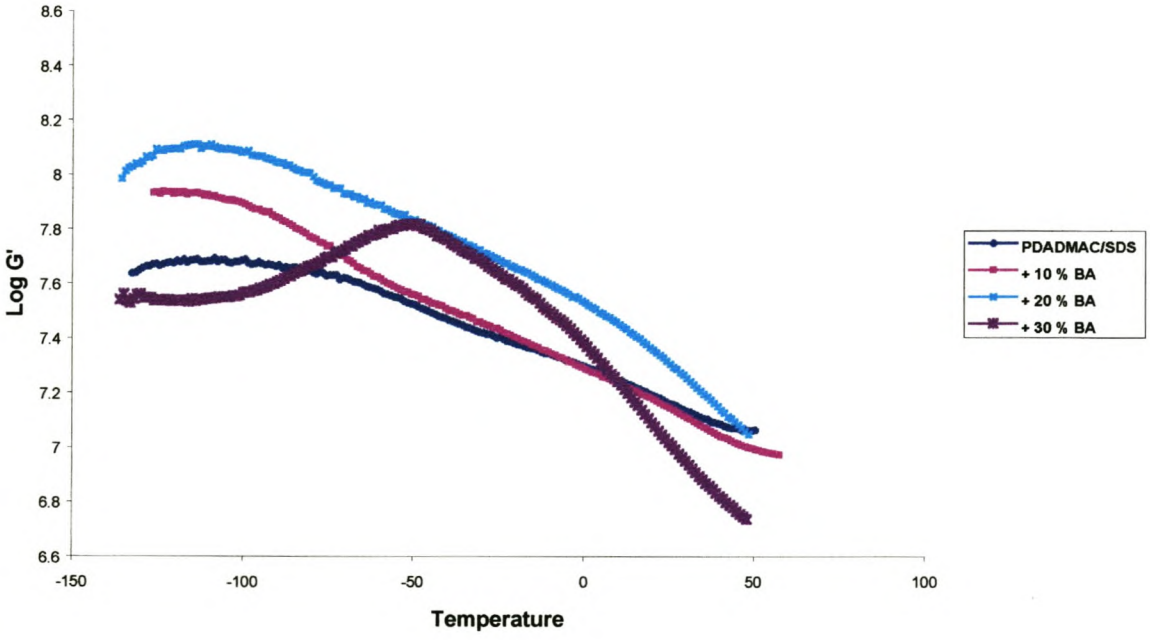

Figure 6.3-6 DMA analyses of complex films swollen with BA

Stellenbosch University http://scholar.sun.ac.za

At high BA content (30 %) the log G' values decreases significantly, showing the probable onset of phase disruption. This is in agreement with results found for EGDMA swollen films. Once again the change in the properties of the alkyl phase reflects the presence of the monomer in this phase.

A very similar, close-to ideal swelling behaviour of the solid PE-surf films is also found for styrene as a swelling agent. A summary of the changes in scattering vector was presented in Figure 6.3-2, and the corresponding shift of the Bragg distance with concentration was already shown in Figure 6.3-5, underlining the close similarities of styrene and BA.

DMA analyses (Figure 6.3-7) supports this view in that for styrene the mobility of the loaded host increases with the percentage of swelling in the complete temperature range examined. This shows that styrene swells and plasticizes the hydrophobic subphase and obviously does not enter, or changes the ionic domains of the host.

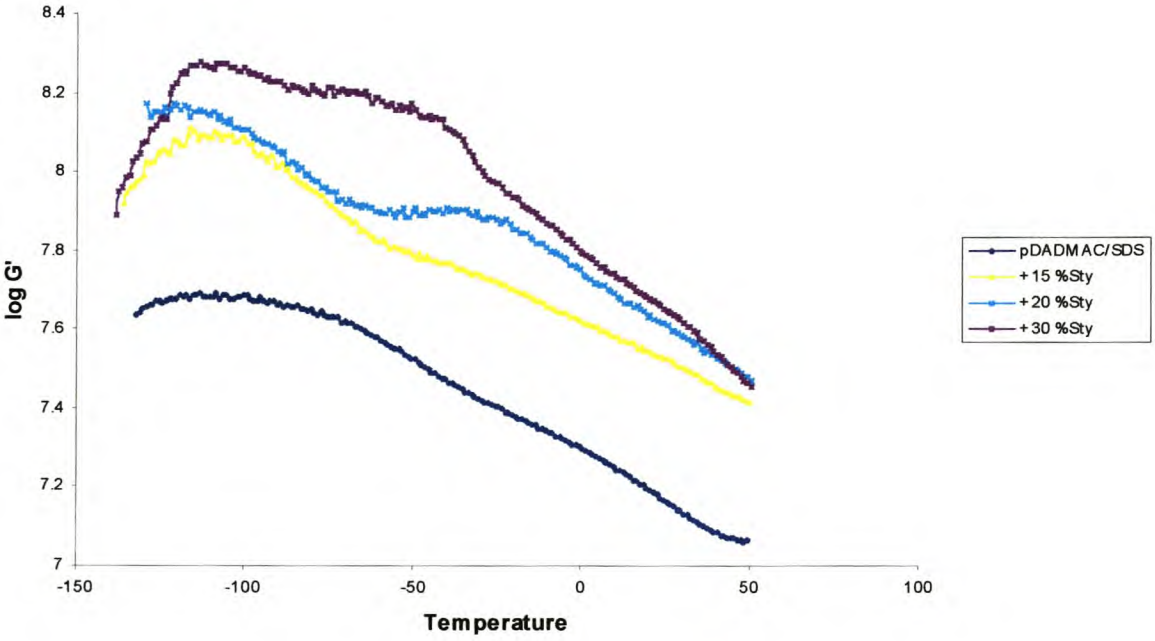

Figure 6.3-7 DMA analyses of complex films swollen with styrene

Since the synthesis of cross-linked species within the PE-surf films would be necessary for the investigation of particle morphology, the swelling behaviour of m-DIB (a cross-linker of similar chemical structure to styrene) was also examined. A similar increase of the Bragg distance with swelling was found, except the fact that the maximal swelling under preservation of the lyotropic order was 20 w%, as indicated by SAXS (see Figure 6.3-2). Obviously, the host just tolerates a certain volume and size of monomer, and larger subunits cannot be included while preserving the alkyl tail packing.

Stellenbosch University http://scholar.sun.ac.za

6.3.3 Films after polymerization

Films containing guest polymer were analysed according to the following scheme. Both crosslinked and uncrosslinked systems were investigated by SAXS and DMA. To characterize the polymerization process, the linear polystyrene was extracted and characterized by means of gel permeation chromatography. In case of the crosslinked systems, it was possible to remove the complex matrix with hot methanol and investigate the morphology of the polymer subphase by TEM.

Since we know from the data of the monomer containing films that there is a maximal concentration where the host keeps the ability to direct the structure, a variety of concentrations of guest polymer (3, 10, 15, 20 and, in the case of pSty and pBA 30 %) were examined

For the polymerization of polystyrene, SAXS analyses (Figure 6.3-8) show that up to 16 w% pSty the scattering diagram shifts towards larger sizes, but the peak broadens. This indicates that the lyotropic order is essentially preserved, but the guest polymer is disrupting the polyelectrolyte-surfactant phase in one or the other way, resulting in a system of lower order. The comparison to the films swollen with monomer reveals that the complex matrix tolerates less polymer than monomer, that is the critical concentration where the SAXS peaks go back to higher q-distances is decreased from over 30 w% to 15 w%.

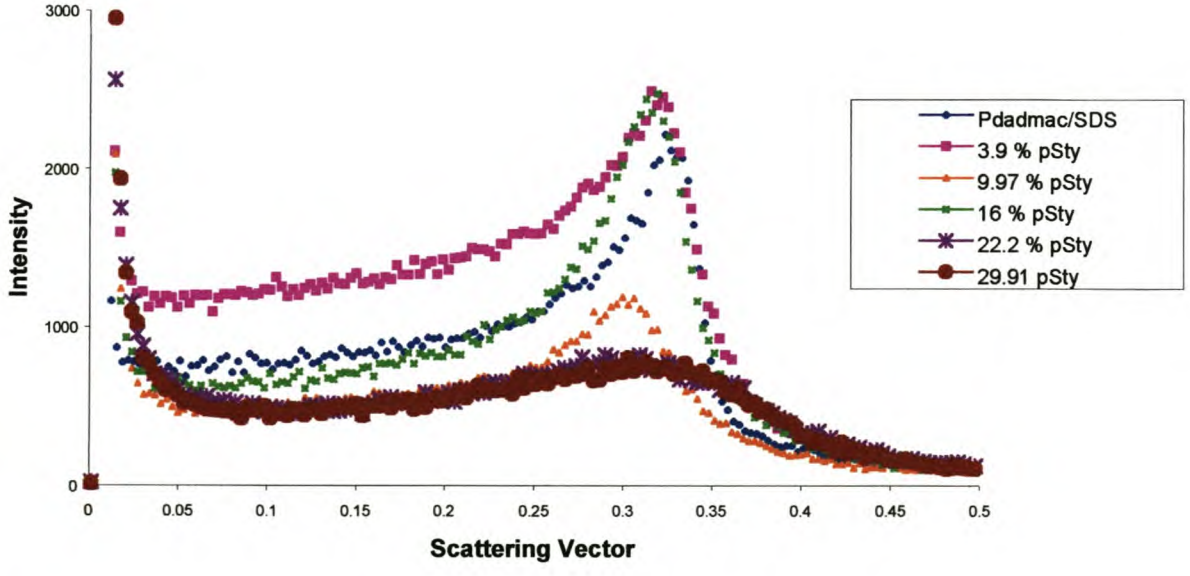

Figure 6.3-8 SAXS analyses of complex films containing pSty guest polymer

Stellenbosch University http://scholar.sun.ac.za

Isolation of the polystyrene from the matrix gives further information about the size and connectivity of the polystyrene domains. Values for molecular weights as found with GPC are listed in Table 6.3-1.

As expected for free radical polymerisation the polydispersity is high (between 3 and 7), but still lower than values found for polymerisations in layered minerals [4]. The M_w-values are quite high, which hints towards the fact that both the termination reaction and growth are slowed down in a similar manner. In any way, the polymers are "real polymers", that is the polymer subphase is larger that the characteristic length of the polyelectrolyte-surfactant structure and the polymer is confined in the nano-environment. No specific trend could be detected in the variation of the molecular weight or polydispersity with volume fraction of monomer, a good sign that all polymerisations occurred under the same confined conditions.

% Guest Polymer	M_n	M_w	D
3 %	63 500	429 000	6.75
9.57 %	113 500	422 700	3.73
14 %	89 400	449 700	5.03
18.83 %	126 400	513 500	4.06
29.5 %	67 9000	346 600	5.13

Table 6-1 Molecular weight distributions for pSty guest polymer extracted from pDADMAC-SDS templates.

In case of poly-m-diisopropenylbenzene, the SAXS analyses show that with increasing guest polymer content (up to 17 w% guest polymer) the template keeps its mesostructure, but the system loses some order, as it can be seen in the increase in the widths of the main scattering peaks. Exceeding the 17 w% limit leads again to a break-up of the phase structure and practically to a vanishing of order. See Figure 6.3-9 for a summary of the data for polystyrene and poly-(mDIB) in terms of change in scattering vector with increasing guest polymer concentration.

Stellenbosch University http://scholar.sun.ac.za

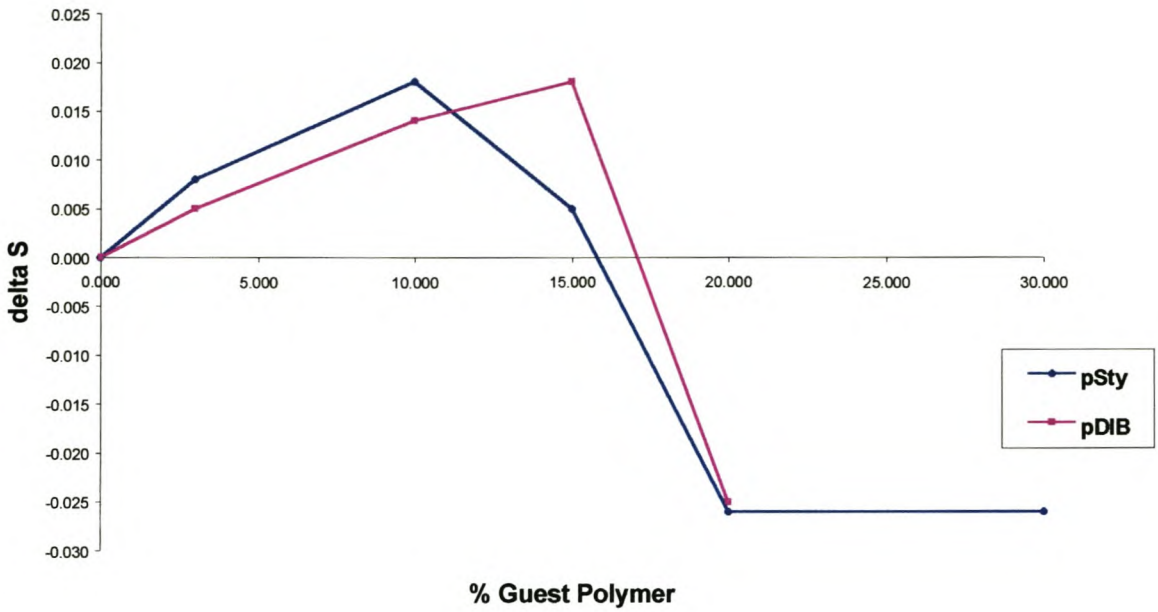

Figure 6.3-9 Summary of swelling behaviour of guest polymer containing complex films

With DMA we (Figure 6.3-10) observe that the presence of the guest polymer increases the modulus and decreases the mobility of the system in the temperature region where just the oleophilic or alkyl phase can move. This means that the poly(m-DIB) is located within the alkyl phase or forms a common phase with lowered mobility.

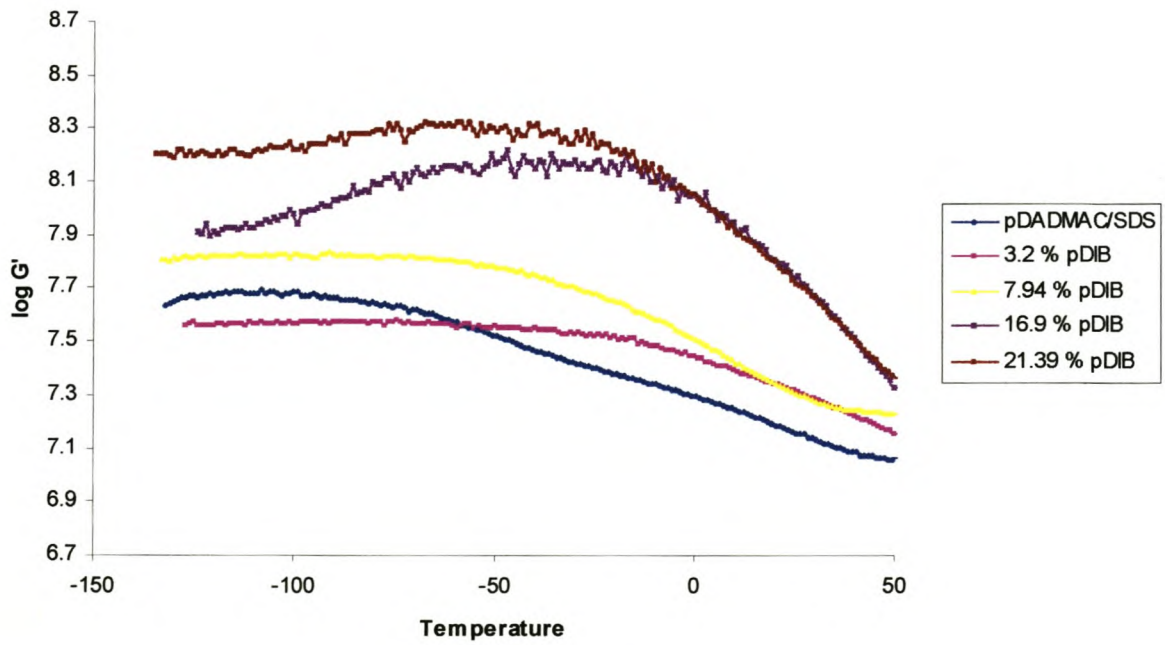

Figure 6.3-10 DMA analyses of complex host films swollen with poly-(mDIB) guest polymer

Stellenbosch University http://scholar.sun.ac.za

Since poly(m-DIB) is a highly cross-linked network polymer, electron microscopy gives important information about the location and the morphology of the final polymer phase.

In the case of template containing 3 % guest polymer, the crosslinked polymeric particles take the shape of thin wires or fibers, with size dimensions of approximately 4 nm in width and between 75 nm to 100 nm in length (see Figure 6.3-11). The amount of guest polymer included in the host is still very low, with consequent formation of particles whose width of 4 nm mimics the dimensions of the structure-directing host very closely (i.e. sizes are on the same lengthscale).

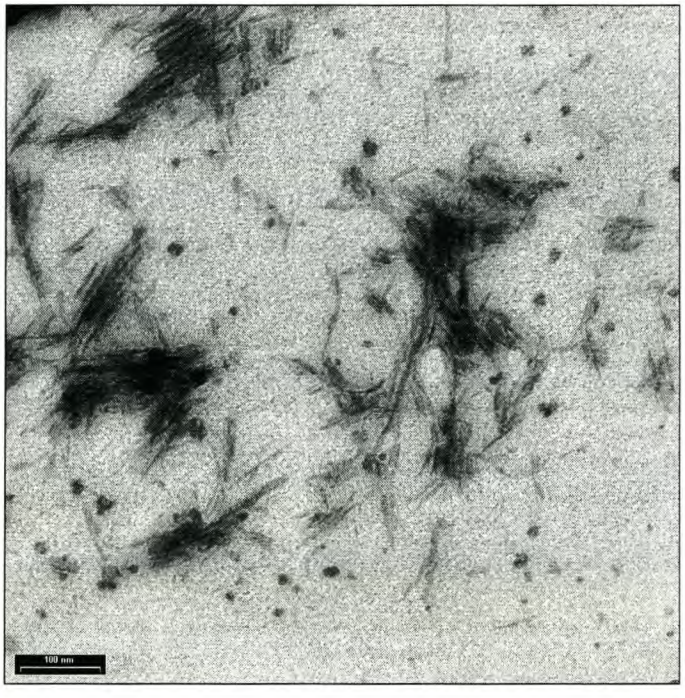

Figure 6.3-11 Structures of particles formed from 3 % crosslinked guest polymer

At 10 % included guest polymer, the particles now form very monodisperse cigar-shaped particles with size dimensions of 8 nm by 50 nm in length (see Figure 6.3-12). The size and morphology of the particles change as the concentration increases and the mimicking of the particles' size to the dimensional changes in the host is not as close. The presence of the guest polymer does therefore influence the host, as is also confirmed by the width of the scattering peaks in the SAXS analyses that indicate a lowering by displaying a broader range of dimensions in the polyelectrolyte-surfactant matrix. This is presumably due to the variable inclusion of the polymer in the host during polymerisation to form the cigar-shaped nanodomains. The comparison of the integrated scattering

Stellenbosch University http://scholar.sun.ac.za

intensities after polymerisation with the one of the original template shows that the areas are similar, but the scattering peak of the polymerised system is considerably broader.

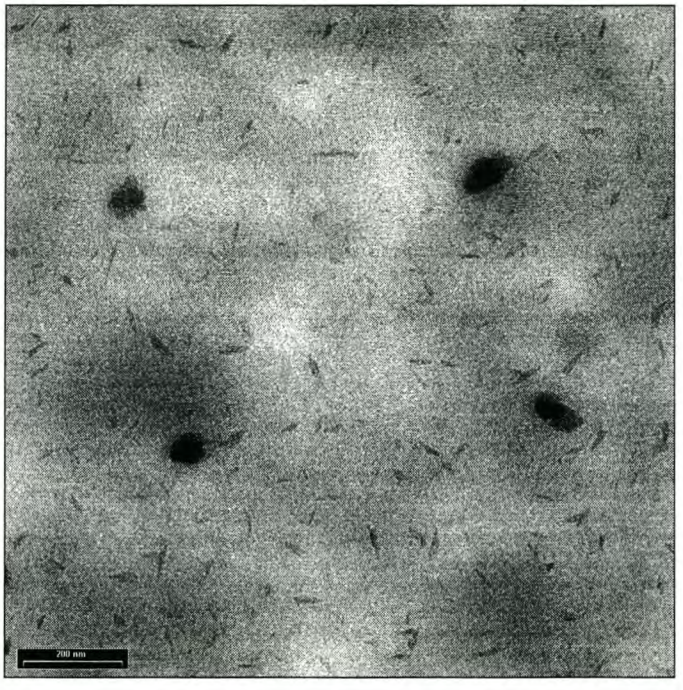

Figure 6.3-12 Cigar-shaped particles formed from 10 % cross-linked guest polymer.

When the concentration of the guest polymer (16.9 %) reaches a point close to where total phase disruption or lowering of the order of the template was observed with SAXS, the morphology of the formed particles also changed. Larger objects were formed (larger than 200 nm), many particles showing bent shapes (see Figure 6.3-13 below), which might be indicative of the transformation into a bent micellar phase or a disordered, sponge-like phase beyond the critical loading with polymer. Larger unstructured particles are also present in larger amounts, which reflect disordered or differently ordered regions.

Stellenbosch University http://scholar.sun.ac.za

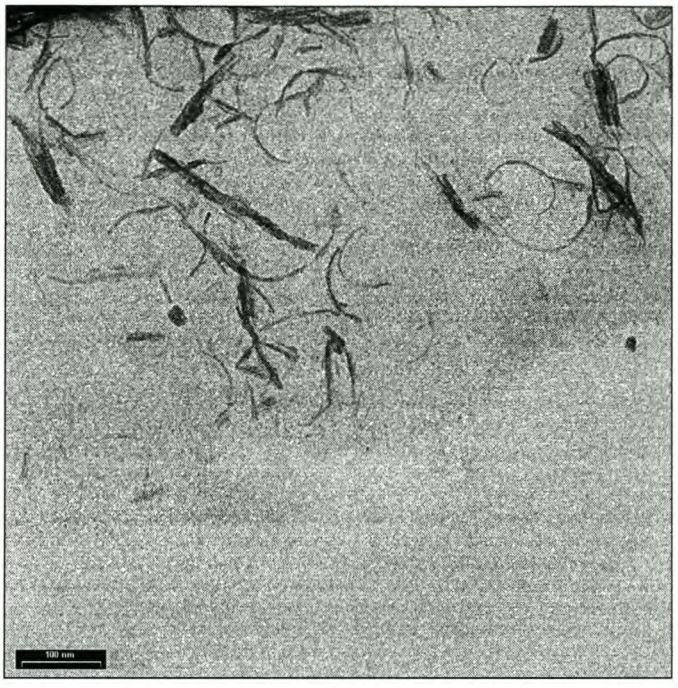

Figure 6.3-13 Bent fibrillar particle shapes from 16.9 % cross-linked guest polymer.

The TEM images show very clearly that the poly(m-DIB) does not form a continuous copy of the 3D hexagonal structure, but rather colloidal copies of a part of the host structure that swelled the most. Different morphologies were found for the different concentrations of guest polymer.

Structure-directing polymerisations were also tried with pBA and pEGDMA as chemically different polymers guests, but the lower miscibility already indicated in the monomer swelling experiments was amplified in the polymerised systems. SAXS analyses of the films containing pBA show that the presence of the pBA lowers the order of the templating phase very quickly, and the system containing 3 w% pBA guest polymer was essentially already disordered. Due to this, no further experiments were performed with the pBA system. A similar failure already at 2 w% guest polymer was also obtained for the pEGDMA system. These films were however subjected to TEM investigation to compare the results with the pDIB systems.

Only at low guest polymer concentrations (2 % pEGDMA) where particles found with shapes visibly influenced by the host. These particles are also roughly cigar-shaped, but approximately 50 nm in width by 150 nm in length (see Figure 6.3-14). In addition, high polydispersity indicates that loss of dimensional order of the host has occurred. This supports the previous statement that preservation of the order of the host is required to obtain reasonable shape control.

Stellenbosch University http://scholar.sun.ac.za

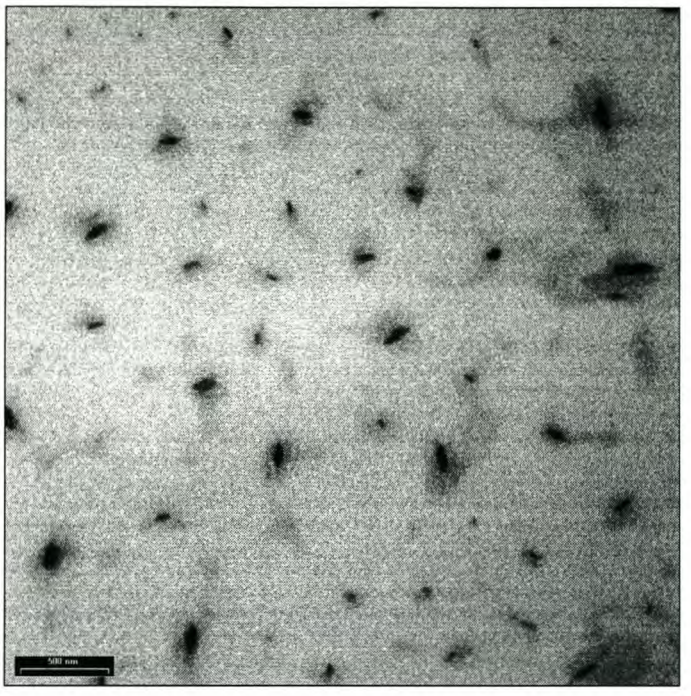

Figure 6.3-14 Shaped pEGDMA guest polymer particles obtained

6.4 Conclusions

Swelling of the inverse hexagonally structured polydiallyldimethylammonium chloride - sodium dodecyl sulphate complex (pDADMAC-SDS) with styrene, m-diispropenylbenzene, butylacrylate and ethyleneglycoldimethacrylate indicated that the polyelectrolyte-surfactant host is able to deform by swelling with the degree of swelling dependant on alkyl chain - monomer compatibility. Butylacrylate and ethyleneglycoldimethacrylate absorbed to 30 % and 15 % respectively before disruption of the phase of the host in the latter case, and styrene and m-diispropenylbenzene absorbed up to 30 % and 20 %, with only m-diispropenylbenzene disrupting the host phase at higher concentrations. This has been proved by small angle x-ray scattering. Small angle x-ray scattering also showed a broadening of the main scattering peak which indicated more varied repeat distances in the hexagonal structure, and therefore lower order. This is consistent with a deformable template that is not defined but maintains the hexagonal structure up to the mentioned percentages.

It was shown that polymerisation reactions performed within monomer swollen polyelectrolyte-surfactant complexes leads to an interesting shaping of the formed polymers, but it is still not possible to know how accurate the copy is imprinted by the host without molecular modelling. An exact one to one copy or cast, but preferably a "colloidal copy" is formed, where typical features of

Stellenbosch University http://scholar.sun.ac.za

the structure-directing host such as cross-dimensions or bending are imprinted into the guest polymer particles.

Polymerisations were carried out with varied amounts of monomers. It was found that the inverse hexagonal structure of the polyelectrolyte-surfactant host was maintained up to 15 % for polystyrene, 17 % for poly-mDIB, 3 % and 2 % respectively for polybutylacrylate and pEGDMA. A colloidal copy is obtained under disordering, but with preservation of the original phase structure up to where dimensional order is lost as concentration increases, i.e. it must be assumed that the system microphase-separates into an ordered subphase of the complex and the confined polymer nanoparticle has to follow the structurally limiting or directing features of its environment. From these results therefore, it seem that even with a strong, deformable host such as the polyelectrolyte-surfactant complex, the polymerisation process exerts a disruptive influence on the hexagonal phase

Since non-crosslinked polystyrene particles will lose shape once they are removed from the template due to thermodynamic influences, polystyrene was used as a non-crosslinked analogue to determine the molecular weight. No specific trend could be detected in the variation of the molecular weight or polydispersity with volume fraction of monomer.

When the polymer is produced from crosslinkable difunctional monomers, polymeric wires (4 x 100 nm), monodisperse cigar-shaped particles (8 x 50 nm) and bent wire-like particles (6 x 200 nm) were produced. These shapes may be regarded as excitingly new but odd polymer nano-structures.

The research described in this chapter has been accepted for publication in Langmuir: Directed Polymerization in Mesophases of Polyelectrolyte-Surfactant Complexes, Faul C.F.J., Antonietti M., Sanderson R.D., Hentze H-P, accepted 28 November 2000.

6.5 References

1. Polymerization in Organised Media" (Ed. C. M. Paleos) Gordon and Breach Science Publishers, Philadelphia, 1994.

2. Göltner C.G., Weissenberger M.C. Acta. Polym. 1998, **49**, 704

3. Frisch H.L., Mark J.E. Chem.Mater. 1996, **8**, 1735

4. Tieke,B.; Wegner, G. Makromol.Chem.Rapid.Commun. 1981, **2**, 543

Stellenbosch University http://scholar.sun.ac.za

5. Stoffer J.O., Bone T., J. Polymer Sci. Polym. Chem Ed. 1980, **18**, 2641

6. Stoffer J.O., Bone T. J. Dispersion Sci. Technol. 1980, **1**, 37

7. Vaskova V., Juranicova V., Barton J. Macromol. Chem. Macromol. Symp. 1990, **131**, 201

8. Gan L.M., Chew C.H., Friberg S.E. J. Macromol. Sci. Chem. 1983, **A19**, 739

9. Gan L.M., Chew C.H., Friberg S.E. Higashimura T. J. Polymer Sci. Polym. Chem Ed. 1981, **19**, 1585

10. Gan L.M., Chew C.H., Friberg S.E. J. Polymer Sci. Polym. Chem Ed. 1983, **21**, 513

11. Vrij A. Pure Appl. Chem. 1976, **48**, 471

12. Menger F. Angew. Chem. Int. Ed. Engl. 1991, **30**, 1086

13. Raj P.W.R., Sasthav M., Cheung H.M. Polymer 1993, **34**, 3305 and references cited therein

14. Chieng T.H., Gan L.M., Chew C.H., Lee L., Ng S.C., Pey K.L., Grant D. Langmuir 1995, **11**, 3321 and references cited therein

15. Antonietti M., Hentze H-P. Colloid Polym. Sci. 1996, **274**, 696

16. Antonietti, M.; Göltner, C.G.; Hentze, H.P. Langmuir 1998, **14**, 2670

17. Hentze, H.P.; Göltner, C.G.; Antonietti, M. Ber. Bunsenges. Phys. Chem. 1997, **101**, 1699

18. Antonietti M, Burger C, Thünemann A. Trends Polym Sci 1997, **5**, 262

19. Antonietti M., Conrad J., Thünemann A. Macromolecules 1994, **27**, 6007

20. Antonietti M., Conrad J. Angew. Chem. Int. Ed. 1994, **33**, 1869

21. Zhou S.Q., Yeh F.J., Burger C., Chu B. J Polym. Sci. Pol. Phys. 1999, **16**, 2165

22. Ikkala O., Ruokolainen J., Torkkeli M., Tanner J., Serimaa R., ten Brinke G. Coll. Surf. A. 1999, **147**, 241

23. Luyten M.C., van Ekenstein G., Wildeman J., ten Brinke G., Ruokolainen J., Ikkala O.,

Stellenbosch University http://scholar.sun.ac.za

Torkkeli M., Serimaa R. Macromolecules 1998, **31**, 9160

24. Goddard, E.D. Coll.Surf. 1986, **19**, 301

25. Hayagawa, H., Santerre, J.P.,Kwak, J.C.T. J. Phys. Chem. 1982, **86**, 3866

26. Blumstein A., Kakivaya S.R., Salamone J.C. Polym. Lett. Ed. 1974, **12**, 651

27. Polacco G., Cascone M.G., Petarca L., Maltini G., Cristallini C., Barbani N., Lazzeri L. Polym. Int. 1996, **41**, 443

28. Rainaldi I., Cristallini C., Ciardelli G., Giusti P. Polym. Int. 2000, **49**, 63

29. Dreja, M., Lennartz, W. Macromolecules 1999, **32**, 3528-3530

30. Thünemann A., Ruppelt D., Schnablegger H., Blaul J. Macromolecules 2000, **33**, 2124

31. Antonietti, M., Neese. M., Blum, G., Kremer, F., Langmuir 1996, **12**, 4436

32. Antonietti, M., Radloff, D., Wiesner, U., Spiess, H.W., Macromol. Chem. Phys. 1996, **197**, 2713

Stellenbosch University http://scholar.sun.ac.za

CHAPTER 7

7 CONCLUSIONS

The overall objective of this research work has been satisfied. Results of the research work have been presented as publications submitted to and accepted by the scientific and peer reviewed journal Langmuir (Directed Polymerization in Mesophases of Polyelectrolyte-Surfactant Complexes, Charl F.J. Faul, Markus Antonietti, Ron Sanderson, Hans-Peter Hentze accepted 28 November 2000). Oral and poster presentations have also been given at the following conferences: IUPAC Chemistry in Africa / 34th South African Chemistry Institute Conference, Durban, South Africa July 1998; IUPAC World Polymer Congress (Macro '98) Gold Coast, Brisbane, Australia, July 1998; ACS/European Polymer Division Macromolecules '99 (Polymers in the new Millennium), Bath, UK, September 1999 and IUPAC World Polymer Congress (Macro 2000), Warsaw, Poland, July 2000.

The basic objective was to create shaped polymer nano-particles as a one to one copy of (or as close as possible to) a template by using a structure-directing host based on sodium dodecyl sulphate - initially alone, and later in a more stable host structure, using polyelectrolyte-surfactant complexes with polydiallyldimethylammonium chloride.

By using the deformable, mesostructured polyelectrolyte-surfactant complex of polydiallyl-dimethylammonium chloride and sodium dodecyl sulphate, higher stability (versus that found in the case of sodium dodecyl sulphate alone) was provided to the structure-directing host by the presence of a high molecular weight polyelectrolyte backbone. It was shown that polymerisation reactions performed within monomer swollen polyelectrolyte-surfactant complexes lead to shaping of the formed guest polymers. Typical features of the structure-directing host such as cross-dimensions or bending are imprinted into the guest polymer particles.

When the guest polymer was produced from crosslinkable difunctional monomers, polymeric wires (4 x 100 nm), monodisperse cigar-shaped particles (8 x 50 nm) and bent wire-like particles (6 x 200 nm) were produced.

Stellenbosch University http://scholar.sun.ac.za

These are the first shaped, polymer nano-particles produced in a soft, self-assembled, organic templating host to be reported. These particles are not one to one copies or casts of the host and could rather be referred to as a colloidal copy of the deformable host. The host allows the diffusion of monomer and polymerisation loci to exist within the lyotropic structure without loss of overall hexagonal structure, up to determined guest polymer concentrations of 17 % in the case of poly-(mDIB).

There are two major advantages of this new route for the production of shaped polymeric particles i) the synthetic scheme is simple, easy and robust, and uses readily available materials, and ii) the host is recoverable; removal of the host, although it must be done with caution, does not present any great problem. With the present technology yields are restricted to 3 - 17 % (monomer-type dependent) shaped guest polymer nano-particles.

7.1 Recommendations for future research

Since this study was basically a proof-of-principle study, the following recommendations can be made.

Future work should focus on obtaining a better understanding of the deformation of the template and loss of order. This can be done by:

- Theoretical investigation and interpretation of SAXS data, to obtain variations in the thickness of the alkyl and ionic layers in polyelectrolyte-surfactant complexes, and to determine fine phase morphologies (such as undulations or perforations)
- Mesoscopic modelling of the polyelectrolyte-surfactant complex with molecular modelling software
- Gathering more data on the influence of varying monomer – surfactant alkyl chain compatibility, for a range of crosslinkable monomers and initiators, on the shape control of the polymeric particles
- Studying the kinetics of the formation of shaped, polymeric nano-particles as a function of time in the various polymerisations

Stellenbosch University http://scholar.sun.ac.za

- Studying structural changes in the deformable host by means of SAXS analyses during the respective polymerisations, to obtain better understanding of the process of particle formation

- Studying the influence of various phase morphologies of deformable hosts on the shape control of the polymeric particles